Hydrological impacts of wildfire and climate change on sediment and organic carbon loads at the watershed scale

by

Danielle Loiselle

A thesis submitted in partial fulfillment of the requirements for the degree of

Master of Science

Department of Earth and Atmospheric Sciences
University of Alberta

ABSTRACT

Climate change, extreme weather events, and disturbances such as wildfires alter hydrology, which in turn influences the cycling of water quality constituents such as sediments and nutrients. Organic carbon (OC) is an important element affecting water quality, as it can transport heavy metals, contaminants, and can support bacteria and biofilms. A study was undertaken with the goal of identifying the dominant hydrological processes affecting sediment and OC load, transport, and fate at the watershed scale, and developing a framework for simulating the impacts of future climate change and wildfires on sediment and OC export, and downstream water quality. The Soil and Water Assessment Tool (SWAT) hydrological model was used to simulate hydrology, erosion, and sediment transport at the watershed scale. The Elbow River watershed of southern Alberta, Canada was chosen as a study watershed due to its diverse landscapes, heterogeneous hydro-climate conditions, and access to long-term water quality data set. An in-stream OC module was incorporated into the SWAT model in order to connect terrestrial and aquatic OC processes, and simulate in-stream transformations between OC compounds. The new module successfully captured the seasonality of monthly loads, and indicated that snowmelt and rainfall are responsible for peak total organic carbon (TOC) loads, and peak streamflow and sediment loads in late spring and early summer. The calibrated model was then used for scenario analyses, in which the downscaled climate projections from five General Climate Models (GCMs) for RCP 2.6 and RCP 8.5 emission scenarios were fed into the model. To model wildfires, land cover and soil properties were updated in the SWAT source code to replicate post-wildfire conditions. The average results from the ensemble of GCMs indicated a sharp decrease in near future (2015–2034) streamflow and sediment yields compared to baseline conditions (1995–2014), particularly between May-August. The distant future (2043–

2062) scenario results indicated a slight increase in streamflow and sediment yields relative to the near future, but were still significantly lower than baseline conditions. In both near and distant future scenarios the TOC loads decreased, however, their relative concentrations increased, indicating poorer water quality compared to baseline conditions. Wildfire simulations largely influenced processes within the wildfire boundary, where surface runoff and the transport of sediments and TOC increased by more than 500% relative to climate change scenarios without wildfires. Impacts were also detectable at the watershed outlet, where annual streamflow, sediment yields, and TOC yields increased by a maximum of 9.3%, 6.5%, and 13.1%, respectively. Greater relative changes were observed for wildfires combined with the high emission climate change scenario (RCP 8.5) compared to the low emission scenario (RCP 2.6), and the watershed responded more strongly to burn severity than burn area. In summary, the development of the SWAT Organic Carbon Simulation Module for in-stream process representation and simulation of the impacts of wildfire was deemed a substantial step in modelling water quality under a changing environment. Model results indicated that climate change and wildfires would act in a synergistic fashion and negatively influence water quality in the future. However, further refinement of model parameters are necessary, such as simulating a top layer of debris and ash following wildfires. As well, this research has highlighted the importance of collecting pre-wildfire and post-wildfire data for quantifying impacts.

PREFACE

This master's research is original work by Danielle Loiselle. It is a paper-based master's thesis where Chapters 2 and 3 are manuscripts that will be submitted to scientific journals. Danielle Loiselle is the secondary author of the first manuscript, forming Chapter 2, and is the primary author of the second manuscript, forming Chapter 3.

The first manuscript (Chapter 2) is undergoing preparations for submission to *Science of the Total Environment*. Xinzhong Du, post-doctoral fellow in the department of Earth and Atmospheric Sciences, is the primary author. Danielle and Xinzhong Du made equal contributions to writing this manuscript and analyzing model results. Co-authors are Dr. Monireh Faramarzi, an Assistant Professor in the Department of Earth and Atmospheric Sciences who led the project and supervised this study, and Dr. Daniel S. Alessi, an Associate Professor in the Department of Earth and Atmospheric Sciences who co-supervised the study. The second manuscript (Chapter 3) is undergoing preparations for submission to the *Journal of Hydrology*, in the "Special Issue on Advances in forest hydrology in the light of land use change and disturbances". Co-authors are Xinzhong Du, Dr. Kevin D. Bladon, Dr. Daniel S. Alessi, and Dr. Monireh Faramarzi. Dr. Kevin Bladon is an eco-hydrologist and Assistant Professor in the Department of Forest Engineering at Oregon State University who provided feedback on simulation of wildfire and its impacts during the development of manuscript 2.

ACKNOWLEDGEMENTS

My sincere gratitude is extended to my supervisors, Dr. Faramarzi and Dr. Alessi, for their continued dedication to this project, and their guidance in navigating the academic world. Dr. Faramarzi with her hydrological modelling background and Dr. Alessi with his field experience offered me unique opportunity not only to learn basics of hydrological modelling but application in understanding real world problems. Both supervisors were generous with their time, provided encouragement and have continuously been forthcoming with new ideas, prompting exciting discussions, and leading to their implementation in this thesis. Both have provided very helpful feedback for countless conference abstracts, and both manuscripts in this thesis. Xinzhong Du has been an invaluable collaborator in this research, which his superior programming abilities and willingness to contribute knowledge. Paul Cabling made substantial contributions by compiling data and reviewing literature in the early stages of this research. I am very appreciative of Dr. Bladon for sharing his forestry and eco-hydrological expertise and helping to steer this research, as being a co-author on the second manuscript. I would also like to acknowledge Dr. Colin Cooke for agreeing to chair my master's thesis defense.

The City of Calgary has been generous in allowing us to use their water quality dataset in this research. In particular, I would like to thank Norma J. Rueker and Eric Camm for their continued interest in this research, willingness to answer questions, and for providing a tour of the Elbow River Watershed.

Finally, I would like to thank my family, friends from Calgary and the University of Alberta, and partner for their continued emotional and intellectual support. They shared advice, knowledge, and ideas, in addition to being excellent company when a break was needed.

TABLE OF CONTENTS

LIST OF TABLES

LIST OF FIGURES

CHAPTER I – INTRODUCTION

1.1 Climate, wildfires and water quality

Water is essential to all life and is undeniably our most valuable resource; however, global freshwater resources are unevenly distributed due to natural factors such as climate, topography, and geography. Various compounds are present within water in suspended or dissolved forms (i.e., nutrients, soil particles, minerals, metals, etc.), and their distributions are controlled by physical, chemical, and biological processes. Their presence can be beneficial to some lifeforms while being detrimental to others. Rapid climate change is increasing global temperatures and altering spatiotemporal precipitation patterns. As a result, extreme events (e.g., drought, storms, and floods), and disturbances such as wildfires are progressively becoming more frequent and severe. Increasing trends in erosion (IPCC, 2013) and dissolved organic carbon (DOC) in surface waters of the northern hemisphere, which can deteriorate water quality, have been linked to climate change (Monteith et al., 2007). Healthy ecosystems achieve balanced nutrient cycling, but excess DOC can support the formation of bacteria and biofilms (e.g., Fischer et al., 2002). Furthermore, DOC can transport metals and organic pollutants, making it an important water quality constituent (Laudon et al., 2012). Treating DOC in drinking water requires coagulant, which is both costly and can result in carcinogenic by-products if chlorine-disinfection is applied (Hohner et al., 2017). According to Health Canada (2017), the filtration of drinking water should result in the lowest possible turbidity levels (i.e., sediments, microorganisms, organic debris), and while there are no specific targets for DOC concentrations, the Canadian province of Ontario (2006) recommends a maximum of 5 mg/L for drinking water.

Anthropogenic greenhouse gas emissions are accelerating global warming, causing some regions to become dryer while others become wetter. Regardless of the direction of change, wildfires, heavy precipitation events, floods, droughts, and storms are increasingly common in many regions (IPCC, 2013). In Western North America, climate change is affecting seasonal patterns. For example, warmer temperatures are resulting in earlier spring melt in snow-dominated watersheds, and drier summers are increasing evapotranspiration rates and reducing streamflow (Islam & Gan, 2015; Rood et al., 2008). However, intense precipitation events are increasingly common, which increase stream power and the risk of floods. Rainfall dislodges sediment and nutrients from the ground surface, subsequently transporting them to streams via surface runoff and subsurface flows, and therefore rain density during storms can be a core predictor of stream water quality (e.g., Rostami et al., 2018). On the other end of the spectrum, longer dry periods reduce streamflow, and can result in warmer water temperatures and higher nutrient concentrations (Wagner et al., 2014). Another risk associated with warming and drying trends are discrete disturbances such as wildfires (e.g., Flannigan et al., 2005), which can affect watersheds for years by altering hydrological processes, sedimentation, and nutrient export (e.g., Emelko et al., 2011; Noske et al., 2010). In fact, if atmospheric carbon dioxide concentrations were to triple, as in the worst-case emissions scenario (IPCC 2013), projections indicate that total annual area burned in Canada and Western U.S.A. could double (Amiro et al., 2009; Flannigan et al., 2005; Rust et al., 2018). The seasonality of wildfires is also likely to shift, with the greatest relative increases projected for May and June (Amiro et al., 2009).

As many Canadians rely upon high quality water originating from forested watersheds, increasing wildfire activity poses a risk to these resources (e.g., Bladon et al., 2014). Forests play an important role in mitigating water yields, groundwater recharge, peak flows, sedimentation

and nutrient transport, as well as filtering pollutants (e.g., Brandt et al., 2013). Given that boreal forests make up 33% of forested area on Earth, and 75% of forested area in Canada (Natural Resources Canada, 2018), it is a key global system for water resources and carbon sequestration. Boreal forests account for approximately 88% of annual area burned in Canada (Amiro et al., 2009), and while wildfires are an integral part of the boreal ecosystem, combustion releases large amounts of greenhouse gases such as carbon dioxide, carbon monoxide, and methane. Therefore, these atmospheric carbon releases can further accelerate climate change and inherently contribute to increased wildfire activity through a positive feedback cycle (Amiro et al., 2009; Wotton et al., 2010). In Alberta, boreal forests make up the majority of forest cover extending north of the Elbow River watershed (Fig. 1.1). Headwaters originate in the Rocky Mountains in the west, and water generally drains to the northeast in the northern reaches, and to the east in the southern agricultural regions. The Eastern Rockies Forest Conservation Board, established in 1948, encouraged aggressive wildfire suppression with the objective of protecting headwater sources and cutting economic losses in the forestry industry (Willmore and Jensen, 1960). However, this has resulted in a wildfire deficit, and expansive fuel connectivity combined with climate change has greatly increased the potential for highly destructive burn events. In addition to natural factors such as lightning strikes, anthropogenic activity such as industry, campfires, and improper disposal of cigarettes commonly cause unintentional ignitions (Alberta Wildfire, 2019). In fact, the number of wildfires and total area burned has been increasing in recent decades and the most destructive events typically occur when conditions are unusually hot and dry (Alberta Wildfire 2019).

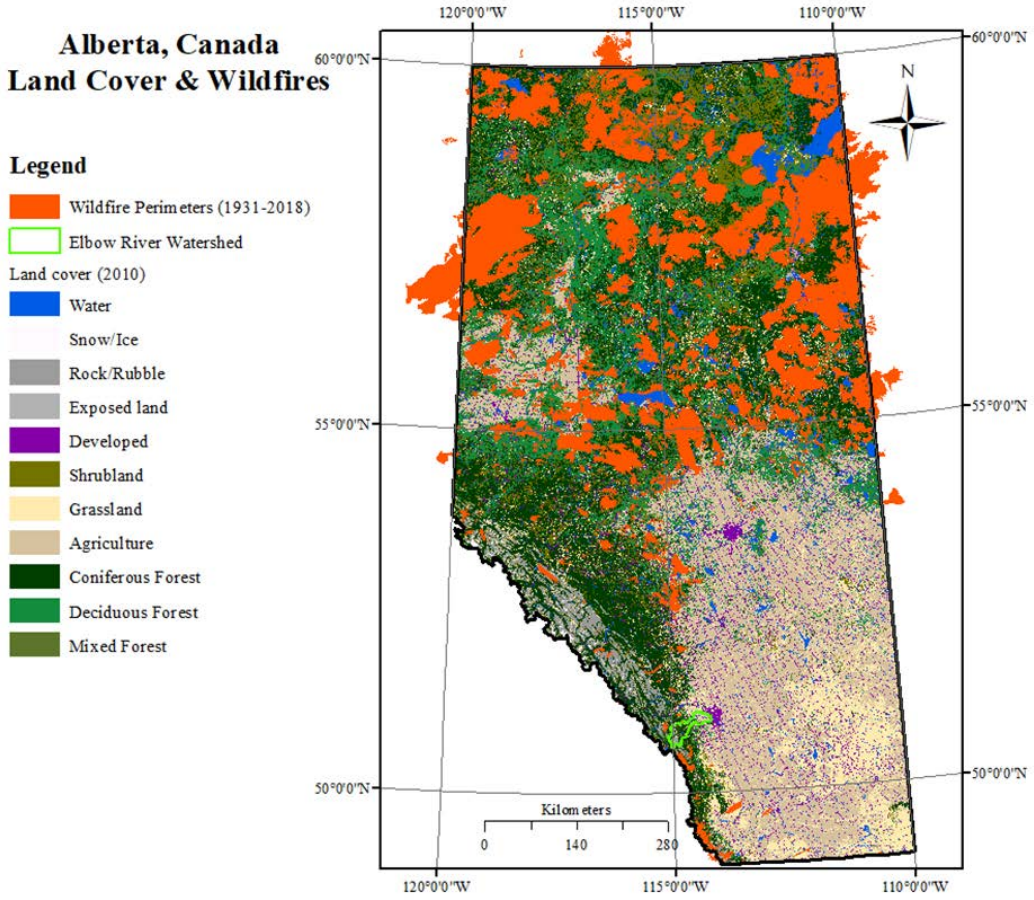

Fig. 1.1. Wildfire perimeters in Alberta, Canada (1961–2018); the Elbow River study watershed is in lime green. Data sources: Alberta land use: ABMI Wall-to-wall Land Cover Map 2010 Version 1.0, accessed July 2019; historical wildfire perimeter from Alberta Wildfire, accessed July 2019.

The removal of canopy shelter and soil organic matter due to wildfire can impact hydrology and water quality for several years, depending on the total area burned, its location within a watershed, and other characteristics such as topography and climate (Emelko et al., 2011; Moody et al., 2013; Noske et al., 2010). Reduced biomass available for evapotranspiration may significantly increases water yield by intensifying surface runoff (Townsend & Douglas, 2004), and thus erosion and nutrient export, particularly in areas with steep slopes (Bladon et al., 2014; Cotrufo et al., 2016; Emelko et al., 2011; Silins et al., 2009; Writer et al., 2014). Wildfires further contribute to surface runoff by altering soil properties, including decreasing hydraulic

conductivity, and increasing water repellency and soil erodibility (Doerr et al., 2009; Ebel & Moody, 2017; Moody & Martin, 2009). Post-wildfire field studies of a mountainous watershed in southern Alberta revealed that in-stream total suspended solids (TSS) increased by 1–3 orders of magnitude (Silins et al., 2009), and DOC increased by 50% (M. B. Emelko et al., 2011). Additionally, the dissolution of nutrients attached to TSS and alluvial sediments can further increase dissolved concentrations, such as DOC, and extend wildfire impacts (Cawley et al., 2018; Cotrufo et al., 2016; Writer et al., 2012). Lower albedo and the loss of shading from trees can lead to warmer water temperatures, accelerating dissolution rates (Wagner et al., 2014), and this will likely be further exacerbated by warming climate. Essentially, most impacts of climate change on freshwater systems are negative and indicate a decreasing trend in both the quantity and quality of water, accentuating the need for a better understanding of how future conditions may influence water resources.

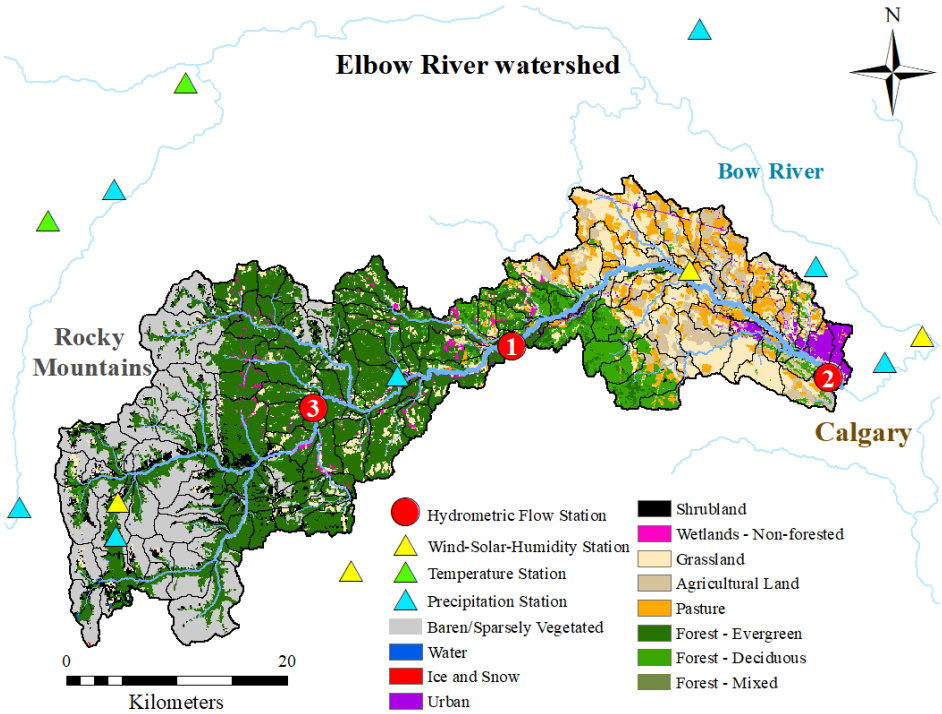

Fig. 1.2. Elbow River watershed in Alberta, Canada, and land use (GeoBase Land Cover Product, 2000). Location within Alberta shown in Fig. 1.1.

1.2 Research objective and hypothesis

Given this context, my research goal was to quantify impacts of climate change and wildfires on sediment and total organic carbon (TOC) transport by simulating watershed processes from landscape (e.g., carbon cycle in the soil, loads, and transport to streams) to in-stream (e.g., transformation between different carbon species and interactions with algae) throughout a watershed. This required a process-based model that can simulate the interaction of both terrestrial and aquatic hydrological processes, and cycling of sediments and TOC. The Elbow River watershed of southern Alberta was chosen as a study area due to its hydrogeological complexity, varying climate, landscapes, vegetation, and soil properties, and its importance as a drinking water source for residents of Calgary (Fig. 1.2). As well, this watershed is overdue for a wildfire (Rogeau et al., 2016), and there is a comprehensive and long-term water quality data set collected by the City of Calgary, making this an ideal study area. Therefore, we hypothesized that the development of a new approach for advancing the existing Soil and Water Assessment Tool (SWAT) model can help to understand hydrological processes affecting water quantity and quality by conducting scenario analyses to reflect climate change and wildfire events. The following objectives were defined to attain this research goal:

1. Modelling terrestrial and aquatic dynamics of water, sediment, and TOC at the watershed scale using an enhanced SWAT model and calibrating and validating model outputs;
2. Assessing performance and uncertainty of the enhanced SWAT model;
3. Developing a framework for modelling the impacts of wildfire by modifying SWAT model inputs to recreate post-wildfire conditions;
4. Using the calibrated model as a tool to project relative changes in sediment and TOC loadings under climate change and wildfire scenarios;

5. Assessing uncertainties and performance of wildfire simulations and identifying areas needing further research.

To achieve objectives 1 and 2 of this research, we used an enhanced SWAT model that embeds the SWAT Organic Carbon Simulation Module (SWAT-OCSM). SWAT is a physical and process-based hydrological model (Neitsch et al., 2011). The model takes into account soil properties, land cover, topography, and climate to simulate key processes related to hydrology, soil water balance, sediment transport, nutrient cycles in the soil and their transport, and plant growth. Simulation of organic carbon (OC) dynamics were previously limited to the soil profile and closely related to cycling of other nutrients such as nitrogen and phosphorous in the soil. However, simulation of its dynamics, transformation, and transport in the water bodies and stream network is crucial for water quality management in the watersheds. The new SWAT-OCSM simulates both terrestrial and aquatic OC processes related to its loads, transport, and fate at the watershed scale. Model outputs were first calibrated to measured streamflow, followed by in-stream sediments, and then in-stream TOC.

Applications of the newly developed module include scenario analyses. As wildfires can alter the transport of water quality constituents, we achieved objective 3 by modifying the SWAT code to change land use and soil properties to reflect post-wildfire conditions. Objective 4 was satisfied by feeding future climate change data into the model from five downscaled General Circulation Models (GCMs), and assessing relative changes in water quantity and quality with and without wildfires. We then achieved objective 5 by comparing our model outputs to those of other studies in order to assess our wildfire modelling approach and identify areas requiring further development.

1.3 Contents and structure of thesis:

Chapter 2 introduces the enhanced SWAT model in the context of previous limitations in simulating TOC dynamics at the watershed scale. In this chapter, we described model set up, the calibration and validation of streamflow, sediment yield and TOC yields, and then discussed uncertainties in model outputs.

Chapter 3 describes and assesses wildfire modelling framework. Climate change scenarios with and without wildfires were applied to the calibrated model in order to project relative future changes in water quantity and quality in terms of sediment and organic carbon. Areas of the wildfire modelling approach requiring further refinement were identified.

Chapter 4 summarizes the findings of previous chapters and draws conclusions about the future of water resources in the face of climate change and extreme events. Finally, the applicability of scenario analysis methods were linked with the importance of monitoring watersheds in order to be proactive about water resources.

CHAPTER II – MANUSCRIPT 1

Incorporation of a process-based in-stream organic carbon module into SWAT to simulate organic carbon load and transport at the watershed scale

Xinzhong Du[1], Danielle Loiselle[1], Daniel S. Alessi[1], Monireh Faramarzi[1].
[1] Department of Earth and Atmospheric Sciences, University of Alberta, 1-26 Earth Sciences Building, Edmonton, AB T6G 2E3

2.1 Introduction

Eroded and leached organic carbon entering streams and other water bodies can cause degradation of water quality, subsequently having negative impacts on both human and aquatic ecosystem health (Larsen et al., 2011; Zhang et al., 2013). A surplus of OC can support the formation of biofilms and bacteria (e.g., Fischer et al., 2002), and ease the transport of organic pollutants and metals (Laudon et al., 2012). The hydrological cycle drives sediment and nutrient transport mechanisms, and is affected by climate, human activity, disturbances, and extreme weather events (e.g., wildfires, storms, droughts, and floods). Climate change and human consumption or diversion of water have already altered water supply in many areas of the world (e.g. Gleeson et al., 2012; Pekel et al., 2016; Rood et al., 2005; Vorosmarty et al., 2010), with implications for water quality. In the case of climate change, it is generally agreed that temperatures will continue to increase, however, changes in precipitation patterns are spatiotemporally variable, and global trends indicate an overall reduction in both the quantity and quality of freshwater (IPCC 2007; IPCC 2013). Higher temperatures and reduced streamflow lead to longer retention times in lakes, during which heat and nutrients can accumulate and influence aquatic life and productivity (Larsen et al., 2011; Schindler and Donahue, 2006). The increase in frequency and severity of events such as wildfires, storms, droughts, and floods are

also associated with climate change, and have implications for both water quantity and quality (e.g., Amiro et al., 2009; Flannigan et al., 2005; Mahat et al., 2016; Rood et al., 2005; Wang et al., 2015). For example, surface runoff from heavy rainfall erodes soil particles and attached nutrients, resulting in turbid waters and higher in-stream nutrient concentrations. Therefore, storm rain intensity and resulting sediment and nutrient export directly affects water quality (Rostami et al., 2018). Wildfire occurrences increase surface runoff through the removal of protective vegetation (Smith et al., 2011), after which both in-stream sediment and OC concentrations can spike dramatically (e.g., Bladon et al., 2008; Bladon et al., 2014; Emelko et al., 2011; Writer et al., 2012) and alter water treatment requirements (Hohner et al., 2016). Health Canada (2017) recommends that filtration systems provide the lowest possible turbidity levels with an upper limit of 1.0 NTU (Nephelometric Turbidity Unit). Particles contributing to turbidity can be organic (e.g. microorganisms, or decomposed plant and animal debris) or made up of inorganic material, such as sediments. As for dissolved organic carbon (DOC) concentrations, there are no specified guidelines for Canada, but a maximum of 5 mg/L is accepted in the Canadian province of Ontario (2006). High DOC fluxes present challenges for water treatment facilities (Emelko et al., 2011; Hohner et al., 2016; Hohner et al., 2017), and removal can result in carcinogenic disinfection by-products (Regan et al., 2017; Roy et al., 2006). Since much of the high-quality drinking water in Canada is sourced from forested watersheds (e.g., Cawley et al., 2018), it is therefore essential to understand how changes in climate and extreme events might impact source water quality in the future.

Watershed models that integrate terrestrial and aquatic processes are useful and cost-effective tools for predicting and assessing the impacts of changes in climate and extreme events on water quality conditions. The Soil and Water Assessment Tool (SWAT) is a widely used

model around the world and has been used extensively for water quality studies. Its applicability to modelling in-stream sediments, or nitrogen or phosphorus compounds is well studied, and scenario analyses are commonly applied in order to quantify possible changes in future water quality (e.g. Malago et al., 2017; Nguyen et al., 2017; Shrestha et al., 2018; Worku et al., 2017; Yang et al., 2014; Zeiger and Hubbart, 2016). For example, Nguyen et al. (2017) used SWAT to model streamflow, nitrate and phosphate loadings into an Australian reservoir, and received satisfactory calibration results, after which they assessed the impacts of scenarios related to climate change, land use, and management practices on water quality. Research conducted by Worku et al. (2017) focused on using SWAT to quantify effects of land use and land cover changes on increased surface runoff and erosion in Ethiopia. In another study, Wei et al. (2018) successfully coupled SWAT with a numerical groundwater model to quantify nitrate concentrations based on nonpoint-source loadings in surface water and leaching into groundwater of an Oregon watershed. The need for a better understanding of interactions between natural factors such as climatic change, human activity and hydrology, as well as models that can better simulate nutrient cycling processes (e.g. concentration and loading from/to groundwater and streams at the watershed scale) was well documented within the aforementioned studies.

Despite numerous SWAT water quality models, the representation of organic carbon (OC) processes in the soil-plant-water continuum within SWAT are simplified. Modelling OC at watershed scale is not only important for understanding regional carbon cycling, but also useful for water quality management in streams and other water bodies. Currently, OC modelling in SWAT is limited to simulation of the soil OC cycle, where it is closely related to processes and relative amounts of nitrogen and phosphorus (Neitsch et al., 2011). To overcome this limitation,

Oeurng et al. (2011) established a strong relationship between lab measurements of suspended sediments and particulate organic carbon (POC), and used calibrated sediment values within the model to predict POC yields in a watershed. In another study, Yang et al. (2016) examined SWAT for simulating the net ecosystem exchange of carbon between the land and atmosphere at ten sites in the U.S.A. and increased model accuracy through the improvement of parameterization and representation of phosphorus cycling, reinforcing the important relationship of OC with other nutrients. Zhang et al. (2013) revised the soil OC CENTURY model, originally developed by Parton et al. (1994), and incorporated it as a new module called SWAT-C. This module improved simulation of soil organic matter residue processes such as decomposition and land-atmosphere carbon exchanges, thereby expanding the applicability of the model to climate change, and carbon sequestration and emission studies. The use of SWAT-C by Zhang (2018) for the simulation of sediment and eroded carbon yields captured long-term trends, despite errors for individual years.

Other researchers have endeavored to model OC at the watershed scale. For example, Lessels et al. (2015) developed a parsimonious watershed DOC model which they coupled with the Hydrologiska Byråns Vattenbalansavdelning (HBV) rainfall-runoff model. However, the soil organic carbon (SOC) cycle was not simulated dynamically, and therefore does not account for temporal changes, such as the addition of OC from plant residue. Additionally, in-stream OC processes were not included in the model. In another study, Futter et al. (2007) developed a watershed scale DOC model called Integrated Catchments Model for Carbon (INCA-C), which simulates both SOC and in-stream DOC processes. However, the in-stream processes only considered the transformation between DOC and dissolved inorganic carbon, and the SOC processes were simulated based on a conceptual model instead of a process-based model. The

INCA-C also does not account for export of OC in suspended sediments. Finally, the Regional Hydro-Ecological Simulation System (RHESSys) model developed by Tague and Band (2004) is capable of simulating carbon fluxes at the watershed scale and includes comprehensive terrestrial plant and soil processes related to carbon and nitrogen cycling. However, the in-stream processes were only explicitly developed for nitrogen, and therefore this module is not applicable to in-stream OC studies. A recent study by Fabre et al. (2019) used SWAT model to simulate DOC and POC loads in Yenisei River basin drained by the Arctic Ocean but the organic carbon modules they used were based on the empirical regression models based on streamflow and sediment concentration.

While there have been significant advances in modelling carbon cycling, the studies described above lack the integration of terrestrial and aquatic processes related to OC cycling. Therefore, this study aimed to develop a new and applicable module for integrated simulation of soil carbon processes and in-stream OC processes within SWAT for modelling upstream to downstream OC loads, dynamics, and transport at the watershed scale. Generally, the goals of this study were twofold. First, we incorporated a process-based parsimonious in-stream OC module by modifying its source code to simulate OC loads and transport at the watershed scale. Secondly, we applied the module to the Elbow River (ER) watershed in Alberta, Canada to verify the model performance for simulating total organic carbon (TOC) loads and transport at a regional scale, and provided a calibrated modelling tool for predicting future OC loadings under the influences of climate change and extreme events. Long-term water quality data sets and dependency on this watershed for drinking water made it an ideal study area for our new methodology. The OC module can contribute to a better understanding of the complex relations between climate, extreme events, OC loading and transport to/from streams within watersheds.

2.2 Materials and Methods

2.2.1 Study area

The hydrology of the Elbow River (ER) watershed is complex due to its diverse landscapes, variable climate and a large elevation range (1040–3200 m), among other factors (Fig. 2.1). This watershed is considered semi-arid, as total rainfall is less than potential evapotranspiration due to its location in the rain shadow of the Rocky Mountains of southern Alberta. As the river flows east, it traverses forested foothills, which make way for more gently sloping grasslands and agriculture. The river then enters urban developments and flows into the Glenmore reservoir in the east of the study area, which supplies approximately 40% of the city of Calgary (half a million people) with drinking water (Valeo et al., 2007), and marks the end of the 1200 km^2 study area (Fig. 2.1). Downstream from the Glenmore dam in downtown Calgary, the ER merges with the larger Bow River, which is a major tributary of the South Saskatchewan River system draining the southern portion of the province of Alberta. Streamflow in the ER is primarily sourced from precipitation and snowmelt in the Rocky Mountains, and groundwater is the main contributor to baseflow, and therefore both climate and land characteristics play significant roles in controlling drainage patterns (Farjad et al., 2016; Farjad et al., 2017; Wijesekara et al., 2012; Wijesekara et al., 2014). Over the last 30 years, average annual precipitation was 608 mm, and the average air temperature was approximately 2.1°C, according to climate data from Alberta Environment and Parks (Table S1). From the western mountains to the eastern plains, annual precipitation generally decreases while average temperatures increase. According to Environment Canada (Table S1), the average streamflow at the watershed outlet from 1986–2015 was 8.8 m^3/s, with June peak flows averaging 30.7 m^3/s and coinciding with both peak rainfall and mountain snowmelt, and January-March baseflow averaged 2.4 m^3/s.

Average annual streamflow exhibited a generally increasing trend over the 1986–2015 period, which contrasts near-mountain gauges of surrounding watersheds in recent decades, including the Bow River (Rood et al., 2005).

In a previous study of the ER watershed, Sosiak and Dixon (2006) analyzed spatial patterns of water quality constituents from 1999–2002. Total suspended solid (TSS) concentrations were found to increase from upstream to downstream, with the highest values near the inlet to the Glenmore Reservoir, and the seasonality of TSS coinciding with streamflow. Suspended solids were defined as residue that had been filtered out, primarily made of soil particles in addition to chemical or biochemical precipitates. Similar to TSS, TOC concentrations increased slightly from upstream to downstream, and peak values coincided with spring runoff and snowmelt. It is also notable that based on thorough water quality monitoring by the City of Calgary, DOC concentrations in the ER watershed have been steadily increasing over the last two decades. The Alberta government and its municipalities follow Health Canada's (2017) drinking water standards (Alberta Environment and Parks, 2012), and the water authorities in Calgary have expressed concern about water treatment if a sharp increase in DOC were to occur (Sosiak and Dixon, 2006). Heavy rainfall events can contribute up to 36–50% of DOC in tributaries of the South Saskatchewan River (Rostami et al., 2018). Therefore, modelling and predicting OC yields is a critical step in understanding the future of water supply.

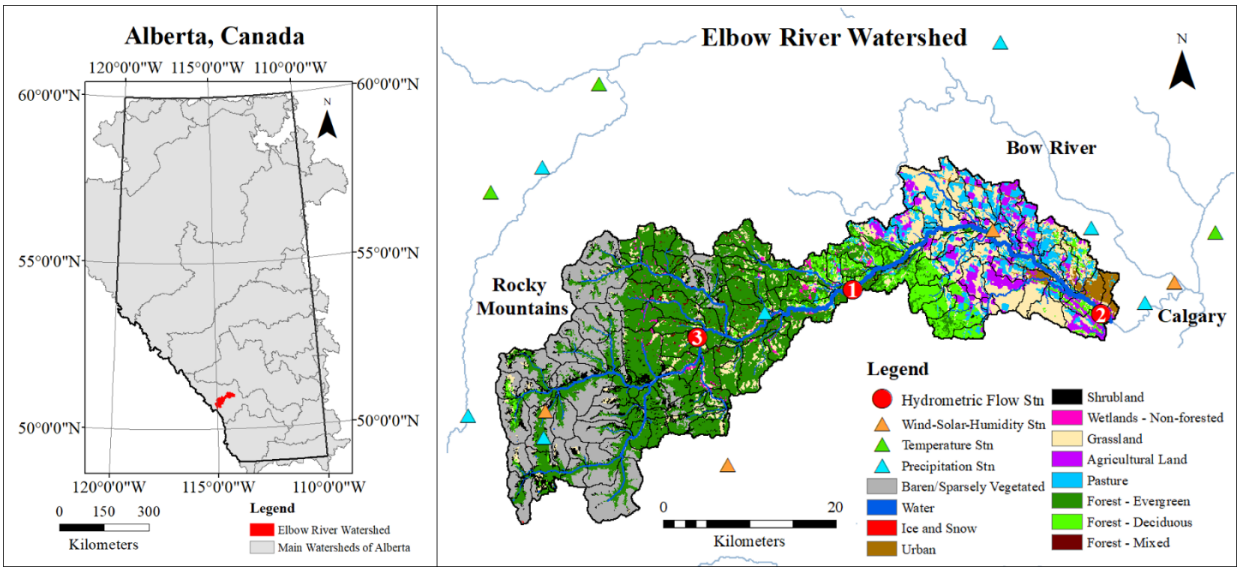

Fig. 2.1. Location of Elbow River Watershed in Alberta, Canada; land use, subbasins (outlined in black) and observation stations of Elbow River Watershed. The hydrometric flow and water quality stations in the map: 1. Bragg Creek; 2. Sarcee Bridge; 3. Elbow Falls; station 2 drains into the Glenmore reservoir of Calgary.

2.2.2 Hydrology and sediment simulation in SWAT model

The Soil and Water Assessment Tool (SWAT) model is a widely used hydrology and water quality model that is used for predicting and assessing environmental impacts of land use change, land management practices, and climate change. Using a digital elevation model (DEM), the model delineates a watershed and divides the watershed into smaller subbasins. The model simulates both landscape processes and water routing in aquatic systems (e.g., streams and reservoirs) at daily time steps within each Hydrologic Response Unit (HRU), which are subdivisions of subbasins. For each time step, the water yield is calculated as the summation of three components simulated in each HRU, including surface runoff, lateral flow (i.e., subsurface runoff) and groundwater discharge to the stream. Water routing through the channel network is simulated based on the Muskingum routing method or variable storage routing methods, in which each reach segment receives inflow and then outflow is calculated. Soil erosion and sediment yield for each HRU are simulated using Modified Universal Soil Loss Equation

(MUSLE), and there are different model options for sediment routing in the channel that simulate sediment transport by calculating both sediment deposition and degradation. For OC processes, SWAT estimates the loads from each HRU transported by soil erosion and water yield components, after which transport, transformation and reactions of chemicals in the stream and streambed through the channel network are not simulated (see section 2.3.3). A more detailed description of SWAT model processes is available from Neitsch et al. (2011).

2.2.3 Organic carbon simulation module in SWAT

Currently, OC modelling in SWAT is limited to simulation of the soil carbon cycle, which does not allow for studying watershed scale organic carbon dynamics, as in-stream OC processes are not simulated. Therefore, we developed a parsimonious organic carbon module to simulate in-stream DOC and POC processes and linked it with the existing SWAT soil carbon module. The major model processes of the developed module can be found in Fig. 2.2.

Presently, there are three options for simulating the soil organic carbon (SOC) cycle in the release version of SWAT, which can be defined using the variable 'cswat' in the 'basin.bsn' file. The first one uses the static SOC content defined by the soil input database. The second uses one multi-layer, one-pool SOC algorithm to model SOC dynamics (Kemanian et al., 2011). The third one (SWAT-C) is the most comprehensive SOC model in SWAT, which combines the CENTURY soil organic matter (SOM) residue algorithm and the modifications in EPIC to simulate SOM residue dynamics (Zhang et al., 2013). In addition, SWAT-C simulates the movement of SOC with water flux in the soil, and loss of POC through soil erosion. Specifically, it calculates the DOC and POC loss from the top soil layer transported by surface runoff and erosion to the stream, and DOC loss from each soil layer transported by lateral flow to the stream. However, it does not simulate the DOC loading transported by groundwater flow to the

stream, nor in-stream processes. In this study, we used SWAT-C to model SOC cycle in the soil layers and the amount of DOC and POC lost from the soil column. To account for DOC load contributions from groundwater, we added the processes using similar approach to those used for calculating dissolved phosphorus load by transported groundwater flow in each HRU and each time step in SWAT (Neitsch et al., 2011):

$$DOC_{gw} = con_{doc,gw} \cdot Q_{gw} \cdot 10^{-2} \qquad (1)$$

where DOC_{gw} is DOC load (kg/ha) transported by groundwater flow, $con_{doc,gw}$ is the DOC concentration in groundwater (mg/L), which is adjusted in calibration, and Q_{gw} is groundwater flow (mm) simulated by SWA

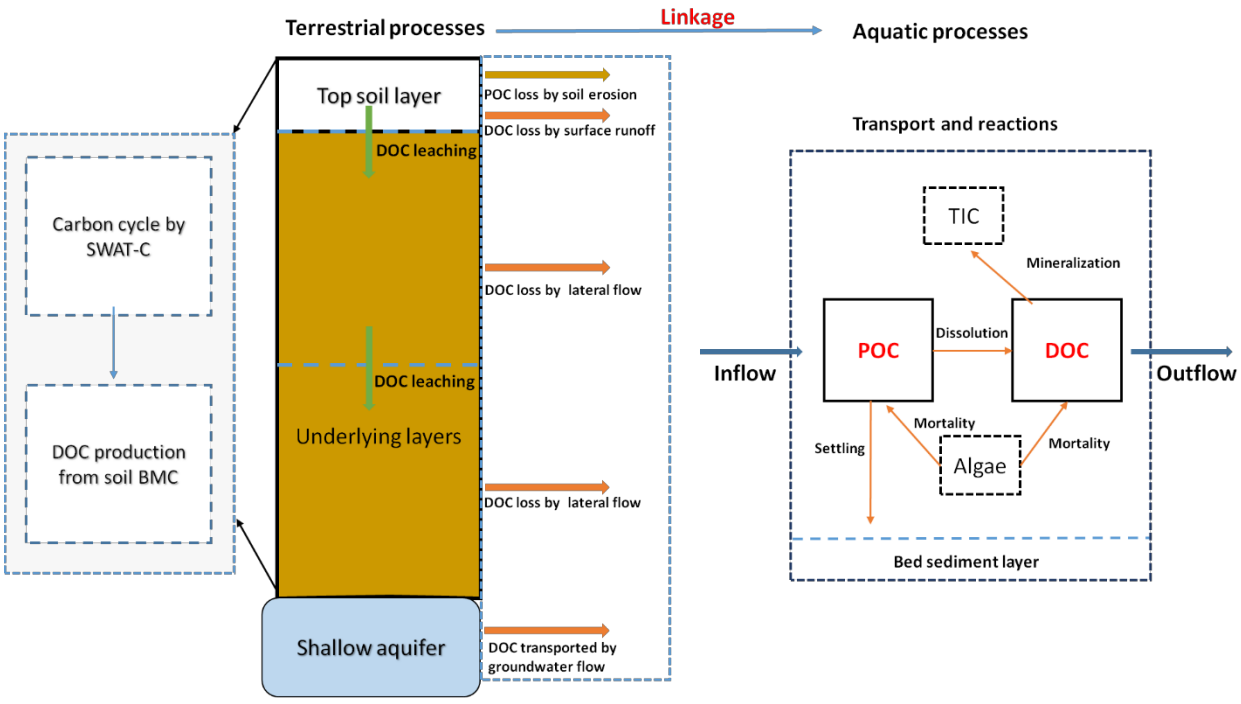

Fig. 2.2. Model processes for SWAT organic carbon simulation module: (a) pre-existing module in SWAT for simulation of landscape processes, (b) in-stream processes developed and linked to the landscape processes in this study.

In order to model the OC load by considering the full spectrum of processes from landscapes to stream networks at the watershed scale, the aforementioned SOC cycling and

transport process was linked with a process-based in-stream OC simulation module. In-stream OC processes with two state variables (POC and DOC) are modeled in the water column (Fig.2). POC represents non-living particulate detrital carbon. The DOC is simply the dissolved portion of TOC rather than the portion of OC in suspension. The in-stream OC module receives inputs (DOC and POC loadings) from the soil carbon module and simulates the transport and transformations of DOC and POC in the stream network. A main channel unit within the subbasin receives OC loadings from inflow, including loadings from local subbasin and upstream channels, and calculates the organic carbon transformations (or reactions) before routing the loadings via outflow to the downstream channel unit. Therefore, the module can output DOC, POC and TOC loads and concentrations for each main channel unit of SWAT at a daily time step. The in-stream DOC and POC processes were incorporated into subroutine 'watqual.f' of SWAT code version 664, which simulates the in-stream nutrient processes. In addition, other 12 subroutines were also modified for the OC module, in which new variables were defined and added within the source code, in order to obtain output data at the HRU and subbasin levels pertaining to OC.

The reactions simulated in the in-stream module include transformations between different carbon species (DOC, POC and inorganic carbon) and the interactions between OC, floating algae, and bed sediment. For in-stream POC reactions, the POC amount increases from algal death and decreases by dissolution of POC to DOC, and settling to the bed sediment (Porcal et al., 2015; Worrall and Moody, 2014). The change in POC concentration for a given day is calculated as follows:

$$\Delta POC = \left(f_{poc} \cdot \alpha_{ca} \cdot \rho_a \cdot algae - k_{poc} \cdot POC - \frac{V_{set}}{h} \cdot POC\right) \cdot TT \qquad (2)$$

where *POC* is POC concentration in the stream (mg/L), f_{poc} is the fraction of algal death to POC, α_{ca} is the carbon to algae biomass ratio, ρ_a is the local death rate of algae (day^{-1}), *algae* is the algal biomass concentration of the day (mg/L) simulated by the existing in-stream water quality module, k_{poc} is the POC dissolution rate to DOC (day^{-1}), V_{set} is the POC settling velocity to river bed (m/d), h is the water depth simulated by SWAT routing module (m), and *TT* is flow travel time in the reach segment (day), which is calculated by the SWAT routing module. The parameters that can be adjusted for calibration are k_{poc} and V_{set} for POC in-stream processes.

For in-stream DOC reactions, DOC amount may be increased through algal death and POC dissolution, and decreased by DOC oxidation to dissolved inorganic carbon (DIC) (Porcal et al., 2015; Worrall and Moody, 2014). The change in DOC concentration for a given day is determined by the following equation:

$$\Delta DOC = \left[\left(1 - f_{poc}\right) \cdot \alpha_{ca} \cdot \rho_a \cdot algae + k_{poc} \cdot POC - k_{doc} \cdot DOC\right] \cdot TT \quad (3)$$

where *DOC* is DOC concentration in the stream (mg/L), k_{doc} is the DOC mineralization rate to DIC (day^{-1}) subject to model calibration, and all other variables are defined in Eq. (2). Overall, there are 7 OC related parameters (see Table 4) needed to be calibrated based on the observed data. In addition, the algae death rate, POC dissolution rate and DOC mineralization rate are defined as the rate at 20 ℃ and are adjusted to the local stream temperature simulated by SWAT using the following relationship:

$$k(T) = k(20) \cdot \theta^{Tw-20} \quad (4)$$

where *k(T)* is the reaction rate at local temperature, *k(20)* is the defined reaction rate at 20 ℃, θ is the temperature correction coefficient and T_w is the stream temperature simulated by SWAT.

2.2.4 SWAT model setup

The 1200 km^2 Elbow River watershed was delineated in SWAT based on a digital elevation model with a resolution of 30 m and separated into 154 subbasins (Fig. 2.1). Next, 373 Hydrologic Response Units (HRUs) were defined based on unique combinations of land use, soil type and slope class in each subbasin. Within each HRU, all hydrological, plant, and soil processes occur homogeneously. The addition of daily climate data between 1980 and 2017, which includes temperature and precipitation, relative humidity, wind speed, and solar radiation, has the model ready to run a simulation and generate monthly output data on HRU, subbasin, and watershed scales. All data used in this study are listed in Appendix A.1. In order to establish baseline watershed conditions and minimize the impacts of initial conditions on model simulations, we used a three-year warm up period.

2.2.5 Model calibration and validation

The Sequential Uncertainty Fitting (SUFI-2) algorithm (Abbaspour et al., 2007; Faramarzi et al., 2009), in combination with a parallel processing scheme, was used for model calibration and validation of streamflow, sediment, and TOC loads. For a cost effective calibration, we used a similar approach as Gorgan et al. (2012) and developed a parallel processing program (PP-program) to calibrate and validate our multi-variable SWAT model using a 200-core windows-based computer. We parallelized swat simulation runs on 200 independent cores to reduce calibration-processing time. Prior to calibration, both one-at-a-time and global sensitivity analyses were performed to identify the most important parameters for calibration purposes (Faramarzi et al., 2009; Faramarzi et al., 2017). We then set an initial range for each sensitive parameter based on literature values and our earlier studies. Input parameter ranges were sampled using Latin Hypercube Sampling technique (Ficklin et al., 2013) to create

500 samples of parameter sets. Each parameter set was fed into the SWAT model to generate output variables from SWAT for comparison with measured data using SUFI-2. If the comparison results were not successful, a new iteration was performed and the procedure continued until satisfactory results were reached or no further improvements were obtained. In this study, we used the Nash-Sutcliffe efficiency (NSE) as an objective function, and also considered the coefficient of determination (R^2) and percent bias (PBIAS) as performance measures. Previous studies have demonstrated that there are trade-offs between different model performance measures in the context of multi-objective calibration (Confesor et. al., 2007), since different measures tend to capture distinct aspects of model performances (Du et al., 2019b). Therefore, we considered the trade-offs of the three performance measures and aimed for an overall balance in calibration results. In addition, we also qualitatively assessed the model outputs based on the criteria for watershed model performances summarized by Moriasi et al. (2007; 2015), which evaluate performance from 'unsatisfactory' to 'very good' based on the range of values of measures statistics. In addition, Moriasi et al. (2015) also summarized and defined performance measure values as being 'unacceptable'. Specifically, $R^2 < 0.18$, NSE < 0.0, PBIAS $\geq \pm 30\%$ for flow, PBIAS $\geq \pm 55\%$ for sediment and PBIAS $\geq \pm 70\%$ for nutrients represent 'unacceptable' model performance. In this study, we tried to get 'acceptable' model performances based on NSE, R^2 and PBIAS and above-mentioned thresholds.

Due to the heterogeneous nature of this watershed, streamflow was calibrated individually for two areas draining into hydrometric stations (Bragg Creek and Sarcee Bridge, Fig. 2.1) for the period of 2000-2015. For this purpose, we used a parameter regionalization approach developed by Faramarzi et al. (2009). The calibrated parameters were then used to validate the model for the 1999-1986 period, in addition to the Elbow Falls station, which was

operational until 1995. Water quality parameters (i.e., sediments and TOC) were then calibrated based on measurements obtained by the City of Calgary through grab samples located near the Bragg Creek and Sarcee Bridge hydrometric stations. The trends of both TSS and TOC concentrations from 2001 to 2015 closely followed streamflow trends, demonstrating the strong relationship between water quantity and quality. Earlier attempts for sediment load calibration were unsuccessful due to variability within the watershed, and the high sensitivity of the channel sediment parameters, which are uniform within the entire watershed. Other studies (e.g., Du et al. 2019; Zabaleta et al. 2014) have also demonstrated that sediment routing parameters in the channel are more influential than upland soil erosion parameters in controlling watershed sediment loads. Therefore, we modified the SWAT code so that the channel sediment parameters could be adjusted by subbasin rather than being uniform. Since many water quality measurements are periodic, many studies have applied the Load Estimator (LOADEST) software developed by USGS (Runkel et al., 2004) to estimate monthly sediment and pollutant loads based on measured streamflow of the concentration sampling dates, and these values were then used for model calibration and validation (e.g., Krishnan et al., 2018; Niraula et al., 2013). Therefore, we used the same approach, in which we calibrated the ER watershed SWAT model to LOADEST estimates of monthly sediment and TOC loads, using a calibration period of 7 years (2001–2007) and a validation period of 8 years (2008–2015). We used the Maximum Likelihood Estimation (MLE) method for estimating loads, as the in-stream sediment and TOC concentrations were uncensored; in other words, measurements below detection limit were not included. The MLE method assumes that model residuals are normally distributed and have constant variance.

2.3 Results and Discussion

2.3.1 Hydrological calibration and streamflow simulation

Monthly streamflow simulations were calibrated to measured volumetric stream discharge at two hydrometric stations from 2000–2015 with the NSE as the objective function (Fig. 2.3), and was validated using three hydrometric stations from 1986–1999, one of which stopped operating after 1995 (Table 2.1, Fig. 2.1). A total of 87 parameters were used for streamflow calibration in three subbasin groups that drained into the different hydrometric flow stations, (i.e., 31 parameters for western subbasins into the Elbow Falls station, 27 parameters for central subbasins into the Bragg Creek station, and 28 parameters for the easternmost subbasins into the Sarcee Bridge station). Our one-at-a-time and global sensitivity analysis indicated that streamflow was typically the most sensitive to channel parameters (Appendix A.2), including Manning's "n" value for the main channel (CH_N2.rte), effective hydraulic conductivity of the main channel alluvium (CH_K2.rte), and bank storage factor (ALPHA_BNK.rte). This supports findings of previous studies, in which Wijesekara et al. (2012; 2014) state that complex surface-groundwater interactions are prominent in the ER watershed. Other sensitive parameters included the adjustment of temperature with elevation in the western mountainous region (TLAPS.sub), and the average slope length (SLSUBBSN.hru). The top 10 sensitive parameters and their locations within the watershed are listed in Appendix A.2. Not surprisingly, four of the ten most sensitive parameters were for the headwater region draining into the Elbow Falls station (Fig. 2.1). Monthly hydrographs for the calibration period demonstrate that the model effectively captured the seasonality of streamflow, although flashiness was underestimated for all years in the final calibration (Fig. 2.4). The final NSE values for Bragg Creek and Sarcee Bridge stations were 0.62 and 0.60, respectively (Table 2.1). During initial calibration, peak flows were well-

represented, but overall water balance was significantly overestimated according to the PBIAS values which were greater than 30%. In order to bring the PBIAS to an acceptable level, the trade-off was underestimation of spring peak flows (Fig. 2.1, Table 2.1). According to Faramarzi et al. (2015), the largest sources of error in physical and process-based modelling are related to input data, misrepresentation of processes, and oversimplification. Flashiness and peak flow rates in the spring (e.g., the 2005 flood caused by heavy rains and the 2013 flood caused by a rain-on-snow event) were significantly underestimated. This may be attributed to the lack of climate data after 2008 for certain climate stations, as well as SWAT's misrepresentation of insulation provided by snow cover for a large part of the year as described by Qi et al. (2016; 2017). Winter streamflow may also be misrepresented due to partial or complete freezing of the top layer of the stream. Additionally, the lack of climate stations within the boundaries of the study area may also have contributed to underestimation of streamflow during these years, as mountainous regions are prone to spatially variable precipitation and temperature (Fig. 2.1). In spite of these potential sources of error, a visual form of performance assessment demonstrated correlation of the timing and seasonality of base and peak flows (Fig. 2.4), which is important to consider in conjunction with statistical measures (Krause et al., 2005).

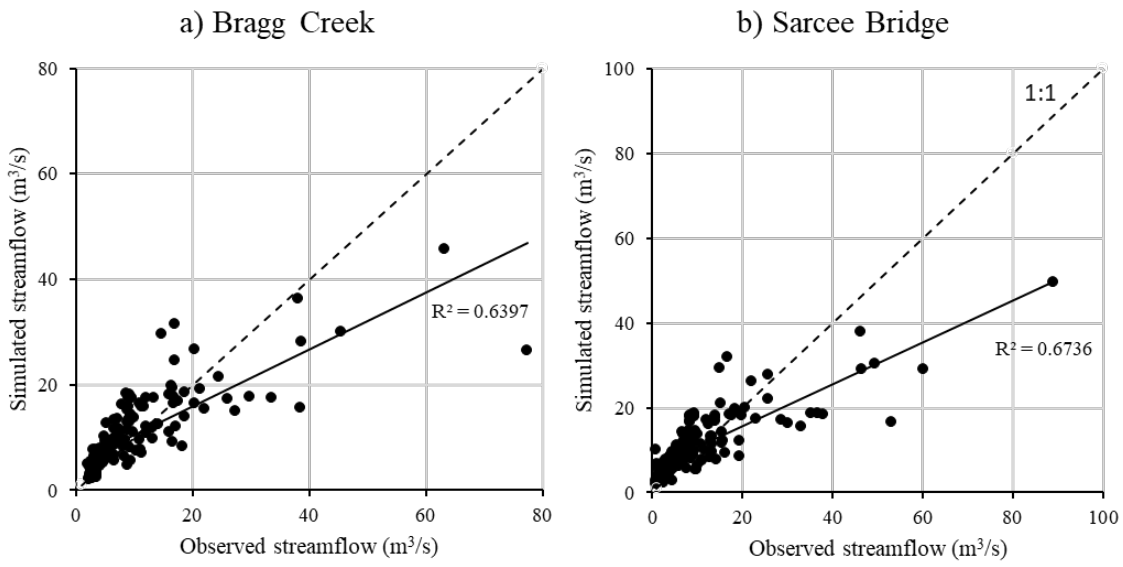

Fig. 2.3. Scatter plot of monthly streamflow simulation results for a) Bragg Creek, and b) Sarcee Bridge (watershed outlet).

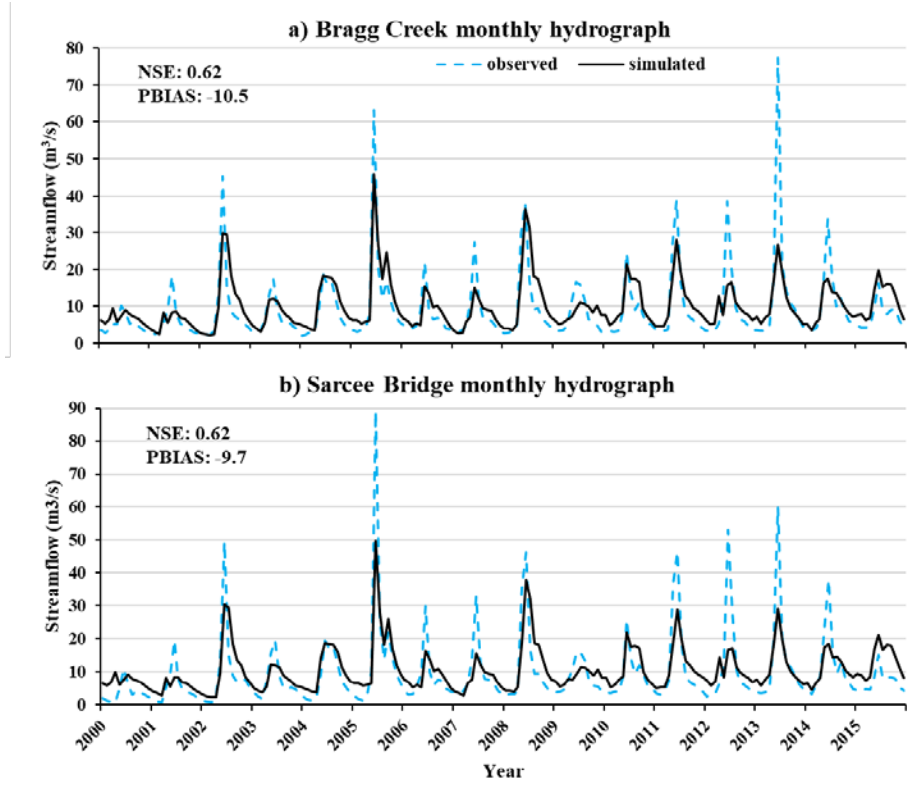

Fig. 2.4. Monthly average hydrographs: a) Bragg Creek; b) Sarcee Bridge (watershed outlet).

Table 2.1. Monthly streamflow calibration and validation statistics; Elbow Falls operational from 1986–1995; Bragg Creek and Sarcee Bridge operational from 1986–2015.

Stations	Calibration (2000–2015)			Validation (1986-1999)			All (1986–2015)		
	NSE	R^2	*PBIAS*	*NSE*	R^2	*PBIAS*	*NSE*	R^2	*PBIAS*
Elbow Falls	-	-	-	0.62	0.62	-0.3	0.62	0.62	-0.3
Bragg Creek	0.62	0.64	-10.5	0.75	0.73	-9.3	0.66	0.68	-9.9
Sarcee Bridge	0.62	0.67	-9.7	0.70	0.70	-13.3	0.63	0.68	-11.2

2.3.2 Sediment load simulation

Following streamflow, the sediment load was calibrated (2001–2007) and validated (2008–2015) using the estimated monthly sediment loads of the two stations (Fig. 2.5 and Fig. 2.6). Similar to streamflow, sediment channel routing parameters (PRF, SPCON and SPEXP) were among the most sensitive during model calibration as compared to parameters related to soil erosion in the landscape HRU units (Table S3), mirroring the findings of other studies (Du et al. 2019; Zabaleta et al. 2014). These three parameters determined the sediment mass balance in the channel by impacting sediment deposition and re-suspension, and results were improved by modifying these parameters by subbasin rather than having them be uniform throughout the watershed. Table 2 outlines the model performance statistics for periodic monthly sediment load simulations of the two stations. We assessed model performances of sediment load simulation based on the evaluation criteria suggested by Moriasi et al. (2007; 2015). The final PBIAS values of sediment simulations during the whole simulation period (Fig. 2.5) were all assessed as 'satisfactory' (within ±20%) according to the criteria, indicating that there are no systematic errors and the magnitudes of sediment loads are captured. For the NSE and R^2, performances for Bragg Creek station during calibration period were assessed as 'satisfactory' and 'very good',

respectively and performances for Sarcee Bridge station during calibration period were assessed as 'satisfactory' and 'good', respectively. However, NSE and R^2 values for two stations during validation period were assessed as 'unsatisfactory' based on the criteria but were 'acceptable' according to the recommended thresholds (R^2>0.18 and NSE >0.0), where monthly and seasonal trends are still captured. Nonetheless, some literature suggests that NSE values could be as low as 0.2 for a 'satisfactory' model performance (Tuppad et al., 2011; Ni et al., 2018). Comparisons of simulated and observed monthly sediment loads for the two stations showed satisfactory correlation (Fig. 2.5), and the model was also able to capture seasonal and monthly variations in the correct order of magnitude (Fig. 2.6). A lower performance for sediment load simulation was expected since there are more uncertainties for simulating soil erosion and sediment transport processes in SWAT compared to streamflow simulation (Chen et al., 2017). In addition, in-stream TSS measurements were taken at inconsistent intervals, and any uncertainties from hydrological simulation would have propagated into sediment simulation.

Table 2.2. Monthly sediment load calibration and validation statistics.

Stations	Calibration (2001–2007)			Validation (2008–2015)		
	NSE	R^2	*PBIAS*	*NSE*	R^2	*PBIAS*
Bragg Creek	0.47	0.88	-1.3	0.21	0.27	-95.7
Sarcee Bridge	0.55	0.79	-43.8	0.13	0.29	26.3

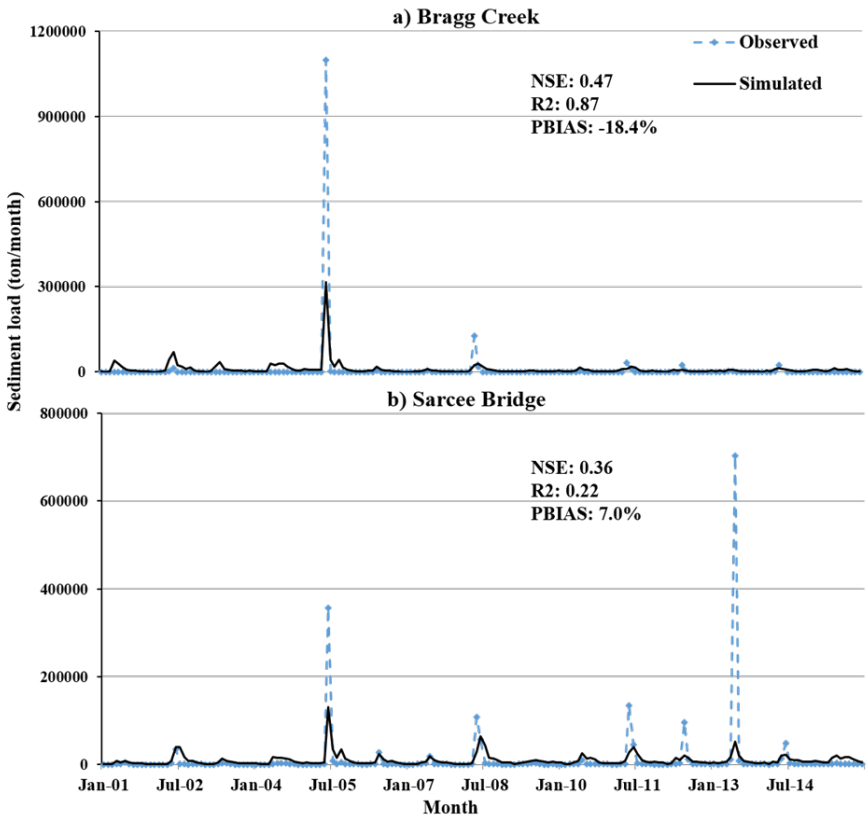

Fig. 2.5. Monthly Sediment load simulations with model performance statistics for the whole simulation period (2001–2015): a) Bragg Creek; b) Sarcee Bridge.

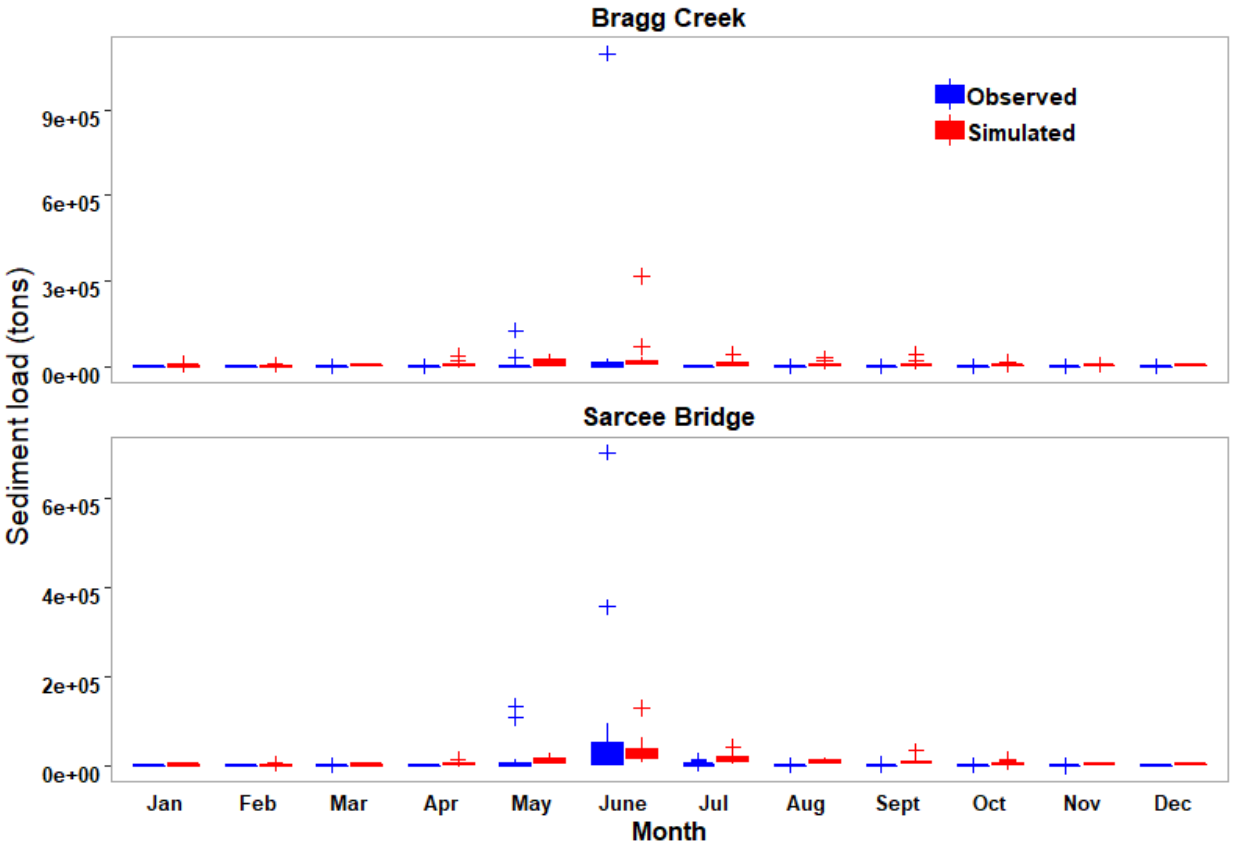

Fig. 2.6. Boxplots of observed and simulated sediment loads for 2001–2015 period at monthly scale: a) Bragg Creek; b) Sarcee Bridge.

2.3.3 Organic carbon simulation in Elbow river watershed

The developed OC module was calibrated and validated using the estimated monthly TOC loads of the two stations and the best parameters obtained from previous streamflow and sediment calibration (Section 2.4.1, and 2.4.2). The calibrated organic carbon parameters for the two stations with their ranges are listed in Table 2.4. Of the seven total parameters for TOC calibration, four are HRU scale parameters, which control the amounts of OC transported from soil to the stream. The remaining three parameters are reach scale parameters for in-stream OC reaction rates. In this study, the performance evaluation criteria for monthly nitrogen and

phosphorus simulations suggested by Moriasi et al. (2015) were used as reference to assess the simulation performances of monthly TOC loads. For the whole simulation period (Fig. 2.6), the performances for monthly TOC loads at Bragg Creek were assessed as 'good' based on NSE, R^2 values and PBIAS value (NSE>0.5, R^2>0.6, PBIAS<±20) and 'very good' for Sarcee Bridge Station (NSE>0.65, R^2>0.7, PBIAS<±15). For the calibration period, all six performance measures of the two stations in Table 2.3 are assessed as 'very good'. For the validation period of Bragg Creek Station, model performance was assessed as 'good' based on NSE and 'satisfactory' based on R^2 and PBIAS. For validation period of Sarcee Bridge Station, model performance was assessed as 'very' good based on NSE and PBIAS and 'good' based on R^2. Therefore, the performance for monthly TOC loads simulations in the ER watershed by the developed module are assessed as 'good' overall. Based on the visual comparisons of simulated and observed monthly TOC loads (Fig. 2.7), the TOC loads were acceptable as they follow a similar temporal trend as the observed data. However, some peak loads during high summer flows were underestimated, which was partially caused by the underestimation of peak streamflow and sediment loads, since flow and sediment processes control the transport of OC in the watershed. The underestimation of peaks can also be attributed to the uncertainties of input data and model structure. As was mentioned previously, the quality of input data, especially the temporal and spatial resolution of the precipitation and temperature data, has substantial impacts on the simulations of peak storm events. Since SWAT is a continuous model that uses a daily time step, it tends to underestimate the peak streamflow, sediment, and chemical loads for days having short intense storm events (e.g., Asadzadeh et al., 2016; Du et al., 2019b, Qiu and Wang, 2014; Zeiger and Hubbart, 2016). This leads to model uncertainties, as short intense storm events are prominent in the ER watershed during summer months (Appendix A.1). The boxplots of

observed and simulated monthly TOC loads during the simulation period (Fig. 2.8) indicate that the long term monthly and seasonal variations in TOC load were successfully captured in the correct order of magnitude, much like the sediment simulation.

Table 2.3. Monthly TOC loads calibration and validation statistics.

Stations	Calibration (2001–2007)			Validation (2008–2015)		
	NSE	R^2	*PBIAS*	*NSE*	R^2	*PBIAS*
Bragg Creek	0.71	0.71	-4.8	0.57	0.58	-27.1
Sarcee Bridge	0.74	0.82	-0.2	0.66	0.66	-9.7

Table 2.4. Model parameters for TOC loads with the ranges and calibrated values

Name	Scale	Description	Unit	Range	Calibrated value	
					Bragg Creek	Sarcee Bridge
enr_poc	HRU	POC enrichment ratio	none	0-5	1.93	1.00
perco_doc	HRU	DOC percolation coefficient for top soil layer	none	0-1	0.98	0.19
$con_{doc,gw}$	HRU	DOC concentration in groundwater flow	mg/L	0-5	0.6	2.6
kd_oc	HRU	Organic carbon partition coefficient for DOC production	none	500-1500	1379.8	499.0
kpoc	Reach	POC dissolution rate to DOC	/day	0.001-0.2	0.15	0.17
V_{set}	Reach	POC settling rate	m/day	0-5	4.52	3.05
k_{doc}	Reach	DOC mineralization rate	/day	0.01-0.2	0.05	0.11

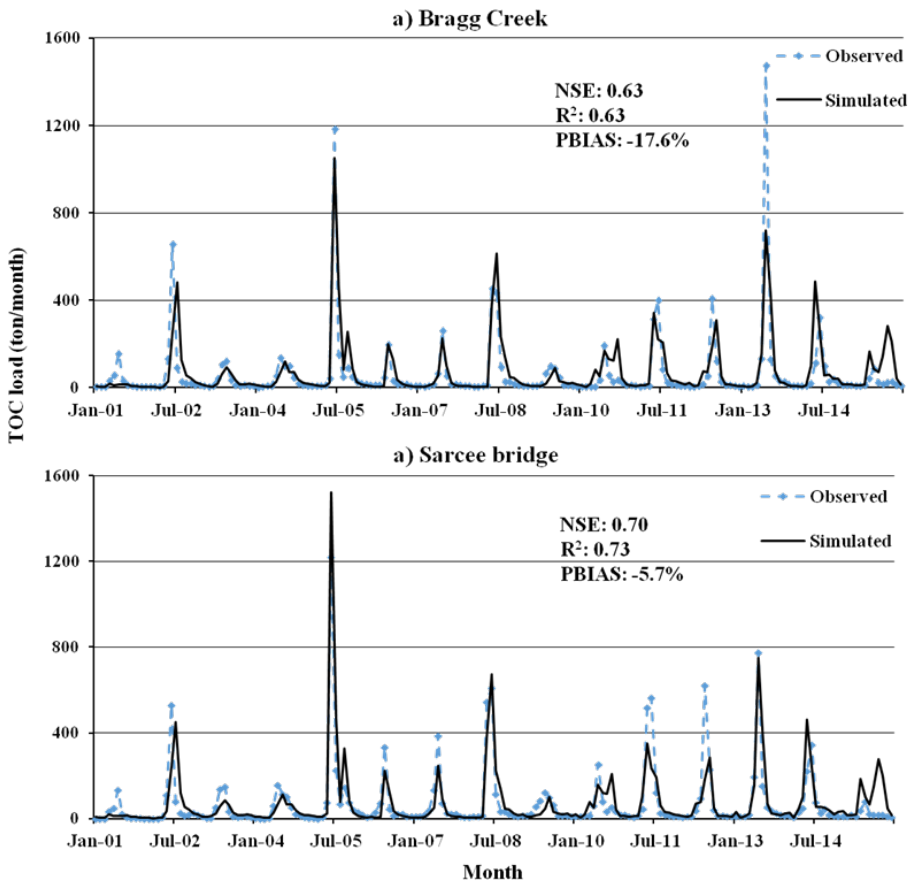

Fig. 2.7. Monthly TOC load simulation results with model performance statistics for the whole simulation period (2001–2015): a) Bragg Creek; b) Sarcee Bridge.

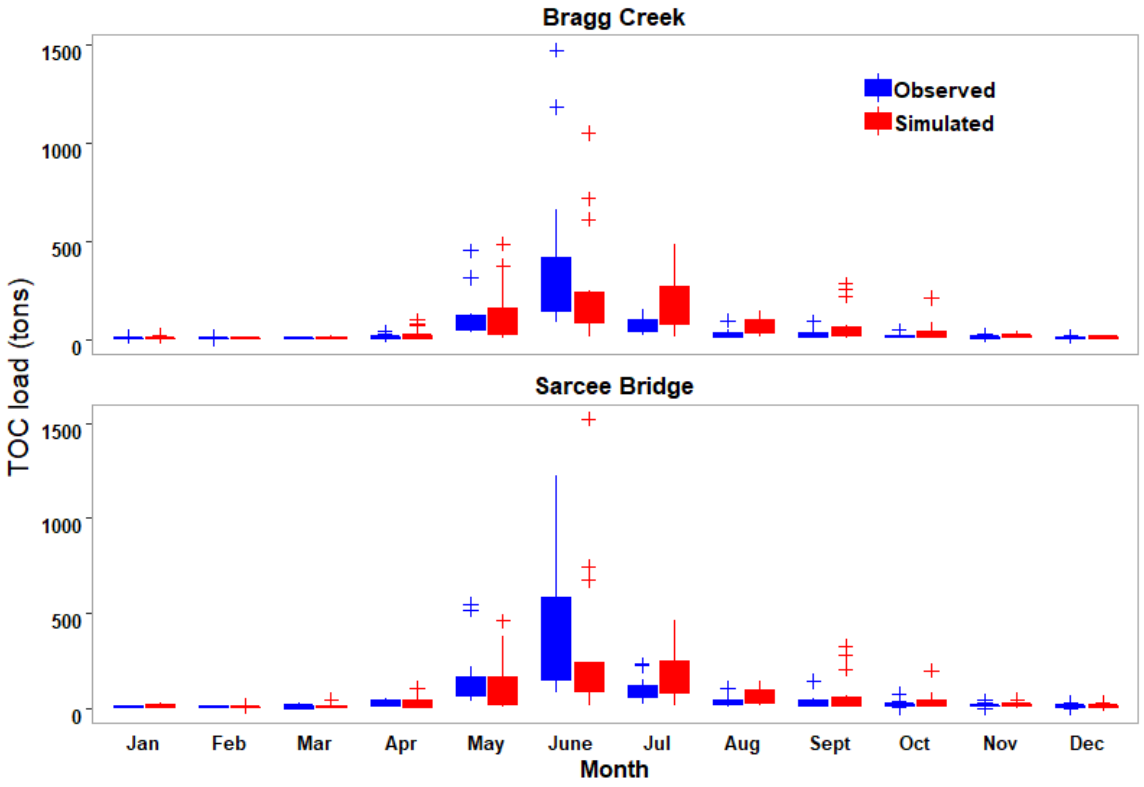

Fig. 2.8. Boxplots of observed and simulated TOC loads at monthly scale for the 2001–2015 period: a) Bragg Creek; b) Sarcee Bridge.

2.3.4 Application of model for identifying key processes controlling TOC dynamics and comparing with other studies

To identify the key processes controlling TOC dynamics, parameter sensitivity was conducted using the global sensitivity approach (Faramarzi et al., 2009). The two most sensitive parameters for the area draining into Bragg Creek station were *kd_oc* and V_{set}, which control the DOC production in the soil layers and POC settling from the water column to riverbed in the reach, respectively (Table 2.5). As for Sarcee Bridge, the most sensitive parameters were *kd_oc*, followed by *enr_poc,* and V_{set}; the *enr_poc* parameter controls the amount of POC transported by soil erosion from the top soil layer to the stream. Parameter sensitivities indicated that the DOC production in the soil is the most important process, followed by POC settling in the stream

(Table 2.5). Overall, our results suggested both landscape and stream processes control TOC dynamics in the ER watershed, confirming the necessity of integrating terrestrial and aquatic OC processes for modelling their combined watershed scale dynamics. Other processes that directly influenced TOC dynamics include climate. For example, SWAT simulates the growth rate of algae adjusted by water temperature (Neitsch et al., 2011), meaning warmer summers or global warming could result in accelerated growth rates, subsequently increasing in-stream POC. Heavy rainfall events increase surface runoff and lateral flow, and therefore the transport of POC and DOC to streams (e.g., Rostami et al., 2018). It follows that streamflow, which is primarily controlled by precipitation, determines the proportion of POC that remains suspended or settles onto the streambed (equation 2), implying that peak flows or storms flows would increase export of particulate matter. Warmer stream temperatures also increase the dissolution rate of POC to DOC (equation 2), as well as the mineralization rate of DOC to dissolved inorganic carbon (equation 3). Therefore, climate change and seasonal variations also play an important role in watershed carbon dynamics. In addition, we also analyzed the impacts of in-stream processes on controlling the TOC flux in the ER watershed based on the modeling results. We summarized the total TOC loads export from the subbasins to the streams and compared it with the load at the watershed out. The results showed that the whole ER watershed exported 2071.1 tons/yr TOC loads during the 15years period to the stream network, while the TOC load at the outlet was 915.3 tons/yr. It indicates that about 55.8% of TOC loads were lost due to the in-stream processes at the whole watershed scale, which were mainly caused by the processes such as POC settling and DOC mineralization

There are some previous studies aimed to model organic carbon at the watershed scale. For example, a parsimonious watershed DOC model based on the Hydrologiska Byråns

Vattenbalansavdelning (HBV) was developed by Lessels et al. (2015). However, the SOC cycle was not simulated dynamically and in-stream organic carbon processes were not included in that model. Futter et al. (2007) developed a watershed scale DOC model, which simulates both soil carbon and DOC in-stream processes. However, the in-stream processes only consider the transformation between DOC and dissolved inorganic carbon and the SOC processes were simulated based on a conceptual model instead of the process-based model. In addition, the Regional Hydro-Ecological Simulation System (RHESSys) is able to simulate the watershed scale organic carbon fluxes (Tague and Band, 2004), but the in-stream processes were not explicitly included.

In this study, we developed a process-based in-stream OC model and integrated it with comprehensive SOC module in SWAT (Zhang et al., 2013), which simulates the SOC cycle using five different SOM pools. Therefore, it is able to mimic the complex OC cycle in both terrestrial and aquatic environments and to simulate the fate and transport of OC at the watershed scale, in addition to in-stream transformations between carbon compounds. In the coupled DOC model developed by Lessels et al. (2015), in-stream DOC concentrations typically followed streamflow patterns, and began to increase during the onset of spring freshet as high water movement displaces more DOC from the soil. Streamflow was also a predictor of OC export in the ER watershed, indicating the importance of snowmelt and precipitation for carbon dynamics. Our model results are also comparable to those of the INCA-C (Futter et al., 2007), in which DOC concentrations were also sensitive to initial soil carbon content. The INCA-C significantly underestimated high DOC fluxes in the summer, which was partly attributed to lower flows, and was likely also influenced by the model's inability to simulate POC transport from the landscape.

Table 2.5. Parameter sensitivity analysis for TOC load simulation at two stations

Bragg Creek station		Sarcee Bridge station	
Parameter name	Sensitivity ranking	Parameter name	Sensitivity ranking
kd_oc	1	kd_oc	1
poc_setl	2	enr_poc	2
perco_doc	3	poc_setl	3
enr_poc	4	perco_doc	4
kdoc_rch	5	kdoc_rch	5
gwc_doc	6	gwc_doc	6
kpoc_rch	7	kpoc_rch	7

In addition to the monthly TOC loads, annual loads at the Sarcee Bridge station were further analyzed in order to characterize temporal TOC dynamics in the ER watershed. Annual TOC loads ranged from 114.9 to 2584.7 tons/year during the simulation period with an annual average of 915.3 tons, representing the approximate amount of TOC entering the Glenmore reservoir. The maximum (2584.7 tons) and minimum (114.9 tons) annual loads occurred in 2005 and 2001, respectively, which were the wettest and driest year during the simulation period. This indicated that hydro-climatic conditions, such as surface runoff and lateral flow resulting from precipitation, are the main drivers for inter-annual variation of TOC loads. To analyze the long-term seasonal variations of TOC loads, monthly averages at Sarcee Bridge during simulation period (2001–2015) are shown in Figure 9. TOC loads became elevated in April when snowmelt typically begins, and peaked in June (Fig. 9). The three months from May to July accounted for 68.8 % of the annual TOC export in the ER watershed, because spring snowmelt runoff and summer rainfall runoff events in the ER watershed are concentrated in this period and are the main driving forces for loads and transport of OC in the watershed. Therefore, if future

conditions change due to climate change or extreme events, it is likely during this period that OC loadings into the reservoir could become problematic.

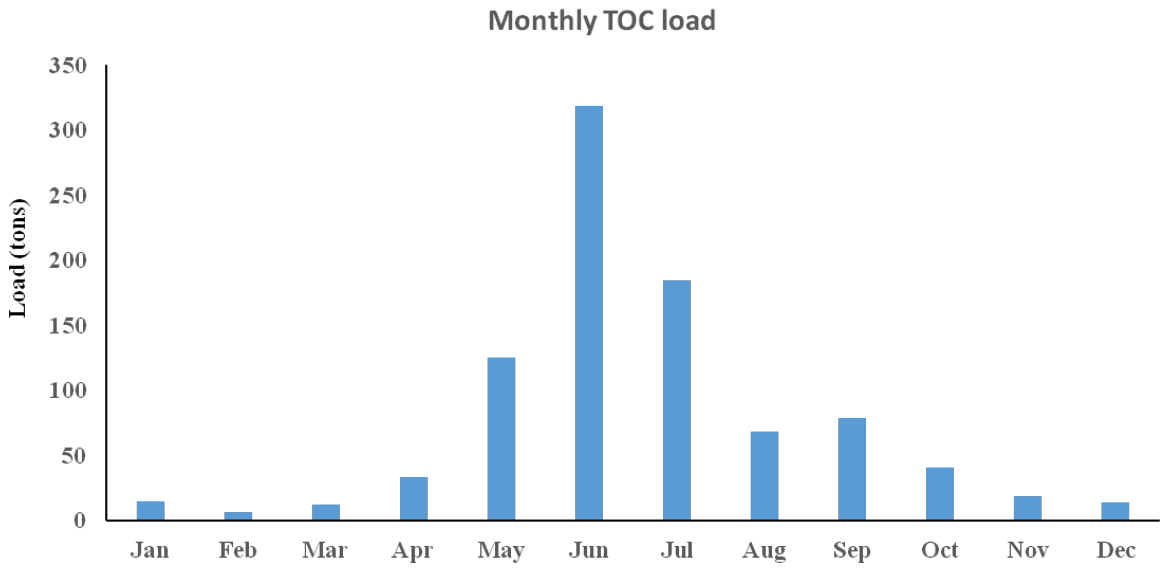

Fig. 2.9. Long-term (2001–2015) average monthly simulated TOC load variation at the Sarcee Bridge station.

2.3.5 Limitations and future studies

Because of the parsimonious nature of this module, some processes were simplified since we opted to minimize the parameter and data input requirements. For instance, the average DOC concentration in groundwater flow was used to calculate DOC loads transported by groundwater flow, rather than simulating detailed DOC mass balance and reactions in shallow aquifers. In addition, two state variables, DOC and POC, were used to model in-stream OC dynamics, although in reality, DOC and POC could be further subdivided into the labile and refractory fractions based on relative different decay rates of organic matter (Sempéré et al., 2000). For example, the turnover time of labile soil OC is typically 1 to 5 years, while the turnover time of refractory fractions could reach 200–1500 years (Parton et al., 1987). Therefore, four state

variables, LPOC, RPOC, LDOC and RDOC, could be used in the future to develop a more complex in-stream OC module to depict in-stream organic transport and reactions. At the same time, this could bring forth more model uncertainty because complex model processes usually require more parameters and input data, and there is usually a trade-off between model complexity and its applicability (Du et al., 2014). Future field and laboratory studies involving in-stream organic carbon could be incorporated into a more complex model that includes additional state variables and parameters. Furthermore, comparison could be performed between the module in this study and a complex in-stream organic carbon module. Despite the long-term water quality record of the ER watershed, it was challenging to capture heterogeneities and fluctuations with the model. We assume in this study that the sample nutrient and sediment concentrations were representative of the entire water column and remain uniform throughout the day, when in reality they would vary spatially and temporally. Another source of error could be the resolution and accuracy of input data such as climate, and geospatial data, including land use, which remained static throughout the simulation, in addition to the soil inputs, which were rather coarse. In terms of scenario analysis related to climate change, anthropogenic activity or extreme events, the calibrated model would likely be better suited for capturing monthly and annual trends rather than immediate changes related to water quality. Natural processes impacting OC also occur in the Glenmore Reservoir, which is outside of the study area, and these could mediate or exacerbate nutrient fluxes before the water reaches the treatment facility by the dam. Furthermore, data obtained from in-stream water samples do not differentiate between DOC and POC fractions of TOC; therefore, it was not possible to verify whether the model is appropriately capturing individual fractions. However, based on the seasonality of measured sediments and TOC, we hypothesized that the particulate fraction is more sensitive to streamflow as it can be

attached to soil particles. The model should be applied to other watersheds with different landscapes and climate, and where both DOC and POC concentration measurements are available.

2.4 Conclusion

A process-based parsimonious in-stream organic carbon (OC) module was developed and incorporated into the SWAT model and linked with the existing soil carbon module in order to simulate OC dynamics at the watershed scale. In-stream OC processes with two state variables (POC and DOC) are modeled in the water column, which considers the transformations (or reactions) between different carbon species and interactions between OC and algae. The model performance was assessed for simulating total organic carbon (TOC) loads in the Elbow River watershed in Alberta, Canada. The hydrological and sediment processes within SWAT were first calibrated and validated on a monthly time step using the observed data. Overall, the calibrated SWAT model achieved 'satisfactory' simulation results for streamflow and sediment loads, and was then used to model TOC loads. The simulation performances for monthly TOC loads of the two stations using the developed module were assessed as 'good' based on evaluation criteria, and the calibrated model successfully captured the seasonal and monthly variations. Model results suggested that snowmelt and rainfall runoff events are two of the main driving forces for OC transport in the Elbow river watershed, which peak in the late spring and early summer. Parameter sensitivities suggested that TOC dynamics in the ER watershed are controlled by both landscape and stream processes, confirming the necessity of integrating terrestrial and aquatic OC processes for modelling their watershed scale dynamics. Therefore, the developed OC module can be an effective tool for simulating the OC cycle at the watershed scale. This study was an important step towards a better understanding of the processes that govern the watershed

OC cycle, and this module may be applied to studies looking at the relationship of OC to nitrogen and phosphorous. Furthermore, scenario analyses regarding climate change, extreme events, and human activity impacts on TOC export in river basins could be useful to water treatment plans and watershed management.

2.5 Acknowledgements

Funding for this study has been received from Campus Alberta Innovation Program Chair (Grant #RES0034497), and Natural Sciences and Engineering Research Council of Canada (Grant #RES0038819). We would like to thank the City of Calgary for providing water quality data. D.L. and X.D. made equal contributions to this study by analyzing results and writing the initial paper draft. D.L. set up and calibrated the initial model. X.D. developed the SWAT Organic Carbon Simulation Module, applied it to the model and calibrated organic carbon; D.S.A. and M.F. supervised this work and revised the paper.

2.6 References

Abbaspour 2007, K. C. (2007). SWAT-CUP: Calibration and Uncertainty Programs – A User Manual. EAWAG: Swiss Federal Institute of Aquatic Science and Technology.

Alberta Environment and Parks, (2012). Standards and Guidelines for Municipal Waterworks, Wastewater and Storm Drainage Systems. Alberta Environment and Sustainable Resource Development, Edmonton, Alberta. ISBN: 978-0-7785-9634-9.

Amiro, B. D., Cantin, A., Flannigan, M. D., & de Groot, W. J. (2009). Future emissions from Canadian boreal forest fires. *Canadian Journal of Forest Research 39*(2). https://doi.org/10.1139/X08-154

Asadzadeh, M., Leon, L., Yang, W., Bosch, D., 2016. One-day offset in daily hydrologic modeling: An exploration of the issue in automatic model calibration. *Journal of Hydrology 534*, 164–177. https://doi.org/10.1016/j.jhydrol.2015.12.056

Bladon, K. D., Emelko, M. B., Silins, U., & Stone, M. (2014). Wildfire and the future of water supply. *Environmental Science and Technology*, *48*(16), 8936–8943. https://doi.org/10.1021/es500130g

Bladon, K. D., Silins, U., Wagner, M. J., Stone, M., Emelko, M. B., Mendoza, C. A., Devito, K. J., & Boon, S. (2008). Wildfire impacts on nitrogen concentration and production from headwater streams in southern Alberta's Rocky Mountains. *Canadian Journal of Forest Research*, *38*(9), 2359–2371. https://doi.org/10.1139/X08-071

Cawley, K. M., Hohner, A. K., McKee, G. A., Borch, T., Omur-Ozbek, P., Oropeza, J., & Rosario-Ortiz, F. L. (2018). Characterization and spatial distribution of particulate and soluble carbon and nitrogen from wildfire-impacted sediments. *Journal of Soils and Sediments*, *18*(4), 1314–1326. https://doi.org/10.1007/s11368-016-1604-1

Chen, H., Luo, Y., Potter, C., Moran, P.J., Grieneisen, M.L., Zhang, M. (2017). Modeling pesticide diuron loading from the San Joaquin watershed into the Sacramento-San Joaquin Delta using SWAT. *Water Research 121*, 374–385. https://doi.org/10.1016/j.watres.2017.05.032

Confesor Jr, R.B., & Whittaker, G.W. (2007). Automatic Calibration of Hydrologic Models With Multi-Objective Evolutionary Algorithm and Pareto Optimization. *JAWRA Journal of the American Water Resources Association 43*(4), 981–989. https://doi.org/10.1111/j.1752-1688.2007.00080.x

Du, X., Li, X., Zhang, W., Wang, H. (2014). Variations in source apportionments of nutrient load among seasons and hydrological years in a semi-arid watershed: GWLF model results. *Environmental Science and Pollution Research 21*(10), 6506–6515. https://doi.org/10.1007/s11356-014-2519-2

Du, X., Shrestha, N.K., & Wang, J. (2019b). Integrating organic chemical simulation module into SWAT model with application for PAHs simulation in Athabasca oil sands region, *Western Canada. Environmental Modelling & Software 111*, 432–443.

https://doi.org/10.1016/j.envsoft.2018.10.011

Emelko, M. B., Silins, U., Bladon, K. D., & Stone, M. (2011). Implications of land disturbance on drinking water treatability in a changing climate: Demonstrating the need for "source water supply and protection" strategies. *Water Research*, *45*(2), 461–472. https://doi.org/10.1016/j.watres.2010.08.051

Fabre, C., Sauvage, S., Tananaev, N., Noël, G.E., Teisserenc, R., Probst, J.L., Sánchez Pérez, S.M. (2019). Assessment of sediment and organic carbon exports into the Arctic ocean: The case of the Yenisei River basin. *Water Research 158*, 118–135. https://doi.org/10.1016/j.watres.2019.04.018

Faramarzi, M., Abbaspour, K. C., Adamowicz, W.L. (Vic), Lu, W., Fennell, J., Zehnder, A.J.B., & Goss, G.G. (2017). Uncertainty based assessment of dynamic freshwater scarcity in semi-arid watersheds of Alberta, Canada. *Journal of Hydrology: Regional Studies, 9*, 48–68. https://doi.org/10.1016/j.ejrh.2016.11.003

Faramarzi, M., Abbaspour, K. C., Schulin, R., & Yang, H. (2009). Modelling blue and green water resources in Iran. *Hydrological Processes 23*, 486–501. https://doi.org/10.1002/hyp.7160

Faramarzi, M., Srinivasan, R., Iravani, M., Bladon, K.D., Abbaspour, K.C., Zehnder, A.J., & Goss, G.G. (2015). Setting up a hydrological model of Alberta: Data discrimination analyses prior to calibration. *Environmental Modelling & Software 74*, 48–65. DOI: 10.1016/j.envsoft.2015.09.006

Farjad, B., Gupta, A., & Marceau, D. J. (2016). Annual and Seasonal Variations of Hydrological Processes Under Climate Change Scenarios in Two Sub-Catchments of a Complex Watershed. *Water Resources Management*, *30*(8), 2851–2865. https://doi.org/10.1007/s11269-016-1329-3

Farjad, B., Pooyandeh, M., Gupta, A., Motamedi, M., & Marceau, D. (2017). Modelling interactions between land use, climate, and hydrology along with stakeholders' negotiation for water resources management. *Sustainability (Switzerland)*, *9*(11), 1–19. https://doi.org/10.3390/su9112022

Ficklin, D.L., Luo, Y., & Zhang, M. (2013). Climate change sensitivity assessment of streamflow and agricultural pollutant transport in California's Central Valley using Latin hypercube sampling. *Hydrological Processes, 27*(18) 2666–2675. https://doi.org/10.1002/hyp.9386

Fischer, H., Sachse, A., Steinberg, C. E. W., & Pusch, M. (2002). Differential Retention and Utilization of Dissolved Organic Carbon by Bacteria in River Sediments. *Limnology and Oceanography, 47*(6), 1702–1711. https://doi.org/10.4319/lo.2002.47.6.1702

Flannigan, M. D., Logan, K. A., Amiro, B. D., Skinner, W. R., & Stocks, B. J. (2005). Future area burned in Canada. *Climatic Change*, *72*(1–2), 1–16. https://doi.org/10.1007/s10584-005-5935-y

Futter, M. N., Butterfield, D., Cosby, B. J., Dillon, P. J., Wade, A. J., & Whitehead, P. G. (2007). Modeling the mechanisms that control in-stream dissolved organic carbon dynamics in upland and forested catchments. *Water Resources Research*, *43*(2), 1–16. https://doi.org/10.1029/2006WR004960

Gleeson, T., Wada, Y., Bierkens, M. F. P., & Van Beek, L. P. H. (2012). Water balance of global aquifers revealed by groundwater footprint. *Nature*, *488*(7410), 197–200. https://doi.org/10.1038/nature11295

Gorgan, D., Bacu, V, Mihon, D., Rodila, D., Abbaspour, K., & Rouholahnejad, E. (2012). Grid based calibration of SWAT hydrological models. *Natural Hazards and Earth System Sciences, 12*(7), 2411–2423. https://doi.org/10.5194/nhess-12-2411-2012

Health Canada, 2017. Guidelines for Canadian Drinking Water Quality—Summary Table. Water and Air Quality Bureau, Healthy Environments and Consumer Safety Branch, Health Canada, Ottawa, Ontario.

Hohner, A. K., Cawley, K., Oropeza, J., Summers, R. S., & Rosario-Ortiz, F. L. (2016). Drinking water treatment response following a Colorado wildfire. *Water Research, 105*, 187–198. https://doi.org/10.1016/j.watres.2016.08.034

Hohner, A. K., Terry, L. G., Townsend, E. B., Summers, R. S., & Rosario-Ortiz, F. L. (2017). Water treatment process evaluation of wildfire-affected sediment leachates. *Environmental Science: Water Research and Technology, 3*(2), 352–365. https://doi.org/10.1039/c6ew00247a

IPCC (2007): Climate Change 2007: Synthesis Report. Contribution of Working Groups I, II and III to the Fourth Assessment Report of the Intergovernmental Panel on Climate Change [Core Writing Team, Pachauri, R.K, & Reisinger, A. (eds.)]. IPCC, Geneva, Switzerland, 104.

IPCC (2013): Climate Change 2013: The Physical Science Basis. Contribution of Working Group I to the Fifth Assessment Report of the Intergovernmental Panel on Climate Change [Stocker, T. F., Qin, D., Plattner, G.-K., Tignor, M., Allen, S. K., Boschung, J., Nauels, A. Xia, Y., Bex, V. & Midgley, P. M. (eds.)]. Cambridge University Press, Cambridge, United Kingdom and New York, NY, USA, 1535.

Kemanian, A. R., Julich, S., Manoranjan, V. S., & Arnold, J. R. (2011). Integrating soil carbon cycling with that of nitrogen and phosphorus in the watershed model SWAT: Theory and model testing. *Ecological Modelling*, *222*(12), 1913–1921. https://doi.org/10.1016/j.ecolmodel.2011.03.017

Krause, P., Boyle, D. P., & Bäse, F. (2005). Advances in Geosciences Comparison of different efficiency criteria for hydrological model assessment. *Advances in Geosciences*, *5*, 89–97. https://doi.org/10.5194/adgeo-5-89-2005

Krishnan, N., Raj, C., Chaubey, I., & Sudheer, K. (2018). Parameter estimation of SWAT and quantification of consequent confidence bands of model simulations. *Environmental Earth Sciences, 77*(470), 1–16. https://doi.org/10.1007/s12665-018-7619-8

Larsen, S., Andersen, T., & Hessen, D. O. (2011). Climate change predicted to cause severe increase of organic carbon in lakes. *Global Change Biology*, *17*(2), 1186–1192. https://doi.org/10.1111/j.1365-2486.2010.02257.x

Laudon, H., Buttle, J., Carey, S. K., McDonnell, J., McGuire, K., Seibert, J., Shanley, J., Soulsby, C., & Tetzlaff, D. (2012). Cross-regional prediction of long-term trajectory of stream water DOC response to climate change. *Geophysical Research Letters, 39*(18), 4–9. https://doi.org/10.1029/2012GL053033

Lessels, J. S., Tetzlaff, D., Carey, S. K., Smith, P., & Soulsby, C. (2015). A coupled hydrology-biogeochemistry model to simulate dissolved organic carbon exports from a permafrost-influenced catchment. *Hydrological Processes, 29*(26), 5383–5396. https://doi.org/10.1002/hyp.10566

Mahat, V., Silins, U., & Anderson, A. (2016). Effects of wildfire on the catchment hydrology in southwest Alberta. *Catena*, *147*, 51–60. https://doi.org/10.1016/j.catena.2016.06.040

Malagó, A., Bouraoui, F., Vigiak, O., Grizzetti, B., & Pastori, M. (2017). Modelling water and nutrient fluxes in the Danube River Basin with SWAT. *Science of the Total Environment*, *603–604*, 196–218. https://doi.org/10.1016/j.scitotenv.2017.05.242

Moriasi, D.N., Arnold, J.G., Van Liew, M.W., Bingner, R.L., Harmel, R.D., & Veith, T.L. (2007). Model evaluation guidelines for systematic quantification of accuracy in watershed simulations. *Transactions of the ASABE. 50*(3), 885–900. doi: 10.13031/2013.23153

Moriasi, D.N., Gitau, M.W., Pai, N., & Daggupati, P. (2015). Hydrologic and water quality models: Performance measures and evaluation criteria. *Transactions of the ASABE 58*(6), 1763–1785. DOI 10.13031/trans.58.10715

Neitsch, S.L., Arnold, J.G., Kiniry, J.R., Williams, J.R. (2011). Soil and water assessment tool theoretical documentation version 2009. Texas Water Resources Institute.

Ni, X., & Parajuli, P.B. (2018). Evaluation of the impacts of BMPs and tailwater recovery system on surface and groundwater using satellite imagery and SWAT reservoir function. *Agricultural water management 210*, 78–87. https://doi.org/10.1016/j.agwat.2018.07.027

Niraula, R., Kalin, L., Srivastava, P., & Anderson, C. J. (2013). Identifying critical source areas of nonpoint source pollution with SWAT and GWLF. *Ecological Modelling*, *268*, 123–133. https://doi.org/10.1016/j.ecolmodel.2013.08.007

Oeurng, C., Sauvage, S., & Sánchez-Pérez, J. M. (2011). Assessment of hydrology, sediment and particulate organic carbon yield in a large agricultural catchment using the SWAT model. *Journal of Hydrology*, *401*(3–4), 145–153. https://doi.org/10.1016/j.jhydrol.2011.02.017

Parton, W.J., Ojima, D.S., Cole, C.V., & Schimel, D.S. (1994). A general model for soil organic matter dynamics: sensitivity to litter chemistry, texture and management. Quantitative modeling of soil forming processes. SSSA spec. 39, Madison, WI, 147–67.

Parton, W.J., Schimel, D.S., Cole, C.V., Ojima, D. (1987). Analysis of factors controlling soil organic matter levels in the Great Plains grasslands. *Soil Science Society of America Journal*

51, 1173–1179. DOI: 10.2136/sssaj1987.03615995005100050015x

Pekel, J.-F., Cottam, A., Gorelick, N., & Belward, A. S. (2016). High-resolution mapping of global surface water and its long-term changes. *Nature*, *540*, 418–422. https://doi.org/10.1038/nature20584

Porcal, P., Dillon, P.J., & Molot, L.A. (2015). Temperature dependence of photodegradation of dissolved organic matter to dissolved inorganic carbon and particulate organic carbon. *PLoS One 10*(6). DOI: 10.1371/journal.pone.0128884

Qi, J., Li, S., Jamieson, R., Hebb, D., Xing, Z., & Meng, F. R. (2017). Modifying SWAT with an energy balance module to simulate snowmelt for maritime regions. *Environmental Modelling and Software*, *93*, 146–160. https://doi.org/10.1016/j.envsoft.2017.03.007

Qi, J., Li, S., Li, Q., Xing, Z., Bourque, C. P. A., & Meng, F. R. (2016). A new soil-temperature module for SWAT application in regions with seasonal snow cover. *Journal of Hydrology*, *538*, 863–877. https://doi.org/10.1016/j.jhydrol.2016.05.003

Qiu, Z., Wang., L., 2014. Hydrological and Water Quality Assessment in a Suburban Watershed with Mixed Land Uses Using the SWAT Model. *Journal of Hydrologic Engineering 19*(4), 816–827.

Regan, S., Hynds, P., & Flynn, R. (2017). An overview of dissolved organic carbon in groundwater and implications for drinking water safety. *Hydrogeology Journal*, *25*(4), 959–967. https://doi.org/10.1007/s10040-017-1583-3

Rood, S. B., Samuelson, G. M., Weber, J. K., & Wywrot, K. A. (2005). Twentieth-century decline in streamflows from the hydrographic apex of North America. *Journal of Hydrology*, *306*(1–4), 215–233. https://doi.org/10.1016/j.jhydrol.2004.09.010

Rostami, S., He, J., & Hassan, Q. K. (2018). Riverine water quality response to precipitation and its change. *Environments*, *5*(1), 1–17. https://doi.org/10.3390/environments5010008

Roy, S., Heidel., K., Creager, C., Chung, C., & Grieb., T. (2006). Conceptual model for organic carbon in the Central Valley and Sacramento-San Joaquin Delta. Tetra Tech, Inc: Lafayette, California, USA

Runkel, R.L., Crawford, C.G., & Cohn, T.A. (2004). Load Estimator (LOADEST): A FORTRAN program for estimating constituent loads in streams and rivers. Techniques and Methods 4-A5, https://doi.org/10.3133/tm4A5

Schindler, D. W., & Donahue, W. F. (2006). An impending water crisis in Canada's western prairie provinces. *Proceedings of the National Academy of Sciences*, *103*(19), 7210–7216. https://doi.org/10.1073/pnas.0601568103

Sempéré, R., Charrière, B., Van Wambeke, F., & Cauwet, G. (2000). Carbon inputs of the Rhône River to the Mediterranean Sea: biogeochemical implications. *Global Biogeochemical Cycles* 14(2), 669–681. https://doi.org/10.1029/1999GB900069

Shrestha, N. K., & Wang, J. (2018). Predicting sediment yield and transport dynamics of a cold

climate region watershed in changing climate. *Science of the Total Environment*, *625*, 1030–1045. https://doi.org/10.1016/j.scitotenv.2017.12.347

Smith, H. G., Sheridan, G. J., Lane, P. N. J., Nyman, P., & Haydon, S. (2011). Wildfire effects on water quality in forest catchments: A review with implications for water supply. *Journal of Hydrology*, *396*(1–2), 170–192. https://doi.org/10.1016/j.jhydrol.2010.10.043

Sosiak, A., & Dixon, J. (2006). Impacts on water quality in the upper Elbow River. *Water Science and Technology*, *53*(10), 309–316. https://doi.org/10.2166/wst.2006.326

Tague, C. L., & Band, L. E. (2004). RHESSys: Regional Hydro-Ecologic Simulation System—An Object-Oriented Approach to Spatially Distributed Modeling of Carbon, Water, and Nutrient Cycling. *Earth Interactions, 8*(19), 1–42. https://doi.org/10.1175/1087-3562(2004)8<1:rrhsso>2.0.co;2

Technical Support Document for Ontario Drinking Water Standards (2006), Objectives and Guidelines, June 2003, Revised June 2006, PIBS 4449e01.

Valeo, C., Xiang, Z., Bouchart, F. J., Yeung, P., & Ryan, M. C. (2007). Climate change impacts in the Elbow River watershed. *Canadian Water Resources Journal*, *32*(4), 285–302. https://doi.org/10.4296/cwrj3204285

Vörösmarty, C. J., McIntyre, P. B., Gessner, M. O., Dudgeon, D., Prusevich, A., Green, P., Gidden, S., Bunn, S. E., Sullivan, C. A., Liermann, R., & Davies, P. M. (2010). Global threats to human water security and river biodiversity. *Nature*, *467*, 555–561. https://doi.org/10.1038/nature09440

Wang, X., Thompson, D. K., Marshall, G. A., Tymstra, C., Carr, R., & Flannigan, M. D. (2015). Increasing frequency of extreme fire weather in Canada with climate change. *Climatic Change*, *130*(4), 573–586. https://doi.org/10.1007/s10584-015-1375-5

Wei, X., Bailey, R.T., Records, R.M., Wible, T.C., & Arabi, M. (2018). Comprehensive simulation of nitrate transport in coupled surface-subsurface hydrologic systems using the linked SWAT-MODFLOW-RT3D model. *Environmental Modelling & Software* (in press, corrected proof) https://doi.org/10.1016/j.envsoft.2018.06.012

Wijesekara, G. N., Farjad, B., Gupta, A., Qiao, Y., Delaney, P., & Marceau, D. J. (2014). A comprehensive land-use/hydrological modeling system for scenario simulations in the Elbow River watershed, Alberta, Canada. *Environmental Management*, *53*(2), 357–381. https://doi.org/10.1007/s00267-013-0220-8

Wijesekara, G. N., Gupta, A., Valeo, C., Hasbani, J. G., Qiao, Y., Delaney, P., & Marceau, D. J. (2012). Assessing the impact of future land-use changes on hydrological processes in the Elbow River watershed in southern Alberta, Canada. *Journal of Hydrology*, *412–413*, 220–232. https://doi.org/10.1016/j.jhydrol.2011.04.018

Worku, T., Khare, D., & Tripathi, S. K. (2017). Modeling runoff–sediment response to land use/land cover changes using integrated GIS and SWAT model in the Beressa watershed. *Environmental Earth Sciences*, *76*(16), 1–14. https://doi.org/10.1007/s12665-017-6883-3

Worrall, F., & Moody, C. (2014). Modeling the rate of turnover of DOC and particulate organic carbon in a UK, peat-hosted stream: Including diurnal cycling in short-residence time systems. *Journal of Geophysical Research: Biogeosciences, 119*(10) 1934–1946. https://doi.org/10.1002/2014JG002671

Writer, J H, McCleskey, R. B., & Murphy, S. F. (2012). Effects of wildfire on source-water quality and aquatic ecosystems, Colorado Front Range. *Wildfire and Water Quality: Processes, Impacts, and Challenges*, (IAHS Publ. 354), 117–123.

Yang, Qi, Leon, L. F., Booty, W. G., Wong, I. W., McCrimmon, C., Fong, P., Fong, P., Michiels, P., Vanrobaeys, J., & Benoy, G. (2014). Land Use Change Impacts on Water Quality in Three Lake Winnipeg Watersheds. *Journal of Environment Quality*, *43*(5), 1690–1701. https://doi.org/10.2134/jeq2013.06.0234

Yang, Qichun, & Zhang, X. (2016). Improving SWAT for simulating water and carbon fluxes of forest ecosystems. *Science of the Total Environment*, *569–570*, 1478–1488. https://doi.org/10.1016/j.scitotenv.2016.06.238

Zabaleta, A., Meaurio, M., Ruiz, E., & Antigüedad, I. (2014). Simulation climate change impact on runoff and sediment yield in a small watershed in the Basque Country, northern Spain. *Journal of environmental quality 43*(1), 235–245. doi: 10.2134/jeq2012.0209

Zeiger, S. J., & Hubbart, J. A. (2016). A SWAT model validation of nested-scale contemporaneous streamflow, suspended sediment and nutrients from a multiple-land-use watershed of the central USA. *Science of the Total Environment*, *572*, 232–243. https://doi.org/10.1016/j.scitotenv.2016.07.178

Zhang, X. (2018). Simulating eroded soil organic carbon with the SWAT-C model. *Environmental Modelling and Software*, *102*, 39–48. https://doi.org/10.1016/j.envsoft.2018.01.005

Zhang, X., Izaurralde, R. C., Arnold, J. G., Williams, J. R., & Srinivasan, R. (2013). Modifying the Soil and Water Assessment Tool to simulate cropland carbon flux: Model development and initial evaluation. *Science of the Total Environment, 463–464*, 810–822. https://doi.org/10.1016/j.scitotenv.2013.06.056

CHAPTER III – MANUSCRIPT 2

Projecting impacts of wildfire and climate change on the downstream transport of sediment and organic carbon

Danielle Loiselle[1], Xinzhong Du[1], Daniel S. Alessi[1], Kevin D. Bladon[2], Monireh Faramarzi[1].
[1] Department of Earth and Atmospheric Sciences, University of Alberta, 1-26 Earth Sciences Building, Edmonton, AB T6G 2E3
[2] Department of Forest Engineering, Resources, and Management, Oregon State University, Corvallis, OR 97331, USA

3.1 Introduction

Climate change has increased the frequency, size, and severity of natural disturbance events such as wildfires, droughts, and storms (e.g., Mahat et al., 2016; IPCC, 2013; Wang et al., 2015) that drive hydrological processes influencing water quality. In particular, the combination of hotter summers with higher frequencies of drought and thunderstorms has favored the ignition of wildfires (Flannigan et al., 2005; Marlon et al., 2012). Since air temperature and fuel moisture are key factors affecting combustion, wildfire severity and frequency are projected to continue increasing (e.g., Coogan et al., 2019; Flannigan et al., 2005). Additionally, aggressive wildfire suppression in many parts of the world, including Western North America, has increased fuel connectivity and the risk of extensive and destructive burn events (e.g., Marlon et al., 2012; Willmore and Jensen, 1960). In the Western Canadian province of Alberta, 10 of the 20 years with the largest burn areas since 1961 have occurred after 2000 (Alberta Wildfire, 2019). One of the most notable occurrences was in 2016, when an uncontrollable wildfire destroyed 589,552 ha of boreal forest and infrastructure within the city of Fort McMurray in northeastern Alberta, resulting in $3.7 billion dollars in insured property losses, the largest natural disaster in Canadian history (MNP LLP, 2017). Another record-setting example was the Lost Creek wildfire in

southwestern Alberta, which ignited during unusually high temperatures in the summer of 2003, burning over 21,000 ha of forest and incurring $38 million in firefighting costs (Kulig et al., 2009).

The source water supplies in many regions of the world are potentially vulnerable to catastrophic wildfire (Robinne et al., 2018; 2016), and in most regions, water and land managers lack the tools to assess potential wildfire- or climate-associated risks (Robinne et al., 2019). Indeed, wildfires can contribute to reduced source water quality following a wildfire, which can challenge the community drinking water treatment process performance and increase operational costs (Emelko et al., 2011; Emelko et al., 2016). For example, wildfires reduce canopy interception, decrease evapotranspiration, and change soil hydraulic properties, resulting in decreased groundwater recharge, and higher soil water content, peak flows, and annual water yields (Ebel & Moody, 2017; Hallema et al., 2018; Townsend & Douglas, 2004). The loss of vegetation also exposes soils to forces exerted by precipitation, increasing the potential for erosion, sediment transport to streams, and debris flows (Gartner et al., 2008; Robichaud et al., 2016; Silins et al., 2009). This increases the delivery of water quality constituents such as sediment and nutrients (i.e., organic carbon, phosphorous and nitrogen) to streams in both the dissolved (Bladon et al., 2008; Rhoades et al., 2019) and particulate forms (Emelko et al., 2016; Rust et al., 2018). For instance, in-stream organic carbon (OC) can increase following wildfires, and the dissolved fraction is particularly challenging to remove from drinking water (e.g., Hohner et al., 2017). OC is a key water quality indicator due to its ability to transport heavy metals and organic contaminants, as well as support bacteria and biofilms (e.g., Fischer et al., 2002; Laudon et al., 2012). Often, high severity wildfires consume soil organic matter (González-Pérez et al., 2004; Smith et al., 2011), leaving mixed layers of ash (Smith et al., 2011)

and other incomplete combustion products, such as charcoal and charred biomass, which contain OC in the form of pyrogenic carbon (PyC) (Abney et al., 2019). Wildfires can cause water-repellency in soils that can persist for over a year, depending on factors such climate and soil type (Abney et al., 2019; Doerr et al., 2009; Plaza-Álvarez et al., 2018). The lower densities of PyC and ash make them easily transportable by surface runoff, and PyC has higher surface area and is more hydrophobic than non-PyC making it a sorbent for organic matter (Abney et al., 2019). As well, alluvial deposits and increased suspended solid levels can facilitate dissolution of particulate organic matter attached to solid particles (Cawley et al., 2018; Cotrufo et al., 2016; Writer et al., 2012). However, the magnitude and longevity of effects from wildfire generally remain uncertain.

Given that the majority of Canadians rely on high-quality drinking water originating from forested watersheds in the Rocky Mountains (e.g., Bladon et al., 2014; Schindler & Donahue, 2006), it is increasingly important to understand the likely range of effects on water resources in the face of climate change and extreme weather events. Many researchers have applied hydrological models to assess watershed responses to climate change, land cover changes, disturbances, and extreme weather events, by analyzing relative changes in water quantity or quality parameters (e.g., Larsen et al., 2011; Malagó et al., 2017; Shrestha et al., 2017; Shrestha & Wang, 2018). Regression models can be useful in those rare instances where local data is available before and after discrete disturbance events (e.g., Rodríguez-Jeangros et al., 2018; Yu et al., 2019), but even then, their application is limited to establishing empirical relationships at specific sites. Therefore, it is not possible to utilize these models to predict changes at the watershed scale under changing climate or land cover. However, process-based models have a distinct advantage in their applicability to “what if” scenarios to project expected changes in

water quantity and quality to future climate change, extreme weather events, or discrete disturbance events.

The SWAT (Soil and Water Assessment Tool) model is a semi-distributed and process-based hydrologic and water quality model that has been extensively applied to water quality studies and scenarios analyses (e.g., Azari et al., 2017; Havel et al., 2018; Hernandez et al., 2018; Morán-Tejeda et al., 2015; Rodrigues et al., 2019; Worku et al., 2014). The majority of these studies addressed changes in hydrological processes, erosion, sediment transport, and nitrogen and phosphorous transport and cycling under various scenarios such as climate change or management practices. Limited studies have recently addressed the effects of discrete disturbance events such as wildfires on water quantity, without assessing water quality parameters such as sediment and organic carbon (OC). For example, Havel et al., (2018) used SWAT to simulate the hydrologic response to the 2012 High Park and Hewlett wildfires in Colorado, using streamflow data that was available before and after the wildfire. In general, their model projected increases in total annual runoff volumes, which were primarily related to increases in surface runoff and corresponding decreases in subsurface flow due to the wildfire. In another study, streamflow accuracy improved when Hernandez et al., (2018) updated land cover annually, rather than every five years in a SWAT model. Canopy interception and surface roughness parameters were updated in the model to reflect disturbances such as wildfires, tree harvest, and pine beetles, using satellite imagery for ten watersheds in the Northern US Rocky Mountains, confirming the importance of vegetation in regulating hydrological processes. Other relevant wildfire studies are related to land cover change and potential impacts on hydrology in models that were calibrated to measured streamflow (Morán-Tejeda et al., 2015; Rodrigues et al., 2019). Rodrigues et al. (2019) found that larger prescribed burn simulations increased

streamflow and considerably reduced aquifer storage in a tropical Brazilian watershed. Moran-Tejeda et al. (2015) combined climate change and land cover scenarios for a mountainous watershed in Spain, and found that overall water yield decreased from 2021-2050 compared to 1961-1990, particularly in spring and summer months. Surface runoff and streamflow increased for wildfire scenarios, and decreased for reforestation scenarios.

While the above-mentioned studies assessed the response of hydrology and water quality to climate change scenarios, to our knowledge, none have used hydrological models to assess the impacts of both climate change and wildfires on water quality parameters (e.g., sediment, OC), by studying landscape and aquatic processes at a watershed scale. Specifically, there are limited studies that assess the impacts of climate change on watershed organic carbon (OC) dynamics. Given the previous limitations of SWAT in simulating OC dynamics, Du et al. (2019a) recently developed the SWAT Organic Carbon Simulation Module (SWAT-OCSM), which can successfully simulate OC transport by erosion and runoff, in-stream OC processes, and OC loading at the watershed scale. It follows that in-stream OC has not yet been considered in scenario analyses. Thus, our objective was to develop a framework to (1) assess watershed responses to climate change and potential wildfires using an improved SWAT model, and (2) interpret model outputs to identify which processes could influence future water quality. This was achieved by simulating processes associated with streamflow, sediment yield, and organic carbon in a watershed with heterogeneous soil, land use, and geospatial conditions characterized by cold region hydrology (e.g., Pomeroy et al., 2007). We then examined both climate change and potential wildfire scenarios and simulated spatiotemporal variation of hydrological and water quality responses (i.e., sediment and OC) for the Elbow River (ER) watershed of southern

Alberta, Canada, which was used as an experimental study area to assess the performance of the SWAT-OCSM.

3.2 Materials and methods

3.2.1 Study area

The Elbow River (ER) is located in the montane and foothills region of southwest Alberta, Canada. This watershed is ideal for modelling water quality processes and conducting scenario analyses due to its unique hydrological characteristics as well as access to a comprehensive water quality data set from the municipal water authorities of the City of Calgary. ydrology of the ER is complex, as the watershed spans diverse landscapes where abrupt weather changes are common due to the influence of the Rocky Mountains (Fig. 3.1). Headwaters originate in the mountains (3,205 m elevation) and flow east through boreal forests (Natural Resources Canada, 2017), after which the landscape becomes flatter and human influences increase in the form of agriculture, pastures and suburban residences. According to Alberta Environment and Parks, climate is semi-arid with average annual precipitation of 608 mm (Appendix A.1.), with the Rocky Mountains receiving nearly twice as much annual precipitation as Calgary. According to streamflow data from Environment Canada (Appendix A.1), peak streamflow occurs in June, coinciding with both peak snowmelt and rainfall, and baseflow occurs between January and March, which is primarily sourced from groundwater (Farjad et al., 2016; Wijesekara et al., 2014). In the ER watershed, the distribution of vegetation is highly correlated with soil type (Fig. 3.1c & 1d), and details about soil properties are found in Table 3.1. The lower reach of our study was the mouth of the Glenmore Reservoir in Calgary (1,039 m elevation), which is the primary source of drinking water for 40% of the city's population of 1.3

million people (City of Calgary, 2018). The reservoir has a surface area of 3.8 km^2 and a mean depth of 6.1 m, and water has predominantly low turbidity (Crosby et al., 1990). Previous research by Sosiak & Dixon (2006) has linked water quality in the Glenmore Reservoir to the impact of land use changes and cohesive sediment in the ER watershed. These cohesive sediments are stored in the upper part of the gravel riverbed, and are re-entrained during high flows, eventually making it into the reservoir.

The mean annual area burned in Alberta from 1961 to July of 2019 was 168,436 ha, with 10 of the 20 years with the highest burned area occurring since 2000 (Alberta Historical Wildfire database 2019). Specific to our study, the Rocky Mountain region encompasses 7.4% of the area of Alberta but, accounts for 12.6% of the annual area burned. Wildfires in the montane and foothills region previously occurred at intervals of approximately 26–39 years (Rogeau et al., 2016), and with the last notable wildfire occurring in 1936, the ER watershed is statistically overdue for a large wildfire. The majority of other reported wildfires were either Class A (<0.1 ha) or Class B (0.1–4.0 ha), and were typically recreational or lightning-caused (Alberta Wildfire, 2019).

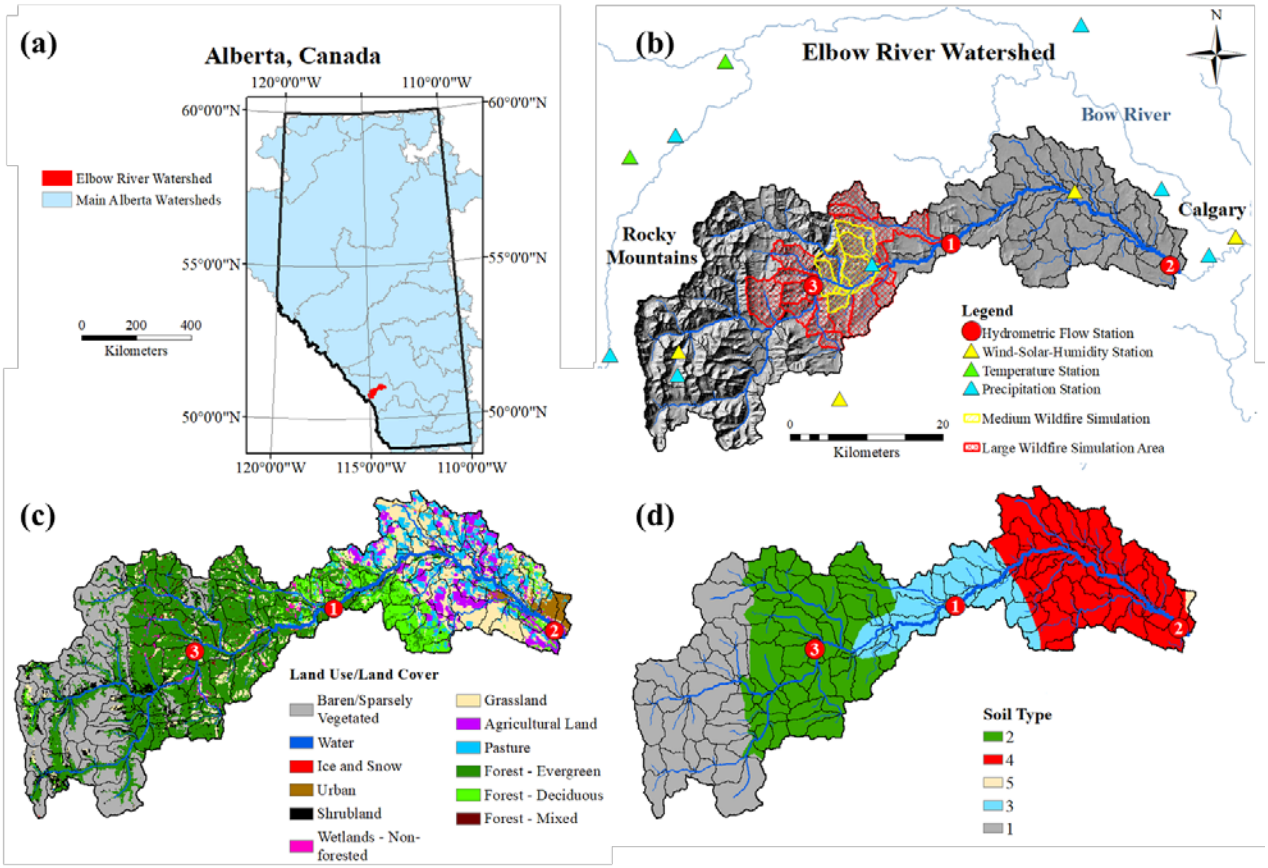

Fig. 3.1. (a) Location of Elbow River watershed in Alberta; (b) location of hydrometric stations (1. Bragg Creek; 2. Sarcee Bridge; 3. Elbow Falls) and climate stations. Areas for wildfire simulation are shown in yellow (6,108 ha), and red (23,984 ha), based on local wildfire history (Rogeau et al., 2016); (c) land use/land cover distribution; (d) soil type distribution.

Table 3.1. Soil types, primary land uses, soil hydrologic group, and top layer composition. Note: rock refers to gravel; sand, silt and clay portions were normalized to 100%, and soil organic carbon is by weight.

Soil type	Land cover	Soil hydrologic group	Rock	Sand	Silt	Clay	Soil OC
1	Exposed rock with no vegetation - some evergreen forests in valleys	D: composed of solid rock with very low infiltration rates and low water transmission	N/A	N/A	N/A	N/A	N/A
2	Foothills or subalpine region - covered in evergreen forests	B: moderate infiltration rates, and moderately to moderately-well drained	2%	61%	17%	22%	7%
3	Mixture of evergreen and deciduous forest, with small urban land use in Bragg Creek	A: high water infiltration and transmission rates, and low runoff potential	15%	22%	60%	18%	30%
4	Agriculture, pasture, and grassland, with Calgary making up the easternmost portion	C: slow water infiltration and transmission rates, and high runoff potential	0	4%	54%	42%	4.8%

3.2.2 Hydrology and water quality simulation in SWAT

SWAT (Soil and Water Assessment Tool) simulates both landscape and in-stream processes related to hydrology, in addition to plant growth, and sediment and nutrient transport. Sub-basins within the model are further subdivided into hydrological response units (HRU), within which all simulated processes occur homogeneously. Key hydrological variables simulated in the model are surface runoff, percolation, evapotranspiration, soil moisture, lateral flow, shallow groundwater recharge and flow, as well as streamflow (Neitsch et al., 2011). Surface runoff is a key process impacting water quality, as it transports sediment and nutrients from hillslopes to the main stream, and subsurface flow can also transport dissolved nutrients. For sediments and nutrients, SWAT simulates erosion and deposition on the ground surface, as well as resuspension and deposition within streams. Nutrients (i.e., carbon (C), nitrogen (N) and

phosphorus (P)) are closely interrelated through soil, microbial and plant processes, including mineralization, immobilization, and humification (Neitsch et al., 2011). The rates at which any of these reactions occur depend on factors such as temperature, moisture, clay content of soil, C:P and C:N ratios, as well as nutrient availability. Generally, carbon is added to soils through plant residue, and removed from soil via erosion and runoff. Because soil particulate organic carbon (POC) is primarily attached to finer clay particles that are more susceptible to erosion, the model calculates an OC enrichment ratio during storms, and therefore the proportion of POC in surface runoff is typically higher than that in the top soil layer.

As mentioned previously, the original SWAT model lacked in-stream OC processes and outputs, and therefore we developed and incorporated in an earlier study the SWAT-OCSM, which simulates in-stream processes associated with particulate and dissolved fractions of OC in the water column as well as OC loading at the watershed scale (Du et al., 2019a). This module incorporates the SWAT-C module developed by Zhang et al., (2013) for soil organic matter processes, and simulates DOC and POC loadings entering the stream from surface runoff and erosion, as well as DOC transported by lateral flow and groundwater to the stream. Other simulated processes include in-stream reactions between OC, floating algae and streambed sediments, and instream transformations between POC, DOC, and inorganic carbon. A detailed description of the SWAT-OCSM including formulae, parameters, and model testing are described in Du et al., (2019a). Model output data relevant to scenario analyses in this study include daily streamflow, sediment yield, and organic carbon yield at a HRU-to-subbasin spatial scale, as this allows us to investigate fluxes in water quantity and quality.

3.2.3 Scenario analysis

3.2.3.1 Climate change

We applied the calibrated SWAT model to assess changes in water quantity and quality for two climate scenarios in the near future (2015–2034) and the distant future (2043–2062). Hydrologic parameters, sediment yield and TOC yield from the four scenarios were compared to historical simulations (1995–2014) in order to calculate relative changes. For our analysis, we considered the best-case and worst-case representative concentration pathways (RCP) for greenhouse gas emissions, as defined in the IPCC Fifth Assessment Report (2013). The RCP 2.6 projection is the optimistic case, in which global cooperation and cleaner technologies lead to reduced greenhouse gas emissions and CO_2 concentrations peak in mid-century. In the RCP 8.5 scenario, economic growth and emphasis on burning of fossil fuels lead to exponential growth in CO_2 concentrations throughout the century. For climate change simulations, CO_2 concentrations for near and distant future scenarios were 465 ppm and 485 ppm for RCP 2.6 and 485 ppm and 660 ppm for RCP 8.5, respectively. For each of the four scenarios, we used climate projections of five general circulation models (GCMs) in order to address uncertainty associated with GCM projections (Appendix A.1). It is noteworthy that projected GCM data have been statistically downscaled to Canada (Cannon et al., 2015) and further bias corrected to local climate conditions in Alberta (Masud et al., 2018, 2019; Faramarzi et al., 2015). The future weather data was loaded into the calibrated SWAT model, after which we investigated the impacts of climate change on water quantity and quality in subbasins and at the watershed outlet, Sarcee Bridge.

3.2.3.2 Wildfire simulation

Wildfires of moderate and high burn severities were simulated for two areas (Fig. 3.1b), generating a total of four wildfire scenarios, which were combined with near future climate

change scenarios (i.e., RCP 2.6 and RCP 8.5). Wildfire severity refers to the loss of biomass above or below ground (Keeley, 2009), for which low severity burns result in considerable tree survival and shallow burn depths within the soil, compared to nearly all vegetation and root systems being incinerated in the case of high severity burns. The smaller of the two areas for burn simulations comprises 6,108 ha and is located in the central-western part of the watershed, intersecting the main stream (Fig 1b). At 23,984 ha, the larger wildfire encompasses the 6,108 ha area and over half of the evergreen forests of the ER watershed; this is comparable to the 2003 Lost Creek wildfire in southwest Alberta that burned approximately 21,000 ha of forest in a mountainous region (Silins et al., 2009). The wildfire scenarios will herein be referred to first by size, followed by burn severity: medium-moderate, medium-high, large-moderate, and large-high wildfire scenarios. Due to spatiotemporal dynamics of hydrological processes and water quality (e.g., Rust et al., 2018), we chose to simulate impacts of wildfires occurring on the 1st day of June for five separate years to allow for analysis of changes on a monthly basis and address inter-annual climate variability. This month was chosen for our analysis because peak precipitation in June is likely to have the highest impact on water quality through erosion and OC loading, based on climate data from Alberta Environment and Parks (Appendix A.1). Wildfires were applied as separate simulations to years 2026, 2027, 2028, 2030, and 2032, because future climate change data indicated lower precipitation in May compared to other years, and dry conditions favor wildfire ignition. HRUs considered for wildfire simulations were chosen based on local wildfire history and elevation, as forests at lower elevations are hotter, drier, and thus more likely to burn (Rogeau et al., 2016). Therefore, we analyzed results of 200 individual wildfire simulations: 4 (wildfire scenarios) × 2 (RCP climate change scenarios) × 5 (GCMs) × 5 (wildfires years) = 200 (total simulations).

Due to limited research on addressing the impact of wildfires on hydrology and water quality, we considered few existing studies for our post-wildfire model parametrization (e.g., Ebel & Moody, 2017; Havel et al., 2018; Moody & Martin, 2009). In order to simulate post-wildfire conditions in SWAT, we modified the code to change land use type and soil parameters in affected HRUs in the 'crop.dat' input file (Table 3.2). The curve number is one of the most sensitive hydrologic parameters, and determines what proportion of rainfall infiltrates into the soil or becomes surface runoff (e.g., Gartner et al., 2008). Curve numbers are updated on a daily basis based on the soil's permeability, land use type and vegetation growth, and initial soil water content from the previous day (Neitsch et al., 2011). In order to simulate the occurrence of wildfires in SWAT, evergreen forests in impacted HRUs were replaced by shrubs for moderate burn severity, and by grasses for high burn severity. The increase in curve numbers are reflective of burn severity, and the approach in changing land cover was reminiscent of another study, in which a SWAT model was calibrated to pre-wildfire and post-wildfire conditions for the High Park and Hewlett wildfires in Colorado (Havel et al., 2018). Wildfires can decrease soil hydraulic conductivity according to burn severity (B. A. Ebel & Moody, 2017), and therefore we reduced the value in the model input data (Table 3.2). It is important to note that this approach does not consider the temporary impact of highly conductive ash layers left behind by wildfires, as it is short-lived and easily removed by surface runoff due to its low density. The final parameter that was updated is soil erodibility, which increases based on burn severity in the first year or two after burning (Table 3.2) (Moody & Martin, 2009).

Post-wildfire analysis involved assessing local changes in model outputs related to hydrology and water quality, including surface runoff, percolation, lateral flow, soil water content, evapotranspiration, sediment yield and organic carbon yield in impacted subbasins. In

addition, streamflow, in-stream sediment yield and TOC yield were compared to those in non-wildfire simulations. With all wildfire simulations occurring on June 1st, we analyzed relative changes on a monthly basis from June-May in order to cover the 12-month period following the wildfire. Similar to climate change, we analyzed the relative changes due to wildfire at the watershed outlet, Sarcee Bridge; however, we also considered the Bragg Creek station due to its proximity to burned subbasins. As it was not possible to calibrate wildfire simulations, the scenario results were broadly compared to those of limited studies that assess hydrology and water quality impacts (e.g., Emelko et al., 2011; Havel et al., 2018; Silins et al., 2009) in order to assess the performance of our simulations.

Table 3.2. Parameters changed in SWAT to simulate impacts of wildfire. The curve number is in the land use database and varies according to soil type.

SWAT input	Default	Moderate burn severity	High burn severity
Land use	Evergreen forest	Shrubland	Grassland
Curve number			
Soil type 2 (central-west)	55	61	69
Soil type 3 (central-east)	25	39	49
Soil hydraulic conductivity (mm/hr)	300	250	200
Soil erodibility	0.15	0.25	0.35

3.3 Results and discussion

3.3.1 Model calibration and validation

Watershed delineation resulted in 154 subbasins (Fig. 3.1), which were further subdivided into 373 HRUs based on slope, land use type, and soil type, within which all simulation processes occurred homogeneously in the model. Monthly outputs were calibrated to measured streamflow, sediment yield, and organic carbon yield. The Nash-Sutcliffe Efficiency (NSE) was used as an objective function, and data from Bragg Creek and Sarcee Bridge stations were used for calibration (Du et al., 2019a). The calibration period for streamflow was 2000–2015, and the validation period was 1986–1999, for which data from an additional station in the headwater region, Elbow Falls, was used for 1986–1995 (Fig. 3.1). Sediment and TOC concentrations measured by the City of Calgary at Bragg Creek and Sarcee Bridge stations were converted to total yields based on streamflow, after which the Load Estimator (LOADEST) software (Runkel et al., 2004) was used to calculate total monthly sediment and TOC yield outputs. The calibration period was 2001–2007 and the validation period was 2008–2015 for both sediment and TOC loads. The SWAT model was calibrated to LOADEST outputs (e.g., Niraula et al., 2013; Teshager et al., 2016) using the newly-developed SWAT-OCSM for TOC (Du et al., 2019a). For streamflow calibration, the NSE was 0.62 for both Bragg Creek and Sarcee Bridge stations, and for validation, 0.62, 0.75, and 0.70 for Elbow Falls, Bragg Creek and Sarcee Bridge stations, respectively. For sediment load at Bragg Creek and Sarcee Bridge stations, the calibration NSE was 0.47 and 0.55, respectively, and the validation NSE was 0.21 and 0.13, respectively. The lower performance of sediment load for the validation period was partially attributed to missing climate data at several climate stations after 2008. For the TOC loads at Bragg Creek and Sarcee Bridge, the calibration NSE was 0.71 and 0.74, respectively,

and the validation NSE was 0.57 and 0.66, respectively. All data sources are listed in Appendix A.1, and detailed calibration results from Du et al. (2019a) are in Appendix A.2, A.3, and A.4.

3.3.2 Spatial analysis of water, sediment, and TOC yields

As expected, water yield, sediment yield, and total organic carbon (TOC) yields were spatially and temporally correlated, as hydrological processes drive sediment and TOC transport (e.g., Rostami et al., 2018). For the baseline period of 1995–2014, water, sediment, and TOC yields generally decreased moving from upstream to downstream (Fig 3.2). Temporally, winter baseflow periods consistently had the lowest sediment and TOC yields, whereas peak streamflow in June corresponded to highest sediment and TOC yields (Appendix A.2, A.3, and A.4). Average water yield by subbasin for the 1995–2014 period is demonstrated in Fig 2a, which is the sum of surface runoff, lateral flow, and groundwater flow contributing to streamflow in each subbasin, minus transmission losses through riverbed and pond storage (Neitsch et al., 2011). On average, the uppermost subbasins draining into the Elbow Falls station yielded 480 mm annually, and those between Elbow Falls and Bragg Creek yielded 310 mm, compared to only 84 mm in lower reaches between Bragg Creek and Sarcee Bridge. The west-to-east gradient was unsurprising, as there is nearly twice as much precipitation in the Rocky Mountains relative to the east.

Average sediment yield by subbasin for the 1995–2014 period generally followed water yield patterns, decreasing from west to east (Fig. 3.2b). However, the westernmost alpine region with soil type one typically yielded less than five tons of sediment per subbasin annually, although this region receives the most precipitation, has the steepest slopes, and therefore highest potential for runoff. This is because much of the mountainous region does not support true soils,

but is composed primarily of bare, exposed bedrock (Fig 1d; Table 3.1). While the bedrock is mildly erodible, the Rocky Mountain Front ranges are generally underlain by more resistant lithology than the downstream Foothills (Osborn et al., 2006). As such, our model treated these regions as relatively resistant, resulting in sediment yields that predominantly originated from channel and bank erosion processes. The central portion of the watershed with soil type 2 and evergreen forests generated the most sediments, with an average of 3,317 tons per subbasin annually and the top soil layer predominantly composed of sand. Soil type 3 is predominantly composed of silt and generated an average of 33 tons per subbasin annually. The easternmost part of the watershed with soil type 4 has the finest grain size distribution, yet contributed little sediments compared to the forested areas at only 12 tons per subbasin in the agriculture and grassland areas, because of lower precipitation and gentler hillslopes. In contrast, the urban areas near the watershed outlet with soil type 4 yielded an average of 464 tons per subbasin due to higher curve numbers and surface runoff in urban areas.

Spatial distribution of TOC yield by subbasin was comparable to that of sediments (Fig. 3.2c). An average of only 2,834 kg of OC originated from the western subbasins with soil type 1 annually, as the model input data has no initial soil OC content for the exposed bedrock (Fig 1d; Table 3.1), and therefore primary sources of TOC were channel and bank erosion. Additional sources include DOC transported by surface runoff, lateral flow, terrestrial vegetation, and in-stream processes such as dissolution of POC. Similar to sediment, subbasins with soil types 2 and 3 generated the highest amounts of TOC annually at 38,739 kg and 26,082 kg, respectively. This is partially attributable to the initial 7% and 30% soil OC content in the soil database, respectively, in addition to surface runoff and erosion processes on steep slopes. The eastern agricultural land with soil type 4 generated an average of only 2,391 kg of TOC annually by

subbasin due to lower precipitation and initial soil OC content of 4.5%, whereas the urban areas yielded 33,336 kg of TOC.

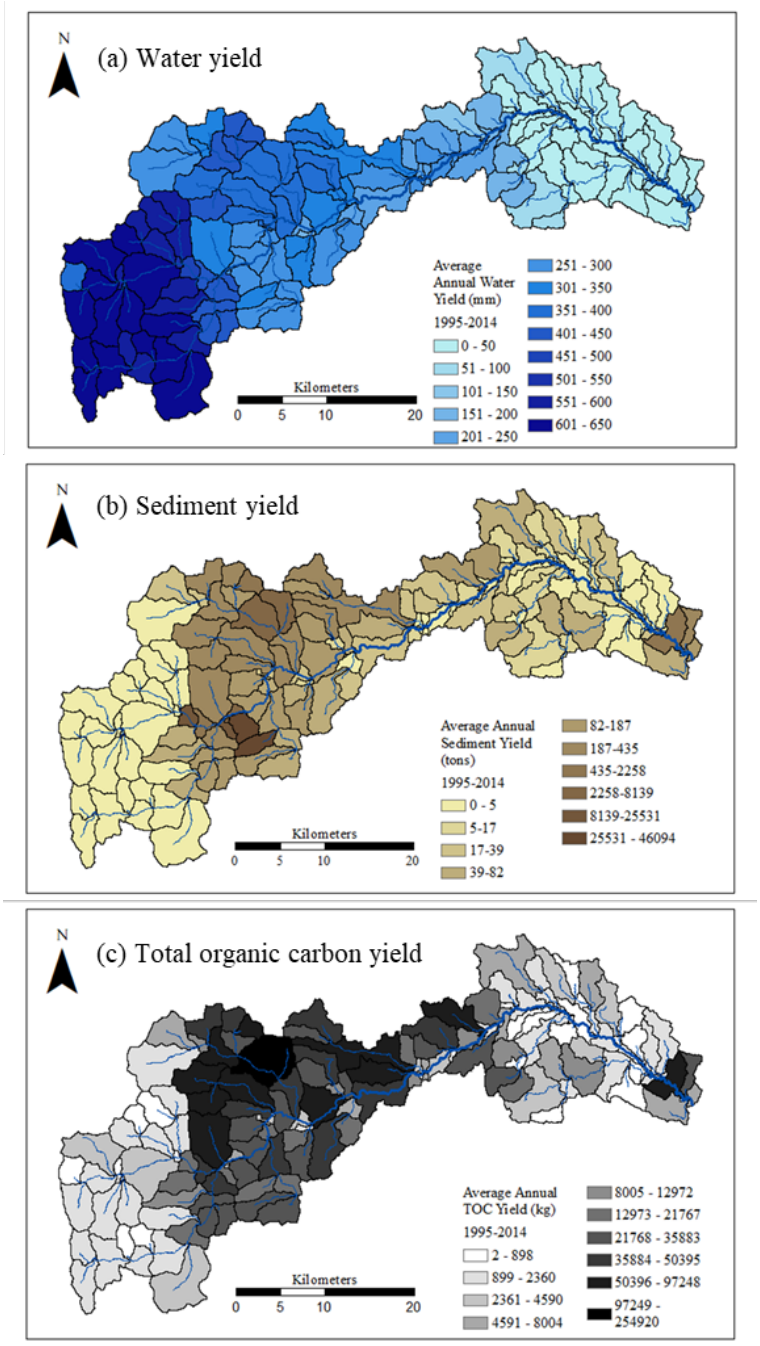

Fig. 3.2. Baseline conditions by subbasin for 1995–2014: (a) Average annual water yield (mm); net amount of water leaving each subbasin and contributing to flow, including surface runoff, lateral flow, and groundwater flow, minus pond storage and transmission losses through riverbed; (b) average annual sediment yield (tons); (c) average annual TOC yield (kg).

3.3.3 Climate change scenarios

3.3.3.1 Streamflow

Both RCP 2.6 and RCP 8.5 scenarios revealed an overall decrease in both near future (2015–2034) and distant future (2043–2062) streamflow at the ER watershed outlet, Sarcee Bridge, compared to the baseline period (1995–2014) (Fig. 3.3a; Table 3.3). Reduced streamflow was most prominent in the summer months of June, July, and August, which was related to lower summer rainfall and hotter temperatures that accelerate evapotranspiration. For each month, the RCP 8.5 scenario projected lower streamflow than the RCP 2.6 scenario, with the largest relative differences in July–November, as the RCP 2.6 scenario has higher precipitation and lower overall temperature than the RCP 8.5 scenario. Annual streamflow decreased by 25.3% and 46.9% for RCP 2.6 and RCP 8.5 scenarios in the near future, respectively, compared to only 9.9% and 31.8% in the distant future, respectively (Table 3.3). Higher streamflow in the distant future period for both scenarios was attributed to slight increases in precipitation relative to the near future. However, it is important to note that hotter temperatures in the distant future would have led to higher evaporation rates. Therefore, we hypothesized that plants required less water because of higher atmospheric CO_2 levels in the distant future, thereby decreasing water uptake by transpiration, according to the Penman-Monteith equation applied to evapotranspiration simulation in the SWAT model (Monteith, 1965; Deryng et al., 2016). In fact, distant future streamflow for the RCP 2.6 scenario showed similar trends to the baseline period, with the exception of notable reductions in May, June, and July. The trends observed in our analysis are consistent with another study of the ER watershed, for which climate change scenario results of a physical process-based model, MIKE SHE/MIKE 11, suggested higher streamflow in the 2050's relative to the 2020's (Farjad, Gupta et al., 2016).

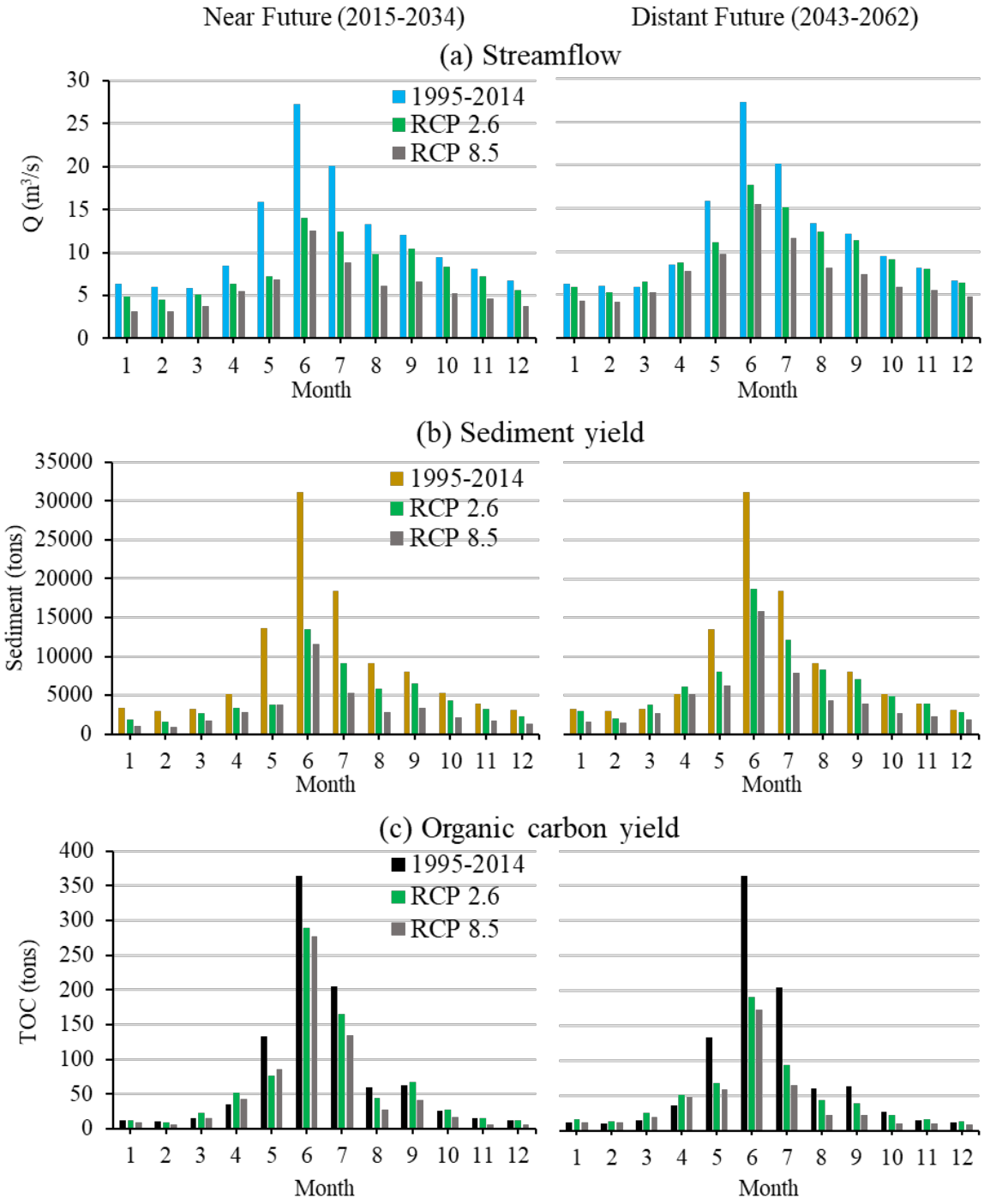

Fig. 3.3. Long-term monthly averages for historical (1995–2014), near future (2015–2034) and distant future (2043–2062) periods at Sarcee Bridge station near watershed outlet: (a) streamflow (m^3/s); (b) sediment yield (tons); (c) organic carbon yield (kg).

Table 3.3. Climate change scenario results for Sarcee Bridge at watershed outlet: % change in streamflow, sediment yield and TOC yield, relative to baseline period (1995–2014): (a) near future; (b) distant future. Note: winter TOC yields are very low between October-March for baseline period.

(a) Near Future (2015-2034)

	Streamflow		Sediment Yield		TOC Yield	
Month	RCP 2.6	RCP 8.5	RCP 2.6	RCP 8.5	RCP 2.6	RCP 8.5
1	-23.0	-49.7	-42.3	-68.4	-0.6	-27.9
2	-24.0	-46.5	-48.9	-69.9	-12.3	-39.5
3	-13.0	-35.4	-18.4	-47.6	+53.8	+6.6
4	-25.2	-35.4	-34.9	-45.8	+45.3	+18.4
5	-54.5	-56.6	-71.7	-72.2	-42.7	-36.1
6	-48.7	-53.9	-56.8	-62.7	-20.7	-24.1
7	-38.3	-56.0	-50.4	-71.3	-19.5	-34.1
8	-25.7	-53.8	-36.3	-69.5	-25.3	-54.7
9	-13.6	-45.2	-18.8	-57.8	+6.0	-34.4
10	-11.3	-44.3	-17.4	-58.6	+5.9	-39.1
11	-10.2	-42.5	-17.2	-57.1	-6.0	-57.0
12	-15.9	-43.2	-25.5	-58.0	-3.2	-50.1
Average	-25.3	-46.9	-36.6	-61.6	-1.6	-31.0

(b) Distant Future (2043-2062)

	Streamflow		Sediment Yield		TOC Yield	
Month	RCP 2.6	RCP 8.5	RCP 2.6	RCP 8.5	RCP 2.6	RCP 8.5
1	-5.8	-32.4	-10.7	-48.7	+37.9	-6.1
2	-11.9	-30.1	-31.4	-51.2	+20.5	+6.9
3	+9.6	-10.9	+15.0	-18.3	+66.1	+27.4
4	+3.2	-8.3	+19.5	-0.2	+44.5	+34.0
5	-30.2	-38.9	-40.8	-53.2	-49.0	-56.1
6	-35.2	-43.5	-39.9	-49.2	-47.8	-52.6
7	-24.7	-42.7	-33.9	-56.7	-54.1	-68.1
8	-7.3	-38.5	-9.2	-51.6	-26.7	-63.9
9	-6.6	-38.4	-10.7	-49.9	-37.0	-64.9
10	-3.4	-37.0	-5.0	-48.2	-14.5	-60.6
11	-1.4	-32.1	-1.6	-41.2	+9.3	-39.1
12	-4.8	-28.9	-6.7	-37.6	+11.7	-23.5
Average	-9.9	-31.8	-13.0	-42.2	-3.3	-30.5

3.3.3.2 Sediment yields

Future sediment yield at the watershed outlet exhibited similar trends to streamflow for both RCP scenarios, reinforcing the strong relationship between discharge and erosion (Fig. 3.3b; Table 3.3). Decreases in annual sediment yield were larger in the near future than in the distant future, with 36.6% and 61.6% reductions in the near future for RCP 2.6 and RCP 8.5 scenarios, respectively, compared to 13% and 42.4% in the distant future, respectively. These results suggested that on average, water entering the Glenmore Reservoir would have lower TSS concentrations compared to the present day period. However, erosion patterns were projected to change heterogeneously within the ER watershed, with Fig. 3.4 demonstrating relative changes in sediment yield by subbasin compared to the baseline period (Fig. 3.3b). In the near future, central subbasins with soil type 2 that yielded the most sediments from 1995–2014 were projected to undergo significantly less erosion. Conversely, both scenarios in the distant future projected sediment yield increases of more than 500% for the same region, which is likely due to overall higher precipitation compared to the near future, and increasingly extreme rainfall events. Furthermore, lower water demand by plants due to elevated CO_2 levels would leave more water available for surface runoff and erosion (Deryng et al., 2016). Although remarkable, these erosion increases in the distant future were not reflected at the watershed outlet, indicating that sediment deposition was a dominant process within the channel due to lower streamflow power. It is notable that analyzing 20-year averages did not address effects of individual extreme rainfall events, during which sediment loads entering the Glenmore Reservoir may have sharp peaks lasting a few days.

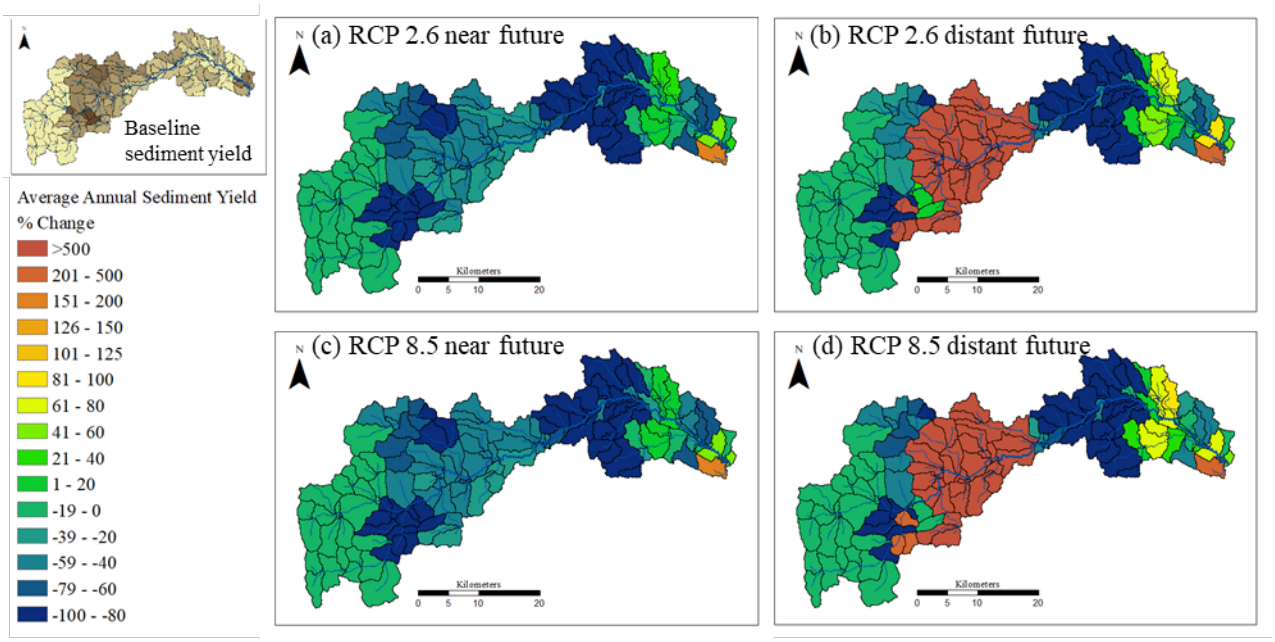

Fig. 3.4. Relative changes in sediment yield (% change) compared to baseline period (1995–2014) in Fig. 3.2b: (a) RCP 2.6 near future (2015–2034); (b) RCP 2.6 distant future (2043–2062); (d) RCP 8.5 near future (2015–2034); (d) RCP 8.5 distant future (2043–2062).

3.3.3.3 Organic carbon yields

Average annual TOC yields declined under both climate change scenarios, but patterns diverged from those of streamflow and sediment yield (Fig. 3.3c and Table 3.3). Similar to streamflow and sediment yield trends, the largest relative decreases in TOC yield occurred in the late spring and summer months; however, a key difference is that TOC yield was higher in the near future compared to the distant future. Annual TOC yields decreased by only 1.6% and 3.3% in the near and distant future of the RCP 2.6 scenario, respectively, compared to the baseline period; however, streamflow decreased by 25.3% and 9.9%, and therefore higher TOC concentrations indicated a deterioration of water quality, particularly in the near future. As well, the RCP 8.5 scenario results suggested poorer water quality compared to the baseline period, particularly in the near future. Relative changes in spatial TOC yields were similar to those of

sediment yields, with near future TOC yields decreasing in central mountain subbasins, compared to large relative increases in the distant future (Fig. 3.5). Eastern agricultural subbasins with soil type 4 revealed higher TOC yields, which were more pronounced in the distant future. While it is understood that surface runoff and erosion are important export mechanisms for TOC (e.g., Rostami et al., 2018), the fact that relative decreases in sediment yields are more pronounced than those for TOC yields suggests that additional processes related to OC play an important role. These processes include DOC transport to the main stream via surface runoff, lateral flow and groundwater flow, in-stream transformations, as well as growth and settling rates of floating algae (Du et al. 2019a). Algae growth rates are a function of temperature (e.g., Nalley et al., 2018), and therefore are likely to increase due to climate change, contributing to higher in-stream POC in addition to higher contributions from landscape erosion. The POC can then remain in suspension, settle to the bed sediment, or dissolve into DOC. Furthermore, in-stream reaction rates of POC and DOC accelerate in warmer waters, and water temperature in SWAT is calculated based on air temperature. Therefore, we hypothesized that in the near future, higher temperatures would lead to faster POC dissolution rates to DOC, and significantly lower summer streamflow would lead to higher concentrations of nutrients. Winter months typically revealed elevated TOC yields relative to baseline conditions for the RCP 2.6 scenario, but not for the RCP 8.5 scenario. This is likely because higher streamflow in RCP 2.6 could transport more POC, which dissolves to DOC and is more easily transported to the watershed outlet. As for the distant future scenarios, higher temperature relative to the near future could even further accelerate POC dissolution to DOC, and subsequently accelerate the rate of DOC mineralization, effectively decreasing the organic fraction of carbon and thus TOC export.

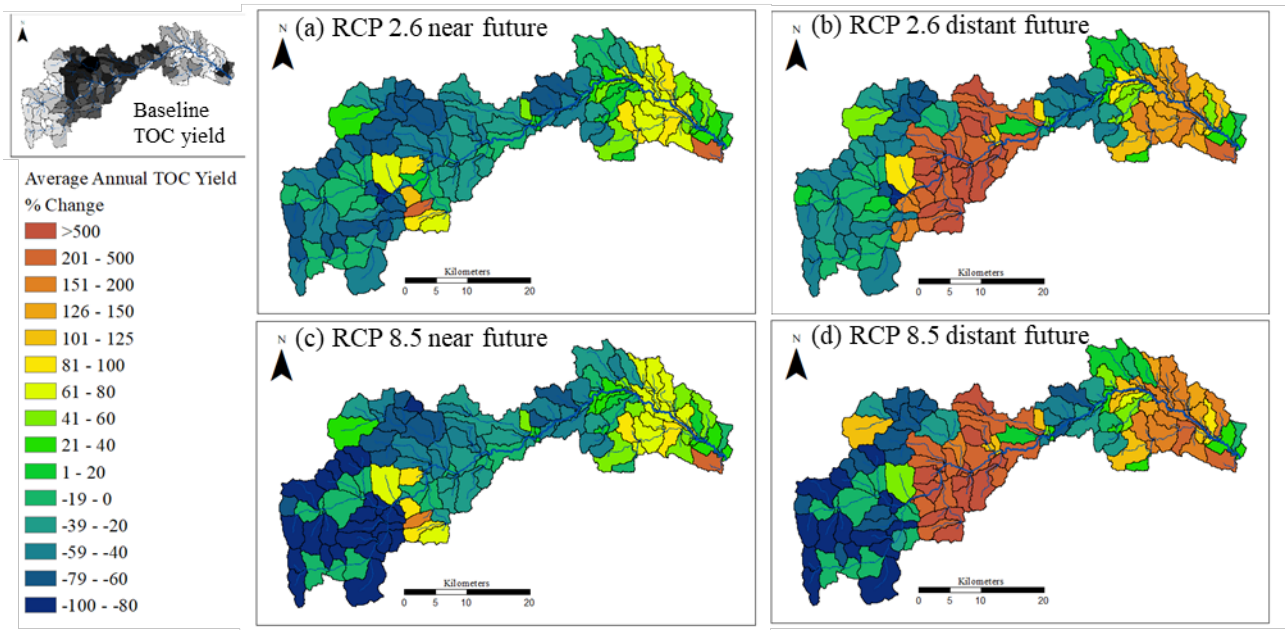

Fig. 3.5. Relative changes in TOC yield (% change) compared to baseline period in Fig. 3.2c: (a) RCP 2.6 near future (2015–2034); (b) RCP 2.6 distant future (2043–2062); (d) RCP 8.5 near future (2015–2034); (d) RCP 8.5 distant future (2043–2062).

3.3.4 Wildfire in combination with climate change Scenarios

3.3.4.1 Local changes

The increase in curve number associated with land cover changes, in addition to reduced soil hydraulic conductivity, resulted in lower soil water content and greater water availability for surface runoff (e.g., Ebel and Moody, 2017), thus increasing sediment and TOC yields. Relative changes in wildfire-impacted subbasins for the large area (23,984 ha) scenarios, i.e., moderate and severe burns, are presented in Fig. 3.6; the medium area (6,108 ha) scenarios are not shown, because they are encompassed by the large area, and relative changes by subbasin were identical to those in the large area scenarios (Fig 3.1b). Therefore, in this section, we discussed the results of the large area wildfire scenarios. For moderate burns, annual surface runoff increased by 11% to over 500% (4–16 mm) in wildfire-affected subbasins for the RCP 2.6 scenario, and by 17% to over 500% (2–16 mm) for the RCP 8.5 scenario. For severe burns, changes ranged from 416% to

over 500% (32–54 mm) for the RCP 2.6 scenario, and from 211% to over 500% (30–55 mm) for the RCP 8.5 scenario (Fig. 3.6). Similarly, Havel et al., (2018) modelled post-fire hydrological changes in SWAT based on measured streamflow in a Colorado watershed, and determined that annual surface runoff in wildfire-impacted subbasins increased between 40–51 mm. However, the greatest observed increase was approximately 75% in subbasins with high burn severities, compared with over 500% for the ER watershed model. The seemingly large variance between the two findings is likely due to differing hydrogeological conditions, in addition to curve numbers in the ER watershed model increasing by 11% and 25% for moderate and high burn severities, respectively, compared to only 10% and 15% in the Colorado study. However, it is important to note that Havel et al., (2018) based spatial their land use changes on satellite imagery, and calibrated curve numbers in their model to hydrometric station data that were available for the pre-wildfire and post-wildfire periods. They also did not directly measure surface runoff in the field, nor modify soil hydraulic conductivity, which can also impact surface runoff (Ebel & Moody, 2017). In comparison, curve numbers in the ER model were obtained from the land use database, and the grass and shrub land use inputs were already present in the ER watershed model in locations outside the wildfire boundary (Fig. 3.1c).

Impacts on annual percolation in the ER watershed were variable within the wildfire boundary, but typically decreased in impacted subbasins (Fig. 3.6). For moderate burns, changes in percolation ranged between -22% (-29 mm) and slight increases (< 1 mm) for the RCP 2.6 scenario, and between -21% (-32 mm) and slight increases (<1 mm) for the RCP 8.5 scenario. For severe burns, changes ranged between -31% (-54 mm) and slight increases (<1 mm) for the RCP 2.6 scenario, and -28% (-54 mm) to slight increases (<1 mm) for the RCP 8.5 scenario. This confirms the important role of forests in regulating water quantity through canopy interception

and evapotranspiration (e.g., Moody and Martin; 2001; Townsend and Douglas, 2004). Percolation in SWAT is a function of existing soil water content, soil water capacity, and plant water uptake among others, and therefore it is conceivable that water available for percolation and soil saturation increased slightly in some subbasins in spite of lower hydraulic conductivity and higher curve numbers (Table 3.2) (Neitsch et al., 2011). Lateral flow occurs when soil water saturation within a given layer reaches a certain threshold, and therefore it generally followed percolation patterns and increased in many wildfire-impacted subbasins. For moderate burns, changes in lateral flow ranged from -21% (-27 mm) to slight increases (<1 mm) for the RCP 2.6 scenario, and -20% (-26 mm) to slight increases (<1 mm) for the RCP 8.5 scenario. For severe burns, changes ranged from -26% (-50 mm) to slight increases (<1 mm) for the RCP 2.6 scenario, and -26% (-47 mm) to slight increases (<1 mm) for the RCP 8.5 scenario. Similar to percolation and lateral flow, post-wildfire soil water content decreased in most subbasins due to higher proportions of water lost by surface runoff. For moderate burns, soil water decreased between -33% to -1% (-254 to -9 mm) annually for the RCP 2.6 scenario, and changed within ranges of -32% to +1% (-277 to +10 mm) for the RCP 8.5 scenario compared to the same years without wildfire. For severe burns soil water decreased between -42% and -6% (-369 to -31 mm) by subbasin for the RCP 2.6 scenario, and by -40% to -5% (-364 to -31 mm) for the RCP 8.5 scenario. Surprisingly, wildfire-affected subbasins experienced higher evapotranspiration, and similar magnitudes of change were observed between scenarios, with increases between 11–39%. For moderate burns, evapotranspiration increased between 24–68 mm annually for the RCP 2.6 scenario, and between 21–62 mm for the RCP 8.5 scenario. For severe burns evapotranspiration increased between 23–70 mm by subbasin for the RCP 2.6 scenario, and between 21–70 mm for the RCP 8.5 scenario. We attributed these increases to soil water

evaporation, given lower plant biomass available for transpiration, and heightened exposure to solar radiation through canopy removal resulting in higher evaporation rates.

Finally, annual sediment and TOC yields increased significantly in all wildfire-affected subbasins, which was the anticipated outcome (e.g., Bladon et al., 2014; Silins et al., 2009). For moderate burns, sediment yields increased by greater than 500% (0.8–547 tons) for the RCP 2.6 scenario, and by 173% to greater than 500% (0.800–805 tons) for the RCP 8.5 scenario. In the case of severe burns, all annual sediment yield increases were greater than 500%, ranging between 1.2–1,364 tons for the RCP 2.6 scenario and 1.3–1,421 tons by subbasin for the RCP 8.5 scenario. Soil erodibility model inputs increased according to wildfire severity (Table 3.2), but it was among the least sensitive parameters affecting sediment yield during the calibration process (Du et al., 2019a). Therefore, we hypothesized that surface runoff was the main driver of sediment transport in the model, which is in agreement with the modified universal soil loss equation (MUSLE) used in SWAT (Neitsch et al., 2011; Williams, 1995). For moderate burns, annual TOC yields increased by 76% to over 500% (123–163,900 kg) by subbasin for the RCP 2.6 scenario, and by 84% to over 500% (115–165,900 kg) for the RCP 8.5 scenario. For severe burns, increases ranged from 227% to over 500% (166–270,400 kg) for the RCP 2.6 scenario, and from 392% to over 500% (173–278,600 kg) for the RCP 8.5 scenario. Since the soil OC model inputs remained the same for wildfire simulations, and erosion caused by surface runoff was also an important driver for TOC export. To further support this hypothesis, the most sensitive parameter for calibration was the POC enrichment ratio (Du et al., 2019a), which determines how much POC sorbs to fine clay particles that are preferentially displaced by surface runoff.

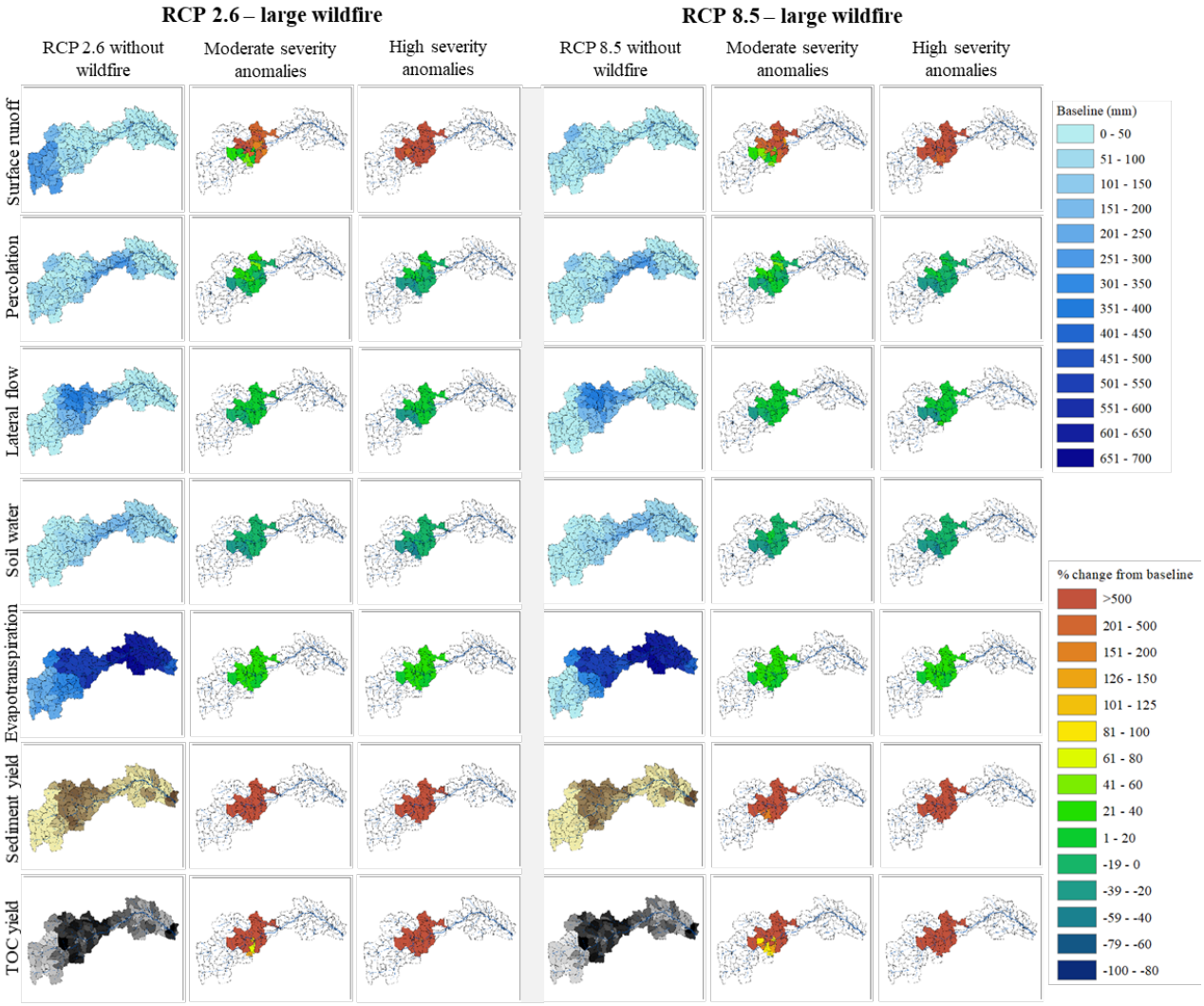

Fig. 3.6. Relative changes in post-fire hydrological processes (surface runoff, percolation, lateral flow, soil water, and evapotranspiration) and water quality parameters (sediment yield and total organic carbon yields) for large burn area – average of wildfire simulations in years 2026. 2027, 2028, 2030, and 2032. The baseline for hydrological processes are climate change projections without wildfire impacts. For baseline sediment yield and TOC yield, refer to Fig. 3.2. Note: relative changes in medium area scenarios (not shown) are identical for impacted subbasins.

3.3.4.2 Regional changes: streamflow

Annual streamflow at both Bragg Creek and Sarcee Bridge stations increased in all wildfire scenarios, with changes most pronounced for the RCP 8.5 scenarios compared to the RCP 2.6 scenarios (Fig. 3.7; Fig. 3.10). For RCP 2.6 scenarios, annual streamflow at Sarcee

Bridge increased by 0.8%, 1.1%, 0.7%, and 1.9% for the medium-moderate, medium-high, large-moderate, and large-high burn scenarios, respectively, and for RCP 8.5 scenarios, annual streamflow increased by 7.7%, 8.1%, 7.9%, and 9.3%, respectively. Annual streamflow increases at the Bragg Creek station were higher in all cases due to burn areas making up a larger proportion of drainage area compared to that of Sarcee Bridge (e.g., Moody et al., 2013). Generally, streamflow increased in the 10 months that followed wildfires relative to the non-wildfire simulations (Fig. 3.7; Fig. 3.10). Intensified streamflow resulted from greater runoff in the wildfire-affected subbasins, highlighting the importance of the forested regions in regulating water yield in the ER watershed. However, streamflow was lower during April and May, following a sharp relative increase in March and February, relative to non-wildfire simulations. This likely resulted from removal of the tree canopy, which would otherwise intercept snowfall during the winter and moderate snow accumulation on the ground, as any form of precipitation that is intercepted by the tree canopy in SWAT evaporates or sublimates before precipitation that has made it to the ground surface (Neitsch et al., 2011). As well, the removal of shading from trees increases snow's exposure to solar radiation (Wagner et al., 2014), thus accelerating snowmelt in February and March, and leaving less snow in April and May. Due to the proximity of Bragg Creek to the wildfire perimeter, relative increases in streamflow were greater compared to the Sarcee Bridge station. For all wildfire simulations, the RCP 8.5 climate change scenario showed a higher increase in streamflow than the RCP 2.6 scenario, due to more extreme precipitation and higher atmospheric CO_2, which can lower evapotranspiration rates (Deryng et al., 2016). Because of high surface runoff, annual streamflow at the ER watershed increased by a range of 0.7–9.3% for large area wildfire scenarios, in which 40% of total forest cover was lost and the wildfire perimeter encompassed approximately 20% of the entire watershed. The

magnitude of these changes are comparable to SWAT model results of another study, in which annual streamflow increased by 2.4% after simulating the burning of 16% of a mountainous watershed in northern Spain (Morán-Tejeda et al., 2015). In the post-wildfire study in Colorado, little changes in streamflow were observed at the watershed scale, but the wildfire location was near the watershed outlet and not in the headwater region (Havel et al., 2018). Conversely, burned areas of the ER watershed were located at higher elevations where the majority of water originates, and therefore impacts of land cover changes were more pronounced.

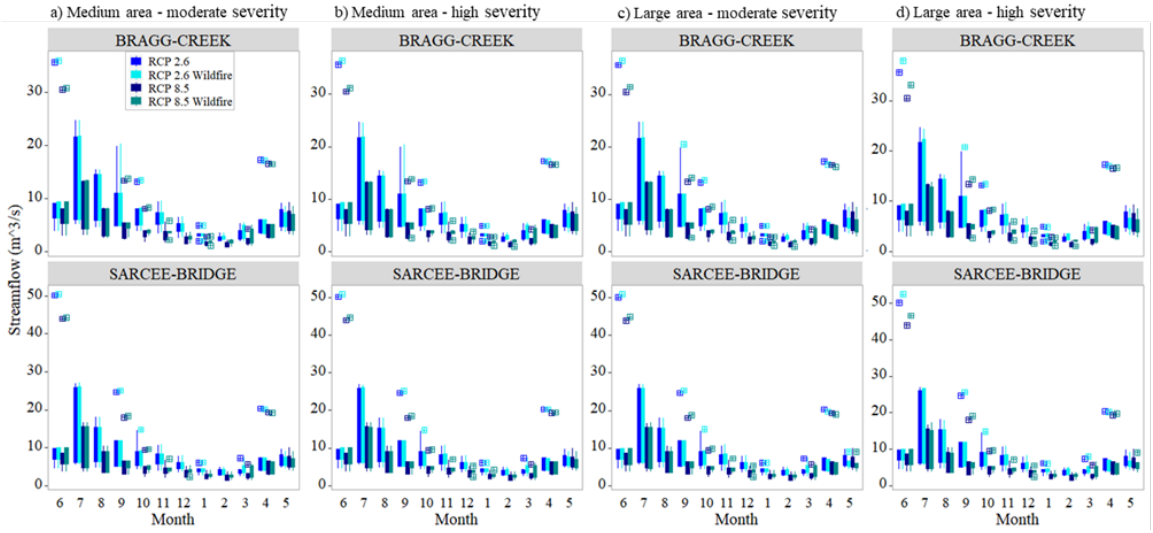

Fig. 3.7. Post-fire streamflow at Bragg Creek and Sarcee Bridge for June 1st wildfire in years 2026, 2027, 2028, 2030 and 2032, and four wildfire scenarios: (a) MM; (b) MH; (c) LM; (d) LH. The ranges illustrated by box plots are based on the annual variabilities in the five simulation years (2026, 2027, 2028, 2030 and 2032).

3.3.4.3 Regional changes: sediments

As was anticipated based on other studies (e.g., Emelko et al., 2011; Writer et al., 2012), the average annual sediment yield in our study increased significantly for all wildfire scenarios (Fig. 3.8; Fig. 3.10). For the RCP 2.6 scenarios, annual sediment yield at Sarcee Bridge increased

by 0.6%, 1.6%, 0.6% and 4.4% for the medium-moderate, medium-high, large-moderate, and large-high burn scenarios, respectively. Comparatively, for the RCP 8.5 scenarios, sediment yield increased by 1.2%, 2.4%, 1.9% and 6.5% for the medium-moderate, medium-high, large-moderate, and large-high burn scenarios, respectively. Sediment yield increases were significantly higher at the Bragg Creek station compared to the Sarcee Bridge station (Fig. 3.10). Although sediment yield by subbasin ranged between 173% to more than 500% (Fig. 3.6), annual increases for in-stream sediment yield ranged from 25–193% at the Bragg Creek station, compared to only 0.6–6.5% at the Sarcee Bridge station. This is because Bragg Creek and Sarcee Bridge stations are over 10 km and 40 km downstream of wildfire-affected areas, respectively, and therefore model results are indicative of in-stream sediment deposition and dilution on the way to the watershed outlet.

In another study area with similar characteristics to the ER watershed, Silins et al., (2009) determined from field-collected data that annual average TSS yields were more than 1000% greater within streams of burned areas compared to non-burned areas. However, a key difference is that their water sampling sites were within the boundaries of the wildfire, and a larger proportion of the drainage area had burned. Water quality impacts depend on total area burned and its location within the watershed (Moody et al., 2013). Similar to the case of streamflow, relative changes were slightly greater for the medium-high scenario than the large-moderate scenario, suggesting that wildfire severity had a larger influence on erosion rates than the total area burned. Reduced TSS transport in the ER watershed typically coincided with decreased streamflow in April and May at the Sarcee Bridge station. The exception was a few slight decreases in August and October for the large-moderate and large-high scenarios, which are likely attributable to high sediment yields in prior months, which can lower availability of

sediments for erosion; in other words, sediments that would otherwise settle and become available for resuspension, were instead transported out of subbasins by surface runoff.

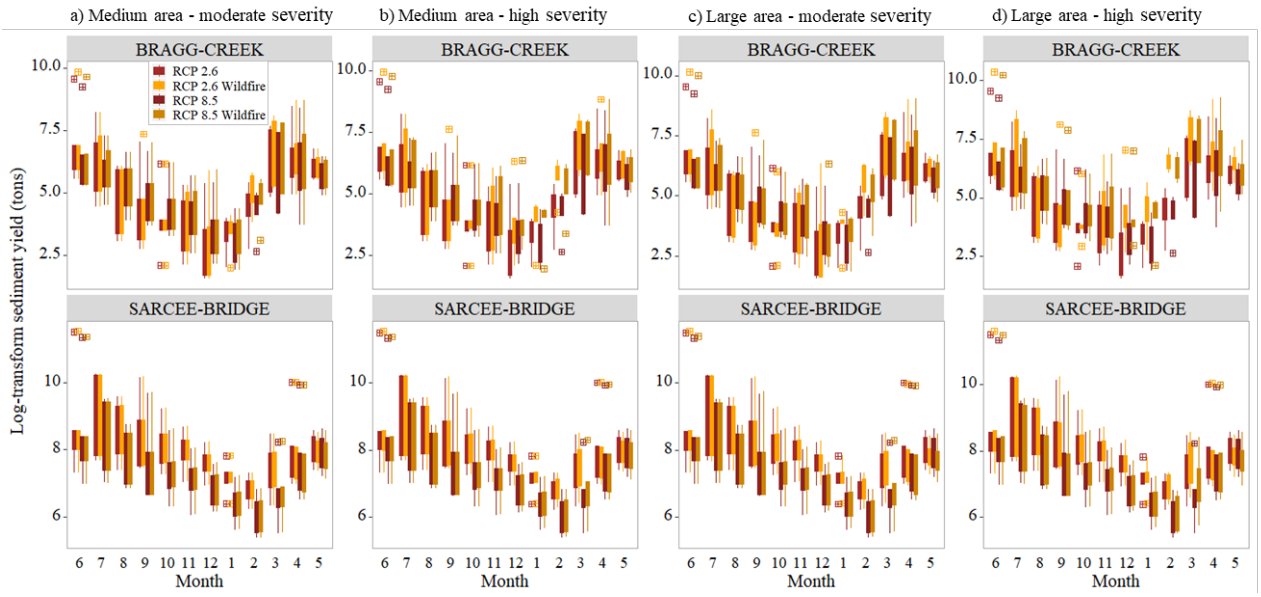

Fig. 3.8. Post-fire sediment yield (log-scale) at Bragg Creek and Sarcee Bridge for June 1st wildfire in the five simulation years (2026, 2027, 2028, 2030 and 2032), and four wildfire scenarios: (a) MM; (b) MH; (c) LM; (d) LH. The ranges illustrated by box plots are based on the annual variabilities in the five simulation years.

3.3.4.4 Regional changes: organic carbon

Wildfire simulations typically resulted in higher annual TOC yields than climate change only scenarios, and all relative changes were greater for the RCP 8.5 than the RCP 2.6 scenarios (Fig. 3.9; Fig. 3.10). For the RCP 2.6 scenario, annual TOC yield at Sarcee Bridge increased by 1.5%, 3.8% and 6.3% for the medium-moderate scenario, the medium-high, and large-high scenarios, respectively, but decreased by 0.47% for the large-moderate scenario. Comparatively, for the RCP 8.5 scenario, annual TOC yield at Sarcee Bridge increased by 1.8%, 5.8% and 13.1% for the medium-moderate scenario, the medium-high, and large-high scenarios, respectively, but decreased by 1.5% for the large-moderate scenario. Relative TOC increases and

decreases were greater for the Bragg Creek station in all scenarios, with the largest relative increase being 19.5% for the large-high scenario. Comparatively, results of the Lost Creek study suggested that DOC concentrations were 50% higher in burned catchments, and that the increases were most pronounced in the first year after the wildfire (Emelko et al., 2011; Silins et al., 2009). However, as mentioned previously, the Lost Creek sampling sites were within the wildfire boundary, where wildfire impacts on water quality were more prominent. Comparable to sediment export, the medium-high scenario yielded more TOC than the large-moderate scenario, meaning wildfire severity has greater impacts on TOC than wildfire size, which in in agreement with findings of other studies (e.g., Abney et al., 2019).

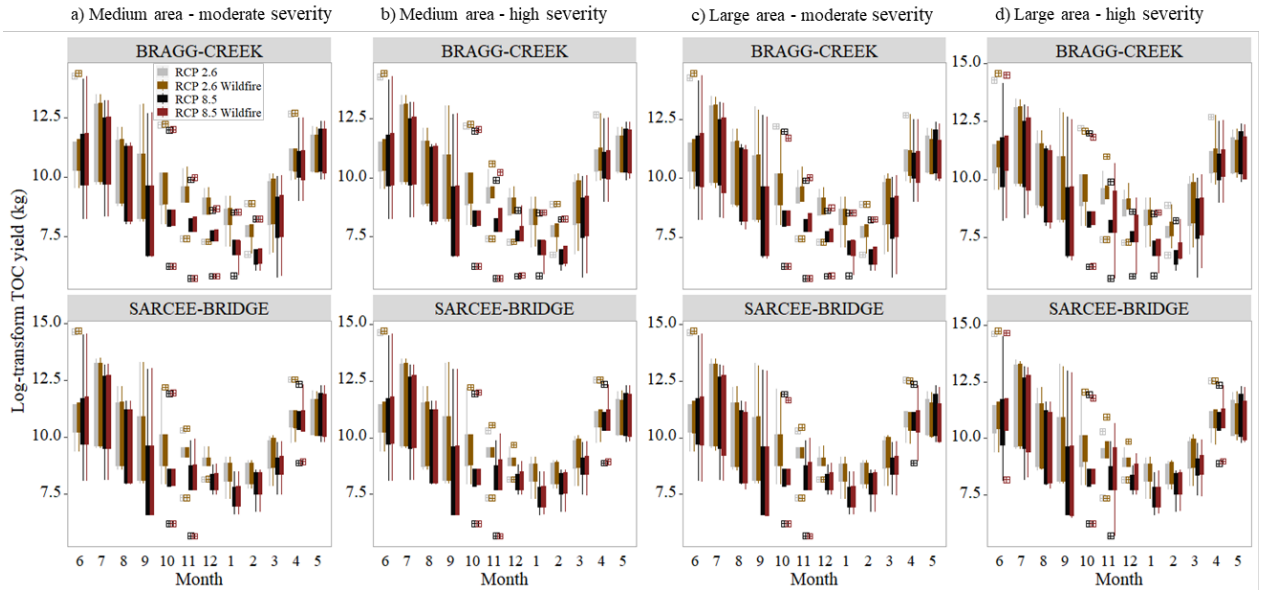

Fig. 3.9. Post-fire total organic carbon yield (log-scale) at Bragg Creek and Sarcee Bridge for June 1st wildfire in years 2026, 2027, 2028, 2030 and 2032, and four wildfire scenarios: (a) MM; (b) MH; (c) LM; (d) LH. The ranges illustrated by box plots are based on the annual variabilities in the five simulation years.

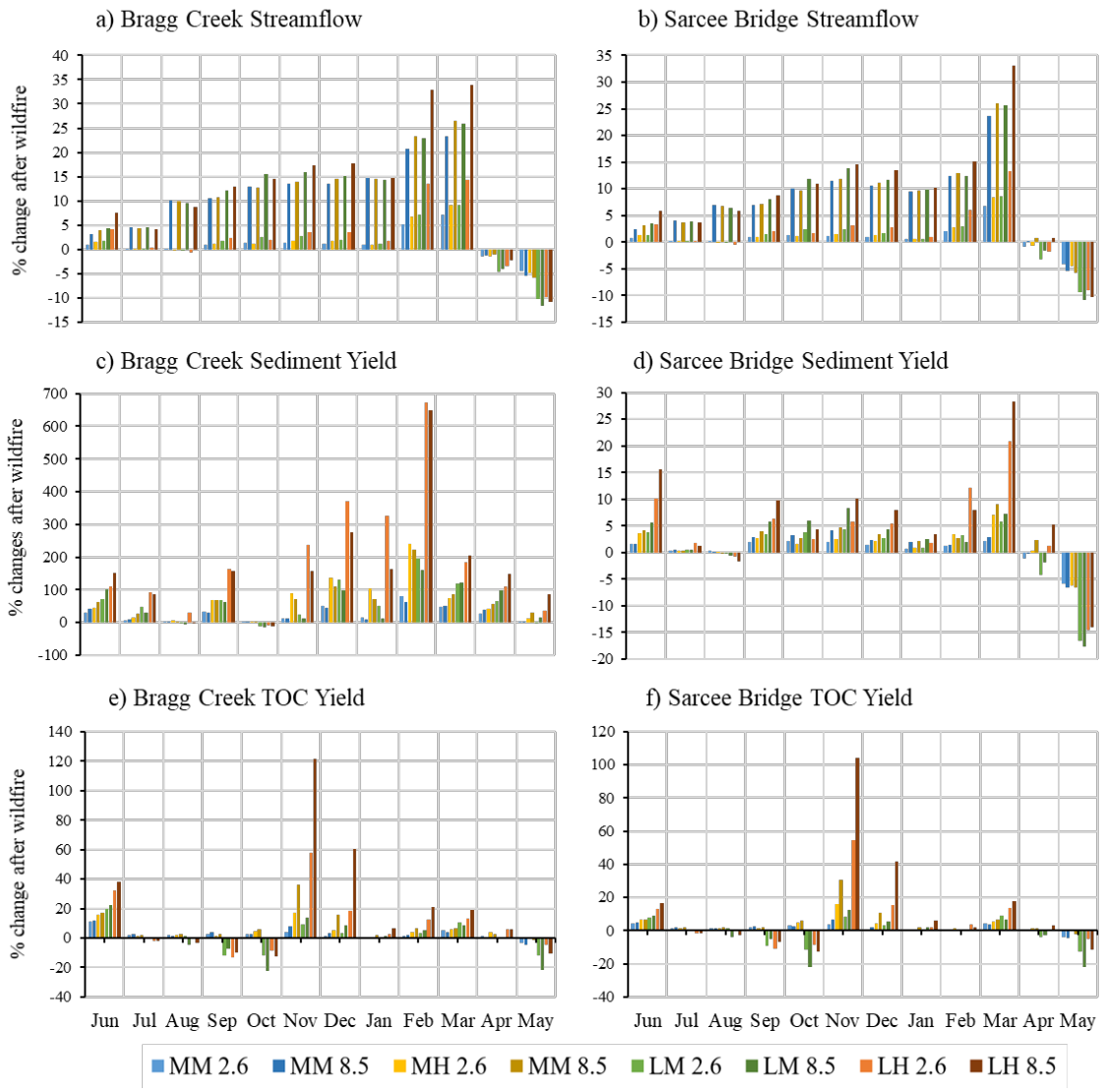

Fig. 3.10. Relative changes in water quantity and quality due to wildfires at Bragg Creek station and Sarcee Bridge station at watershed outlet. All results are the average from wildfire simulations in the year 2026, 2027, 2028, 2030, and 2032. MM = medium area, moderate burn severity; MH = medium area, high burn severity; LM = large area, moderate burn severity; LH = large area, high burn severity.

All wildfire scenarios resulted in higher TOC yields in June. For the medium area wildfires, TOC yields generally increased in all months, with the exception of April and May, due to earlier snowmelt and reduced surface runoff. Water from snowmelt is an important transport mechanism for DOC (Writer et al., 2012), which the model captured in the month of March. However, TOC yields at both stations decreased in summer months and early autumn for

the large burn area scenarios, which contrasted field studies (e.g., Emelko et al., 2011; Writer et al., 2012). In a post-wildfire study of Fourmile Creek, a watershed in Colorado, USA, Writer et al., (2012) determined that in-stream DOC concentrations peaked during the first heavy precipitation event that followed the wildfire, and subsequent summer storms notably increased concentrations. After heavy rains, sediment and DOC levels remained elevated due to dissolution of POC, which underwent repeated deposition and resuspension within streams. As well, sediments in wildfire-affected areas are enriched in OC (Abney et al., 2019), and this was reflected in field data collected by Silins et al., (2009) for the Lost Creek wildfire. In the case of the ER watershed model, we hypothesized that post-wildfire rainstorms in June and snowmelt stripped the top soil layer of OC, and that this deficit led to lower yields in subsequent months. This is because our post-wildfire model inputs did not reflect plant debris, ash and incomplete combustion products, which can act as important sources of OC (e.g., Abney et al., 2019; Smith et al., 2011). In November, TOC yields increased substantially for all wildfire simulations, and these changes were most significant for the high burn severity scenarios. We believe that the OC available for export increased in November because of the addition of plant residue in autumn, which marks the end of the growing season in SWAT, thereby accounting for falling leaves and the death of seasonal plants and replenishing the soil OC supply through decomposition (Zhang et al., 2013).

3.4 Conclusion

Many Western North American regions are statistically overdue for wildfires (e.g., Coogan et al., 2019; Marlon et al., 2012; Rogeau et al., 2016), which could further exacerbate the impacts of climate change on water quality. Few studies have addressed the effects of climate change combined with discrete disturbance events, such as wildfires, on both water quantity and

water quality by linking terrestrial and in-stream processes at the watershed scale. As such, this study aimed to develop a framework to assess the potential response of water quantity and quality to wildfires and climate change scenarios using a physical process-based model, in which the recently developed SWAT Organic Carbon Simulation Module (SWAT-OCSM) was applied to analyze total organic carbon (TOC) loading at the watershed scale. Changes were assessed locally and at the watershed outlet in order to quantify potential changes to water quality entering a reservoir.

For best-case (RCP 2.6) and worst-case (RCP 8.5) climate change scenarios, streamflow, sediment yields, and TOC yields in both near future (2015–2034) and distant future (2043–2062) were compared to baseline conditions (1995–2014). Results indicated that both water quantity and quality will likely decrease in the future, based on reduced streamflow and increased TOC concentrations. Model results suggested that streamflow would drop dramatically in the near future, with distant future streamflow increasing slightly relative to the near future, and less overall water in the RCP 8.5 scenarios compared to the RCP 2.6 scenarios. Thus, our model results reflected projections from other studies (e.g., IPCC, 2014; Schindler and Donahue 2006), with lower overall precipitation and higher temperatures causing earlier spring snowmelt, and significantly lower streamflow in late spring and summer. Intensified precipitation events accelerated erosion, particularly for the RCP 8.5 scenario. On average, results suggested reduced in-stream sediment concentrations (Fig 3.3b; Table 3.3). However, higher erosion rates increase sediment available for transport during storms through resuspension, which can cause higher sediment fluxes for individual events. Suspended sediments can also facilitate the dissolution of organic matter attached to the sediment particles (Cawley et al., 2018). In-stream TOC yields were projected to increase relative to sediments due to faster POC dissolution rates and higher

DOC mobility (Fig. 3c; Table 3.3), diminishing the quality of water entering the reservoir. It is noteworthy that GCMs reflect climate change resulting from anthropogenic greenhouse gas emissions. However, they do not address natural variabilities such as the El Nino Southern Oscillation or the Pacific Decadal Oscillation (e.g., Vaghefi et al., 2019), and these multiannual cycles would likely mediate or exacerbate climate change impacts on water supply.

Results of simulations involving wildfires indicated greater streamflow, sediment yields and TOC yields due to increased surface runoff relative to non-wildfire simulations, and these impacts were evident at the watershed outlet (Fig. 3.10). Much of the sediment and TOC yielded from wildfire-affected subbasins did not reach the reservoir due to in-stream deposition. However, in the event of individual storms, increased availability of sediment and TOC for transport means that remobilization occurs during high water fluxes, and this process can extend wildfire impacts for several years (Emelko et al., 2011; Noske et al., 2010). Wildfires alter local hydrological process, and heavy precipitation events are projected to increase in both frequency and severity, which can ultimately lower downstream water quality through increased sediment and nutrient export, particularly for high severity burns (e.g., Abney et al., 2019; Writer et al., 2012). As our study area ended at the reservoir inlet (Fig 1), this research did not address processes within the reservoir such as deposition of particulate matter or biological nutrient consumption. However, during peak runoff in June, water can be turbid throughout the reservoir (personal observation), and therefore it is likely that both POC and DOC can be present in larger quantities, increasing the need for coagulant and potentially creating harmful disinfection by-products through water treatment processes (Emelko et al., 2011; Hohner et al., 2017).

As it was not possible to calibrate the wildfire scenarios, we compared results to studies in other locations to assess our framework (e.g., Havel et al., 2018; Writer et al., 2012). Based on

these correlations, the approach developed herein was determined to be a substantial step towards simulating impacts of potential wildfires. Notwithstanding this progress made, further improvements could be incorporated into future work. Post-wildfire parameterization for the ER watershed SWAT model assumed uniform burning within wildfire perimeters, whereas burn severity is often heterogeneous and based on factors such as elevation and aspect (e.g., Rogeau & Armstrong 2017). Therefore, allowing patches of trees to remain could create scenarios that are more realistic. This approach would maintain a proportion of canopy protection from rainfall, in addition to intercepting a portion of surface runoff and the transport of water quality constituents. Additionally, post-wildfire parameters within the model remained static, when in reality they would change with time. As an example, while relative changes in soil erodibility (Moody et al., 2009) and hydraulic conductivity (Ebel et al., 2017) can linger for several years after a wildfire, they typically diminish over time. As well, plant debris and ash accumulate after wildfires, and can be transported to streams by surface runoff, decreasing water quality for years after wildfires (e.g., Smith et al., 2011). Since the only terrestrial OC sources in our model were initial soil content and plant residues (Zhang et al., 2013), in-stream TOC was elevated for a short period following wildfire simulations, during which a large proportion of soil OC was removed by surface runoff during post-wildfire rain events. This occurred more quickly than plant residue could replenish the OC supply, and therefore relative in-stream TOC levels decreased for several months afterwards relative to non-wildfire simulations, when they would be expected to remain elevated (e.g., Emelko et al., 2011; Writer et al., 2012). Therefore, we propose the addition of highly erodible and low-density soil layer with elevated TOC content that gradually erodes with storms (e.g., Doerr et al., 2009). Additionally, it would be beneficial for the SWAT-OCSM to differentiate between different OC compounds such as pyrogenic carbon, which acts as a sorbent

for organic matter and can remain within watersheds for decades (Abney et al., 2019). Finally, since impacts can persist for years, additional scenarios such as tree planting or natural succession could provide a long-term perspective on the impacts of wildfires on watersheds.

Although many researchers have collected post-wildfire field data (e.g., Abney et al., 2019; Cotrufo et al., 2016; Ebel et al., 2012; Emelko et al., 2011; Silins et al., 2009; Writer et al., 2014), relevant pre-wildfire data rarely exist for the same study areas due to the unpredictability of wildfire occurrences. Furthermore, responses to wildfire are highly variable, both between watersheds and within a single wildfire boundary, as they are affected by properties such as soil, vegetation, topography, climate, and burn severity (e.g., González-Pérez et al., 2004; Plaza-Álvarez et al., 2018; Smith et al., 2011). The previous statements highlight the necessity for environmental monitoring in various watersheds in order to establish baseline conditions. This could include the installment of climate stations, hydrometric stations, or the collection of soil and water quality samples, which provide valuable data for identifying key environmental changes that result from extreme weather events, human activity, climate change, or any combination thereof. In short, field data spanning a diversity of landscapes and climatic regimes are an important precursor to scenario analyses and future projections, particularly in the case of extreme events and disturbances, which can have almost immediate impacts on water quality.

3.5 Acknowledgements

We would like to thank the City of Calgary for providing water quality data. D.L. was the primary author and executor of scenario analyses. X.D. modified the SWAT code to simulate wildfires. K.D.B. was a consultant for parameterization of the wildfire simulations and revised the paper. D.S.A. and M.F. supervised this work and revised the paper.

Funding for this study has been received from Campus Alberta Innovation Program Chair (Grant #RES0034497), and Natural Sciences and Engineering Research Council of Canada (Grant #RES0043463).

3.6 References

Abney, R. B., Kuhn, T. J., Chow, A., Hockaday, W., Fogel, M. L., & Berhe, A. A. (2019). Pyrogenic carbon erosion after the Rim Fire, Yosemite National Park: the role of burn severity and slope. *Journal of Geophysical Research: Biogeosciences*, *124*(2), 1–18. https://doi.org/10.1029/2018jg004787

Alberta Wildfire (2019). accessed May 2019, <https://wildfire.alberta.ca/resources/historical-data/historical-wildfire-database.aspx>

Azari, M., Saghafian, B., Moradi, H. R., & Faramarzi, M. (2017). Effectiveness of Soil and Water Conservation Practices Under Climate Change in the Gorganroud Basin, Iran. *Clean - Soil, Air, Water*, *45*(8), 1–12. https://doi.org/10.1002/clen.201700288

Bladon, K. D., Emelko, M. B., Silins, U., & Stone, M. (2014). Wildfire and the future of water supply. *Environmental Science and Technology*, *48*(16), 8936–8943. https://doi.org/10.1021/es500130g

Bladon, K. D., Silins, U., Wagner, M. J., Stone, M., Emelko, M. B., Mendoza, C. A., Devito, K. J., & Boon, S. (2008). Wildfire impacts on nitrogen concentration and production from headwater streams in southern Alberta's Rocky Mountains. *Canadian Journal of Forest Research*, *38*(9), 2359–2371. https://doi.org/10.1139/X08-071

Cannon A. J. (2015). Selecting GCM scenarios that span the range of changes in a multimodel ensemble: application to cmip5 climate extremes indices. *Journal of Climate 28*, 1260–1267. https://doi.org/10.1175/JCLI-D-14-00636.1

Cawley, K. M., Hohner, A. K., McKee, G. A., Borch, T., Omur-Ozbek, P., Oropeza, J., & Rosario-Ortiz, F. L. (2018). Characterization and spatial distribution of particulate and soluble carbon and nitrogen from wildfire-impacted sediments. *Journal of Soils and Sediments*, *18*(4), 1314–1326. https://doi.org/10.1007/s11368-016-1604-1

Coogan, S. C. P., Robinne, F.-N., Jain, P., & Flannigan, M. D. (2019). Scientists' warning on wildfire — a Canadian perspective. *Canadian Journal of Forest Research*, *49*(9), 1015–1023. https://doi.org/10.1139/cjfr-2019-0094

Cotrufo, M. F., Boot, C. M., Kampf, S., Nelson, P. A., Brogan, D. J., Covino, T., Haddix, M. L., MacDonald, L. H., Rathburn, S., Ryan-Bukett, S., Schmeer, S., & Hall, E. (2016). Redistribution of pyrogenic carbon from hillslopes to stream corridors following a large montane wildfire. *Global Biogeochemical Cycles*, *30*(9), 1348–1355. https://doi.org/10.1002/2016GB005467.Received

Deryng, D., Elliott, J., Folberth, C., Müller, C., Pugh, T. A. M., Boote, K. J., Conway, D., Ruane, A. C., Gerten, D., Jones, J. W., Khabarov, N., Olin, S., Schaphoff, S., Schmid, E., Yang, H., & Rosenzweig, C. (2016). Regional disparities in the beneficial effects of rising CO2 concentrations on crop water productivity. *Nature Climate Change*, *6*(8), 786–790. https://doi.org/10.1038/nclimate2995

Doerr, S. H., Woods, S. W., Martin, D. A., & Casimiro, M. (2009). "Natural background" soil

water repellency in conifer forests of the north-western USA: Its prediction and relationship to wildfire occurrence. *Journal of Hydrology*, *371*(1–4), 12–21. https://doi.org/10.1016/j.jhydrol.2009.03.011

Du, X., Loiselle, D., Alessi, D.S., Faramarzi, M. (2019a). Incorporation of a process-based in-stream organic carbon module into SWAT to simulate organic carbon load and transport at the watershed scale. *manuscrip in preparation*.

Ebel, B. A., & Moody, J. A. (2017). Synthesis of soil-hydraulic properties and infiltration timescales in wildfire-affected soils. *Hydrological Processes*, *31*(2), 324–340. https://doi.org/10.1002/hyp.10998

Ebel, B. A., Moody, J. A., & Martin, D. A. (2012). Hydrologic conditions controlling runoff generation immediately after wildfire. *Water Resources Research*, *48*(3), 1–13. https://doi.org/10.1029/2011WR011470

Emelko, M. B., Silins, U., Bladon, K. D., & Stone, M. (2011). Implications of land disturbance on drinking water treatability in a changing climate: Demonstrating the need for "source water supply and protection" strategies. *Water Research*, *45*(2), 461–472. https://doi.org/10.1016/j.watres.2010.08.051

Emelko, M. B., Stone, M., Silins, U., Allin, D., Collins, A. L., Williams, C. H. S., Martens, A. M., & Bladon, K. D. (2016). Sediment-phosphorus dynamics can shift aquatic ecology and cause downstream legacy effects after wildfire in large river systems. *Global Change Biology*, *22*(3), 1168–1184. https://doi.org/10.1111/gcb.13073

Farjad, B., Gupta, A., & Marceau, D. J. (2016). Annual and Seasonal Variations of Hydrological Processes Under Climate Change Scenarios in Two Sub-Catchments of a Complex Watershed. *Water Resources Management*, *30*(8), 2851–2865. https://doi.org/10.1007/s11269-016-1329-3

Fischer, H., Sachse, A., Steinberg, C. E. W., & Pusch, M. (2002). Differential Retention and Utilization of Dissolved Organic Carbon by Bacteria in River Sediments. *Limnology and Oceanography*, *47*(6), 1702–1711. https://doi.org/10.4319/lo.2002.47.6.1702

Flannigan, M. D., Logan, K. A., Amiro, B. D., Skinner, W. R., & Stocks, B. J. (2005). Future area burned in Canada. *Climatic Change*, *72*(1–2), 1–16. https://doi.org/10.1007/s10584-005-5935-y

Gartner, J. E., Cannon, S. H., Santi, P. M., & Dewolfe, V. G. (2008). Empirical models to predict the volumes of debris flows generated by recently burned basins in the western U.S. *Geomorphology*, *96*(3–4), 339–354. https://doi.org/10.1016/j.geomorph.2007.02.033

Hallema, D. W., Robinne, F.-N., & Bladon, K. D. (2018). Reframing the Challenge of Global Wildfire Threats to Water Supplies. *Earth's Future*, *6*(6), 772–776. https://doi.org/10.1029/2018EF000867

Havel, A., Tasdighi, A., & Arabi, M. (2018). Assessing the long-term hydrologic response to wildfires in mountainous regions. *Hydrology and Earth System Sciences*, *22*(25), 2527–

2550. https://doi.org/10.5194/hess-2017-604

Hernandez, A. J., Healey, S. P., Huang, H., & Ramsey, R. D. (2018). Improved prediction of stream flow based on updating land cover maps with remotely sensed forest change detection. Forests, 9(6), 1–19. https://doi.org/10.3390/f9060317

Hohner, A. K., Cawley, K., Oropeza, J., Summers, R. S., & Rosario-Ortiz, F. L. (2016). Drinking water treatment response following a Colorado wildfire. *Water Research*, *105*, 187–198. https://doi.org/10.1016/j.watres.2016.08.034

Hohner, A. K., Terry, L. G., Townsend, E. B., Summers, R. S., & Rosario-Ortiz, F. L. (2017). Water treatment process evaluation of wildfire-affected sediment leachates. *Environmental Science: Water Research and Technology*, *3*(2), 352–365. https://doi.org/10.1039/c6ew00247a

IPCC (2013): Climate Change 2013: The Physical Science Basis. Contribution of Working Group I to the Fifth Assessment Report of the Intergovernmental Panel on Climate Change [Stocker, T. F., Qin, D., Plattner, G.-K., Tignor, M., Allen, S. K., Boschung, J., Nauels, A. Xia, Y., Bex, V. & Midgley, P. M. (eds.)]. Cambridge University Press, Cambridge, United Kingdom and New York, NY, USA, 1535.

Kulig, J. C., Edge, D., Reimer, W. (Bill), Townshend, I., & Lightfoot, N. (2009). Levels of Risk: Perspectives from the Lost Creek Fire. *Australian Journal of Emergency Management*, *24*(2), 33–39.

Larsen, S., Andersen, T., & Hessen, D. O. (2011). Climate change predicted to cause severe increase of organic carbon in lakes. *Global Change Biology*, *17*(2), 1186–1192. https://doi.org/10.1111/j.1365-2486.2010.02257.x

Laudon, H., Buttle, J., Carey, S. K., McDonnell, J., McGuire, K., Seibert, J., Shanley, J., Soulsby, C., & Tetzlaff, D. (2012). Cross-regional prediction of long-term trajectory of stream water DOC response to climate change. *Geophysical Research Letters*, *39*(18), 4–9. https://doi.org/10.1029/2012GL053033

Malagó, A., Bouraoui, F., Vigiak, O., Grizzetti, B., & Pastori, M. (2017). Modelling water and nutrient fluxes in the Danube River Basin with SWAT. *Science of the Total Environment*, *603–604*, 196–218. https://doi.org/10.1016/j.scitotenv.2017.05.242

Marlon, J. R., Bartlein, P. J., Gavin, D. G., Long, C. J., Anderson, R. S., Briles, C. E., Brown, K. J., Colombaroli, D., Hallett, D. J., Power, M. J., Scharf, E. A., & Walsh, M. K. (2012). Long-term perspective on wildfires in the western USA. *Proceedings of the National Academy of Sciences*, *109*(9), 3203–3204. https://doi.org/10.1073/pnas.1112839109

Masud, M.B., Ferdous, J., & Faramarzi, M. (2018). Projected changes in hydrological variables in the agricultural region of Alberta, Canada, *Water, 12*(10), DOI: 10.3390/w10121810.

Masud, M. B., Wada, Y., Goss, G., & Faramarzi, M. (2019). Global implications of regional grain production through virtual water trade, *Science of the total environment 659*, 807–820. DOI: 10.1016/j.scitotenv.2018.12.392.

Monteith, J.L. (1965). Evaporation and the environment. In The state and movement of water in living organisms. 19th symposia of the Society for Experimental Biology. Cambridge University Press, London, U.K. 205–234.

Moody, J. A., & Martin, D. A. (2001). Post-fire, rainfall intensity-peak discharge relations for three mountainous watersheds in the Western USA. *Hydrological Processes*, *15*(15), 2981–2993. https://doi.org/10.1002/hyp.386

Moody, J. A., & Martin, D. A. (2009). Synthesis of sediment yields after wildland fire in different rainfall regimes in the western United States. *International Journal of Wildland Fire*, *18*, 96–115. https://doi.org/10.1071/WF07162

Moody, J. A., Shakesby, R. A., Robichaud, P. R., Cannon, S. H., & Martin, D. A. (2013). Current research issues related to post-wildfire runoff and erosion processes. *Earth-Science Reviews*, *122*, 10–37. https://doi.org/10.1016/j.earscirev.2013.03.004

Morán-Tejeda, E., Zabalza, J., Rahman, K., Gago-Silva, A., López-Moreno, J. I., Vicente-Serrano, S., Lehmann, A., Tague, C. L., & Beniston, M. (2015). Hydrological impacts of climate and land-use changes in a mountain watershed: Uncertainty estimation based on model comparison. *Ecohydrology*, *8*(8), 1396–1416. https://doi.org/10.1002/eco.1590

Nalley, J. O., O'Donnell, D. R., & Litchman, E. (2018). Temperature effects on growth rates and fatty acid content in freshwater algae and cyanobacteria. *Algal Research*, *35*, 500–507. https://doi.org/10.1016/j.algal.2018.09.018

Natural Resources Canada (2017), accessed May 2019, <https://www.nrcan.gc.ca/forests/measuring-reporting/classification/13179>

Natural Resources Canada (2018), accessed July 2019. <https://www.nrcan.gc.ca/our-natural-resources/forests-forestry/sustainable-forest-management/boreal-forest/8-facts-about-canadas-boreal-forest/17394>

Niraula, R., Kalin, L., Srivastava, P., & Anderson, C. J. (2013). Identifying critical source areas of nonpoint source pollution with SWAT and GWLF. *Ecological Modelling*, *268*, 123–133. https://doi.org/10.1016/j.ecolmodel.2013.08.007

Noske, P. J., Lane, P. N. J., & Sheridan, G. J. (2010). Stream exports of coarse matter and phosphorus following wildfire in NE Victoria, Australia. *Hydrological Processes*, *24*(11), 1514–1529. https://doi.org/10.1002/hyp.7616

Osborn, G., Stockmal, G., & Haspel, R. (2006). Emergence of the Canadian Rockies and adjacent plains: A comparison of physiography between end-of-Laramide time and the present day. *Geomorphology*, *75*(3–4), 450–477. https://doi.org/10.1016/j.geomorph.2005.07.032

Plaza-Álvarez, P. A., Lucas-Borja, M. E., Sagra, J., Moya, D., Alfaro-Sánchez, R., González-Romero, J., & De las Heras, J. (2018). Changes in soil water repellency after prescribed burnings in three different Mediterranean forest ecosystems. *Science of the Total Environment*, *644*, 247–255. https://doi.org/10.1016/j.scitotenv.2018.06.364

Pomeroy, J. W., Gray, D. M., Brown, T., Hedstrom, N. R., Quinton, W. L., Granger, R. J., & Carey, S. K. (2007). The cold regions hydrological model: a platform for basing process representation and model structure on physical evidence. *Hydrological Processes*, *21*, 2650–2667. https://doi.org/10.1002/hyp

Rhoades, C. C., Chow, A. T., Covino, T. P., Fegel, T. S., Pierson, D. N., & Rhea, A. E. (2019). The Legacy of a Severe Wildfire on Stream Nitrogen and Carbon in Headwater Catchments. *Ecosystems*, *22*(3), 643–657. https://doi.org/10.1007/s10021-018-0293-6

Robichaud, P. R., Wagenbrenner, J. W., Pierson, F. B., Spaeth, K. E., Ashmun, L. E., & Moffet, C. A. (2016). Infiltration and interrill erosion rates after a wildfire in western Montana, USA. *Catena*, *142*, 77–88. https://doi.org/10.1016/j.catena.2016.01.027

Robinne, F. N., Bladon, K. D., Miller, C., Parisien, M. A., Mathieu, J., & Flannigan, M. D. (2018). A spatial evaluation of global wildfire-water risks to human and natural systems. *Science of the Total Environment, 610–611*, 1193–1206. https://doi.org/10.1016/j.scitotenv.2017.08.112

Robinne, F. N., Bladon, K. D., Silins, U., Emelko, M. B., Flannigan, M. D., Parisien, M. A., Wang, X., Kienzle, S. W., & Dupont, D. P. (2019). A regional-scale index for assessing the exposure of drinking-water sources to wildfires. *Forests, 10*(5), 1–21. https://doi.org/10.3390/f10050384

Robinne, F. N., Miller, C., Parisien, M. A., Emelko, M. B., Bladon, K. D., Silins, U., & Flannigan, M. (2016). A global index for mapping the exposure of water resources to wildfire. *Forests, 7*(1), 1–16. https://doi.org/10.3390/f7010022

Rodrigues, E. L., Jacobi, C. M., & Figueira, J. E. C. (2019). Wildfires and their impact on the water supply of a large neotropical metropolis: A simulation approach. *Science of the Total Environment*, *651*, 1261–1271. https://doi.org/10.1016/j.scitotenv.2018.09.289

Rodríguez-Jeangros, N., Hering, A. S., & McCray, J. E. (2018). Analysis of anthropogenic, climatological, and morphological influences on dissolved organic matter in Rocky Mountain streams. *Water (Switzerland)*, *10*(4), 1–46. https://doi.org/10.3390/w10040534

Rogeau, M.-P., & Armstrong, G. W. (2017). Quantifying the effect of elevation and aspect on fire return intervals in the Canadian Rocky Mountains. *Forest Ecology and Management*, *384*, 248–261. https://doi.org/10.1016/j.foreco.2016.10.035

Rogeau, M.-P., Flannigan, M. D., Hawkes, B. C., Parisien, M.-A., & Arthur, R. (2016). Spatial and temporal variations of fire regimes in the Canadian Rocky Mountains and Foothills of southern Alberta. *International Journal of Wildland Fire*, *25*, 1117–1130. https://doi.org/10.1071/WF15120

Rostami, S., He, J., & Hassan, Q. K. (2018). Riverine water quality response to precipitation and its change. *Environments*, *5*(1), 1–17. https://doi.org/10.3390/environments5010008

Runkel, R.L., Crawford, C.G., & Cohn, T.A. (2004). Load Estimator (LOADEST): A FORTRAN program for estimating constituent loads in streams and rivers. Techniques and

Methods 4-A5, https://doi.org/10.3133/tm4A5

Rust, A. J., Hogue, T. S., Saxe, S., & McCray, J. (2018). Post-fire water-quality response in the western United States. *International Journal of Wildland Fire*, *27*(3), 203–216. https://doi.org/10.1071/WF17115

Schindler, D. W., & Donahue, W. F. (2006). An impending water crisis in Canada's western prairie provinces. *Proceedings of the National Academy of Sciences*, *103*(19), 7210–7216. https://doi.org/10.1073/pnas.0601568103

Shakesby, R. A., Bento, C. P. M., Ferreira, C. S. S., Ferreira, A. J. D., Stoof, C. R., Urbanek, E., & Walsh, R. P. D. (2015). Impacts of prescribed fire on soil loss and soil quality: An assessment based on an experimentally-burned catchment in central Portugal. *Catena*, *128*, 278–293. https://doi.org/10.1016/j.catena.2013.03.012

Shrestha, N. K., Du, X., & Wang, J. (2017). Assessing climate change impacts on fresh water resources of the Athabasca River Basin, Canada. *Science of the Total Environment*, *601–602*, 425–440. https://doi.org/10.1016/j.scitotenv.2017.05.013

Shrestha, N. K., & Wang, J. (2018). Predicting sediment yield and transport dynamics of a cold climate region watershed in changing climate. *Science of the Total Environment*, *625*, 1030–1045. https://doi.org/10.1016/j.scitotenv.2017.12.347

Silins, U., Stone, M., Emelko, M. B., & Bladon, K. D. (2009). Sediment production following severe wildfire and post-fire salvage logging in the Rocky Mountain headwaters of the Oldman River Basin, Alberta. *Catena*, *79*(3), 189–197. https://doi.org/10.1016/j.catena.2009.04.001

Smith, H. G., Sheridan, G. J., Lane, P. N. J., Nyman, P., & Haydon, S. (2011). Wildfire effects on water quality in forest catchments: A review with implications for water supply. *Journal of Hydrology*, *396*(1–2), 170–192. https://doi.org/10.1016/j.jhydrol.2010.10.043

Sosiak, A., & Dixon, J. (2006). Impacts on water quality in the upper Elbow River. *Water Science and Technology*, *53*(10), 309–316. https://doi.org/10.2166/wst.2006.326

Technical Support Document for Ontario Drinking Water Standards (2006), Objectives and Guidelines, June 2003, Revised June 2006, PIBS 4449e01.

Teshager, A. D., Gassman, P. W., Secchi, S., Schoof, J. T., & Misgna, G. (2016). Modeling Agricultural Watersheds with the Soil and Water Assessment Tool (SWAT): Calibration and Validation with a Novel Procedure for Spatially Explicit HRUs. *Environmental Management*, *57*(4), 894–911. https://doi.org/10.1007/s00267-015-0636-4

Townsend, S. A., & Douglas, M. M. (2000). The effect of a wildfire on stream water quality and catchment water yield in a tropical savanna excluded from fire for 10. *Journal of Hydrology*, *229*, 118–137. Retrieved from http://espace.library.cdu.edu.au/view.php?pid=cdu:1488

Townsend, S. A., & Douglas, M. M. (2004). The effect of a wildfire on stream water quality and catchment water yield in a tropical savanna excluded from fire for 10 years (Kakadu

National Park, North Australia). *Water Research*, *38*(13), 3051–3058. https://doi.org/10.1016/j.watres.2004.04.009

Vaghefi, S.A., Iravani, M., Sauchyn, D., Andreichuk, Y., Goss, G., Faramarzi, M. (2019). Regionalization and parameterization of a hydrologic model significantly affect the cascade of uncertainty in climate-impact projections. *Climate Dynamics, 53*(5–6), 2861–2886. DOI: https://doi.org/10.1007/s00382-019-04664-w

Wang, X., Thompson, D. K., Marshall, G. A., Tymstra, C., Carr, R., & Flannigan, M. D. (2015). Increasing frequency of extreme fire weather in Canada with climate change. *Climatic Change*, *130*(4), 573–586. https://doi.org/10.1007/s10584-015-1375-5

Wijesekara, G. N., Farjad, B., Gupta, A., Qiao, Y., Delaney, P., & Marceau, D. J. (2014). A comprehensive land-use/hydrological modeling system for scenario simulations in the Elbow River watershed, Alberta, Canada. *Environmental Management*, *53*(2), 357–381. https://doi.org/10.1007/s00267-013-0220-8

Williams, J.R. (1995). Chapter 25: The EPIC model. P. 909–1000. In V.P. Singh (ed) Computer models of watershed hydrology. Water Resources Publications.

Willmore, N. Jensen, H.G. (1960). Alberta's Forests, Government of the Province of Alberta, Department of Lands and Forests, Edmonton.

Worku, T., Khare, D., & Tripathi, S. K. (2017). Modeling runoff–sediment response to land use/land cover changes using integrated GIS and SWAT model in the Beressa watershed. *Environmental Earth Sciences*, *76*(16), 1–14. https://doi.org/10.1007/s12665-017-6883-3

Writer, J H, McCleskey, R. B., & Murphy, S. F. (2012). Effects of wildfire on source-water quality and aquatic ecosystems, Colorado Front Range. *Wildfire and Water Quality: Processes, Impacts, and Challenges*, (IAHS Publ. 354), 117–123.

Writer, Jeffrey H., Hohner, A., Oropeza, J., Schmidt, A., Cawley, K., & Rosario-Ortiz, F. L. (2014). Water treatment implications after the High Park Wildfire in Colorado. *American Water Works Association*, *106*(4), 189–199. https://doi.org/10.5942/jawwa.2014.106.0055

Yang, Qi, Leon, L. F., Booty, W. G., Wong, I. W., McCrimmon, C., Fong, P., Fong, P., Michiels, P., Vanrobaeys, J., & Benoy, G. (2014). Land Use Change Impacts on Water Quality in Three Lake Winnipeg Watersheds. *Journal of Environment Quality*, *43*(5), 1690–1701. https://doi.org/10.2134/jeq2013.06.0234

Yu, M., Bishop, T. F. A., & Van Ogtrop, F. F. (2019). Assessment of the decadal impact of wildfire on water quality in forested catchments. *Water (Switzerland)*, *11*(3), 1–17. https://doi.org/10.3390/w11030533

Zhang, X., Izaurralde, R. C., Arnold, J. G., Williams, J. R., & Srinivasan, R. (2013). Modifying the Soil and Water Assessment Tool to simulate cropland carbon flux: Model development and initial evaluation. *Science of the Total Environment, 463–464*, 810–822. https://doi.org/10.1016/j.scitotenv.2013.06.056

CHAPTER IV – CONCLUSION

4.1 Research Summary

The primary goal of this research was to develop a framework for assessing the response of water quantity and quality sediment and TOC in watersheds under various climate change and wildfire scenarios. An enhanced Soil and Water Assessment Tool (SWAT) that embeds SWAT Organic Carbon Simulation Module (SWAT-OCSM) was applied to the Elbow River watershed to assess model performance. This study watershed was ideal because of its importance as a drinking water source for residents of Calgary, along with its complexity resulting from varying hydro-climatic conditions, landscapes, vegetation, and soil properties. As well, few watersheds have water quality data as extensive as those collected by the City of Calgary. After calibrating streamflow, sediment yields, and TOC yields, we assessed the performance of the SWAT-OCSM in simulating TOC dynamics in the watershed. The following step was to apply scenario analyses to the calibrated model. First, we developed a framework for simulating wildfires in SWAT, for which we modified the source code to change land cover and soil properties within a specified region to reflect post-wildfire conditions. Previous studies (Ebel & Moody, 2017; Havel et al., 2018; Moody & Martin, 2009) influenced our post-wildfire parameterization. Relative changes in streamflow, sediment yields and TOC yields were then analyzed for climate change scenarios. The second part of scenario analyses involved combining wildfire scenarios with climate change scenarios, for which we analyzed changes relative to the non-wildfire scenarios, both within the wildfire perimeter and at the watershed outlet. Finally, model outputs of our wildfire scenarios were compared to those from other studies, although there is limited research that fits into the scope of this project (e.g., Abney et al., 2019; Emelko et al., 2011; Havel et al., 2018; Morán-Tejeda et al., 2015; Silins et al., 2009).

We incorporated the parsimonious SWAT-OCSM into the existing soil organic carbon module of SWAT by modifying the source code. This module allowed for simulation of both particulate organic carbon (POC) and dissolved organic carbon (DOC) within the water column, in addition to reactions such as interactions of organic carbon with algae, dissolution of POC, and mineralization of DOC. Thus, we could model terrestrial TOC transport, such as erosion or shallow groundwater flow, and their contributions to in-stream TOC content. We obtained satisfactory results for simulating monthly TOC loads at both stations used for calibration. The model successfully captured the seasonality of TOC export, which closely followed streamflow and sediment export patterns, reinforcing the importance of both terrestrial and aquatic processes in TOC cycling. Snowmelt and rainfall runoff events in the Elbow River watershed were the driving forces behind annual peaks in streamflow, sediment yields, and TOC yields that occur in the late spring and early summer. The importance of understanding controls behind the organic carbon cycle is underscored by the close relationship between cycling of different nutrients (e.g., organic carbon, nitrogen, and phosphorous), in addition to water quality impacts of TOC.

Following the successful simulation of TOC dynamics at the watershed scale, we applied climate change and wildfire scenarios. Baseline conditions were defined for the 1995–2014 period, which were used to compare relative changes in streamflow, sediment yields, and TOC yields in both near future (2015–2034) and distant future (2043–2062). For both the best-case (RCP 2.6) and worst-case (RCP 8.5) climate change scenarios, we used the average of an ensemble of five GCMs that are downscaled to local conditions. Future projections indicated significantly lower streamflow, particularly between May–August, and that the distant future would have slightly greater streamflow than the near future time period. Interestingly, annual streamflow decreased by 25.3% and 46.9% for the near future RCP 2.6 and RCP 8.5 scenarios,

respectively, and by 9.9% and 31.8% for the distant future RCP 2.6 and RCP 8.5 scenarios, respectively, compared to the baseline period, due to higher precipitation and lower plant water uptake in the distant future. In each month, the RCP 2.6 scenario showed higher streamflow than the RCP 8.5 scenario. Sediment yield projections followed similar trends to streamflow, and suggested lower average sediment concentrations entering the reservoir. In contrast, TOC yield projections were higher in the near future compared to the distant future, which we partly attributed to the impact of higher temperatures accelerating mineralization of DOC. Higher relative TOC content indicated future degradation of water quality entering the reservoir, particularly in the near future.

The next step was to analyze wildfire impacts combined with near future climate change scenarios, in which two perimeters encompassing 6,108 ha and 23,984 ha were defined for simulating moderate and high severity burns, making four total wildfire scenarios. Due to the removal of forest canopy, surface runoff in wildfire-affected subbasins increased within a range of 11% to over 500%, leading to local increases in sediment yields and TOC yields of similar magnitudes, and increasing streamflow by 0.7–9.3% at the watershed outlet. Low stream power in the near future caused the majority of sediments and TOC yielded from burned catchments to settle on the streambed, and therefore water quality impacts were less prominent at the watershed outlet. However, total loads entering the reservoir increased between 0.6–6.5% for sediments, and changes between -1.5% and +13.1% were observed for TOC loads. All relative changes were more prominent for wildfire simulations combined with RCP 8.5 scenarios, suggesting that the worst-case climate change scenario would have the most detrimental impacts on water quality if a wildfire were to occur. As well, results indicated that the watershed was more sensitive to burn severity than total area burned, as medium area wildfires with high burn

severities had larger impacts on water quality than large area wildfires with moderate burn severities.

4.2 Study limitations and future directions

Hydrological models inherently simplify processes, and therefore are not fully representative of the complexity of water, sediment, and nutrient cycling occurring within watersheds. For example, land cover remained static throughout calibration and scenario analyses, with the exception of land cover changes related to wildfires; however, changes such as urbanization or deforestation alter hydrology and associated sediment and nutrient transport. Additionally, the model simulates consistent streamflow throughout the day and therefore does not account for fluctuations on a smaller timescale, which could also affect transport of water quality constituents. Sediment and TOC concentrations can vary spatially and temporally, but we assumed that concentrations from in-stream samples were representative of the entire water column when calibrating the model. There was only TOC data available for calibration, and while the SWAT-OCSM simulates both POC and DOC, it was not possible to verify how well the model differentiated between the two fractions. As well, the POC and DOC fractions could be further subdivided into different components based on the decay rates of organic matter (Sempéré et al., 2000), or to represent compounds such as pyrogenic carbon in the case of wildfire simulations. Further refinement is required for the wildfire modelling approach in SWAT, which would require testing broader parameter ranges related to land cover and soil properties. However, it is rare to have both pre-wildfire and post-wildfire field data for a single watershed, and therefore few studies were available with which to compare these model outputs. A solid addition to our framework would be a temporary layer of wildfire remains (i.e., ash, plant debris, organic carbon compounds such as pyrogenic carbon) that degrades and erodes over time,

which would alter local hydrology and downstream water quality. Nevertheless, this work has been an important step for projecting possible impacts of wildfire on water quality at the watershed scale. Our research has also highlighted the importance of establishing baseline conditions in watersheds through field monitoring in order to increase general understanding of the processes that govern water, sediment and nutrient cycling, and the relative changes caused by climate change and disturbance events.

It is clear that the cumulative effects of climate change, extreme events, and disturbances are altering the water cycle and associated transport of suspended and dissolved compounds (i.e., nutrients, soil particles, minerals, metals, etc.). Therefore, simulating dynamics at the watershed scale and analyzing various scenarios can be useful for projecting the future of water quantity and quality. Studies such as these may help policy makers and water treatment facilities to be proactive in facing the uncertain future of water resources.

BIBLIOGRAPHY

Abbaspour 2007, K. C. (2007). SWAT-CUP: Calibration and Uncertainty Programs – A User Manual. EAWAG: Swiss Federal Institute of Aquatic Science and Technology.

Abney, R. B., Kuhn, T. J., Chow, A., Hockaday, W., Fogel, M. L., & Berhe, A. A. (2019). Pyrogenic carbon erosion after the Rim Fire, Yosemite National Park: the role of burn severity and slope. *Journal of Geophysical Research: Biogeosciences*, *124*(2), 1–18. https://doi.org/10.1029/2018jg004787

Alberta Environment and Parks, (2012). Standards and Guidelines for Municipal Waterworks, Wastewater and Storm Drainage Systems. Alberta Environment and Sustainable Resource Development, Edmonton, Alberta. ISBN: 978-0-7785-9634-9.

Alberta Wildfire (2019). accessed May 2019, <https://wildfire.alberta.ca/resources/historical-data/historical-wildfire-database.aspx>

Amiro, B. D., Cantin, A., Flannigan, M. D., & de Groot, W. J. (2009). Future emissions from Canadian boreal forest fires. *Canadian Journal of Forest Research 39*(2). https://doi.org/10.1139/X08-154

Asadzadeh, M., Leon, L., Yang, W., Bosch, D., 2016. One-day offset in daily hydrologic modeling: An exploration of the issue in automatic model calibration. *Journal of Hydrology 534*, 164–177. https://doi.org/10.1016/j.jhydrol.2015.12.056

Azari, M., Saghafian, B., Moradi, H. R., & Faramarzi, M. (2017). Effectiveness of Soil and Water Conservation Practices Under Climate Change in the Gorganroud Basin, Iran. *Clean - Soil, Air, Water*, *45*(8), 1–12. https://doi.org/10.1002/clen.201700288

Bladon, K. D., Emelko, M. B., Silins, U., & Stone, M. (2014). Wildfire and the future of water supply. *Environmental Science and Technology*, *48*(16), 8936–8943. https://doi.org/10.1021/es500130g

Bladon, K. D., Silins, U., Wagner, M. J., Stone, M., Emelko, M. B., Mendoza, C. A., Devito, K. J., & Boon, S. (2008). Wildfire impacts on nitrogen concentration and production from headwater streams in southern Alberta's Rocky Mountains. *Canadian Journal of Forest Research*, *38*(9), 2359–2371. https://doi.org/10.1139/X08-071

Brandt, J. P., Flannigan, M. D., Maynard, D. G., Thompson, I. D., & Volney, W. J. A. (2013). An introduction to Canada's boreal zone: ecosystem processes, health, sustainability, and environmental issues. *Environmental Reviews*, *21*(4), 207–226. https://doi.org/10.1139/er-2013-0040

Cannon A. J. (2015). Selecting GCM scenarios that span the range of changes in a multimodel ensemble: application to cmip5 climate extremes indices. *Journal of Climate 28*, 1260–1267. https://doi.org/10.1175/JCLI-D-14-00636.1

Cawley, K. M., Hohner, A. K., McKee, G. A., Borch, T., Omur-Ozbek, P., Oropeza, J., & Rosario-Ortiz, F. L. (2018). Characterization and spatial distribution of particulate and

soluble carbon and nitrogen from wildfire-impacted sediments. *Journal of Soils and Sediments*, *18*(4), 1314–1326. https://doi.org/10.1007/s11368-016-1604-1

Chen, H., Luo, Y., Potter, C., Moran, P.J., Grieneisen, M.L., Zhang, M. (2017). Modeling pesticide diuron loading from the San Joaquin watershed into the Sacramento-San Joaquin Delta using SWAT. *Water Research 121*, 374–385. https://doi.org/10.1016/j.watres.2017.05.032

Confesor Jr, R.B., & Whittaker, G.W. (2007). Automatic Calibration of Hydrologic Models With Multi-Objective Evolutionary Algorithm and Pareto Optimization. *JAWRA Journal of the American Water Resources Association 43*(4), 981-989. https://doi.org/10.1111/j.1752-1688.2007.00080.x

Coogan, S. C. P., Robinne, F.-N., Jain, P., & Flannigan, M. D. (2019). Scientists' warning on wildfire — a Canadian perspective. *Canadian Journal of Forest Research*, *49*(9), 1015–1023. https://doi.org/10.1139/cjfr-2019-0094

Cotrufo, M. F., Boot, C. M., Kampf, S., Nelson, P. A., Brogan, D. J., Covino, T., Haddix, M. L., MacDonald, L. H., Rathburn, S., Ryan-Bukett, S., Schmeer, S., & Hall, E. (2016). Redistribution of pyrogenic carbon from hillslopes to stream corridors following a large montane wildfire. *Global Biogeochemical Cycles*, *30*(9), 1348–1355. https://doi.org/10.1002/2016GB005467.Received

Deryng, D., Elliott, J., Folberth, C., Müller, C., Pugh, T. A. M., Boote, K. J., Conway, D., Ruane, A. C., Gerten, D., Jones, J. W., Khabarov, N., Olin, S., Schaphoff, S., Schmid, E., Yang, H., & Rosenzweig, C. (2016). Regional disparities in the beneficial effects of rising CO2 concentrations on crop water productivity. *Nature Climate Change*, *6*(8), 786–790. https://doi.org/10.1038/nclimate2995

Doerr, S. H., Woods, S. W., Martin, D. A., & Casimiro, M. (2009). "Natural background" soil water repellency in conifer forests of the north-western USA: Its prediction and relationship to wildfire occurrence. *Journal of Hydrology*, *371*(1–4), 12–21. https://doi.org/10.1016/j.jhydrol.2009.03.011

Du, X., Li, X., Zhang, W., Wang, H. (2014). Variations in source apportionments of nutrient load among seasons and hydrological years in a semi-arid watershed: GWLF model results. *Environmental Science and Pollution Research 21*(10), 6506–6515. https://doi.org/10.1007/s11356-014-2519-2

Du, X., Loiselle, D., Alessi, D.S., Faramarzi, M. (2019a). Incorporation of a process-based in-stream organic carbon module into SWAT to simulate organic carbon load and transport at the watershed scale. *manuscrip in preparation*.

Du, X., Shrestha, N.K., & Wang, J. (2019b). Integrating organic chemical simulation module into SWAT model with application for PAHs simulation in Athabasca oil sands region, *Western Canada. Environmental Modelling & Software 111*, 432–443. https://doi.org/10.1016/j.envsoft.2018.10.011

Ebel, B. A., & Moody, J. A. (2017). Synthesis of soil-hydraulic properties and infiltration

timescales in wildfire-affected soils. *Hydrological Processes*, *31*(2), 324–340. https://doi.org/10.1002/hyp.10998

Ebel, B. A., Moody, J. A., & Martin, D. A. (2012). Hydrologic conditions controlling runoff generation immediately after wildfire. *Water Resources Research*, *48*(3), 1–13. https://doi.org/10.1029/2011WR011470

Emelko, M. B., Silins, U., Bladon, K. D., & Stone, M. (2011). Implications of land disturbance on drinking water treatability in a changing climate: Demonstrating the need for "source water supply and protection" strategies. *Water Research*, *45*(2), 461–472. https://doi.org/10.1016/j.watres.2010.08.051

Emelko, M. B., Stone, M., Silins, U., Allin, D., Collins, A. L., Williams, C. H. S., Martens, A. M., & Bladon, K. D. (2016). Sediment-phosphorus dynamics can shift aquatic ecology and cause downstream legacy effects after wildfire in large river systems. *Global Change Biology*, *22*(3), 1168–1184. https://doi.org/10.1111/gcb.13073

Fabre, C., Sauvage, S., Tananaev, N., Noël, G.E., Teisserenc, R., Probst, J.L., Sánchez Pérez, S.M. (2019). Assessment of sediment and organic carbon exports into the Arctic ocean: The case of the Yenisei River basin. *Water Research 158*, 118–135. https://doi.org/10.1016/j.watres.2019.04.018

Faramarzi, M., Abbaspour, K. C., Adamowicz, W.L. (Vic), Lu, W., Fennell, J., Zehnder, A.J.B., & Goss, G.G. (2017). Uncertainty based assessment of dynamic freshwater scarcity in semi-arid watersheds of Alberta, Canada. *Journal of Hydrology: Regional Studies, 9*, 48–68. https://doi.org/10.1016/j.ejrh.2016.11.003

Faramarzi, M., Abbaspour, K. C., Schulin, R., & Yang, H. (2009). Modelling blue and green water resources in Iran. *Hydrological Processes 23*, 486–501. https://doi.org/10.1002/hyp.7160

Faramarzi, M., Srinivasan, R., Iravani, M., Bladon, K.D., Abbaspour, K.C., Zehnder, A.J., & Goss, G.G. (2015). Setting up a hydrological model of Alberta: Data discrimination analyses prior to calibration. *Environmental Modelling & Software 74*, 48–65. DOI: 10.1016/j.envsoft.2015.09.006

Farjad, B., Gupta, A., & Marceau, D. J. (2016). Annual and Seasonal Variations of Hydrological Processes Under Climate Change Scenarios in Two Sub-Catchments of a Complex Watershed. *Water Resources Management*, *30*(8), 2851–2865. https://doi.org/10.1007/s11269-016-1329-3

Farjad, B., Pooyandeh, M., Gupta, A., Motamedi, M., & Marceau, D. (2017). Modelling interactions between land use, climate, and hydrology along with stakeholders' negotiation for water resources management. *Sustainability (Switzerland)*, *9*(11), 1–19. https://doi.org/10.3390/su9112022

Ficklin, D.L., Luo, Y., & Zhang, M. (2013). Climate change sensitivity assessment of streamflow and agricultural pollutant transport in California's Central Valley using Latin hypercube sampling. *Hydrological Processes, 27*(18) 2666–2675.

https://doi.org/10.1002/hyp.9386

Fischer, H., Sachse, A., Steinberg, C. E. W., & Pusch, M. (2002). Differential Retention and Utilization of Dissolved Organic Carbon by Bacteria in River Sediments. *Limnology and Oceanography*, *47*(6), 1702–1711. https://doi.org/10.4319/lo.2002.47.6.1702

Flannigan, M. D., Logan, K. A., Amiro, B. D., Skinner, W. R., & Stocks, B. J. (2005). Future area burned in Canada. *Climatic Change*, *72*(1–2), 1–16. https://doi.org/10.1007/s10584-005-5935-y

Futter, M. N., Butterfield, D., Cosby, B. J., Dillon, P. J., Wade, A. J., & Whitehead, P. G. (2007). Modeling the mechanisms that control in-stream dissolved organic carbon dynamics in upland and forested catchments. *Water Resources Research*, *43*(2), 1–16. https://doi.org/10.1029/2006WR004960

Gartner, J. E., Cannon, S. H., Santi, P. M., & Dewolfe, V. G. (2008). Empirical models to predict the volumes of debris flows generated by recently burned basins in the western U.S. *Geomorphology*, *96*(3–4), 339–354. https://doi.org/10.1016/j.geomorph.2007.02.033

Gleeson, T., Wada, Y., Bierkens, M. F. P., & Van Beek, L. P. H. (2012). Water balance of global aquifers revealed by groundwater footprint. *Nature*, *488*(7410), 197–200. https://doi.org/10.1038/nature11295

González-Pérez, J. A., González-Vila, F. J., Almendros, G., & Knicker, H. (2004). The effect of fire on soil organic matter - A review. *Environment International*, *30*(6), 855–870. https://doi.org/10.1016/j.envint.2004.02.003

Gorgan, D., Bacu, V, Mihon, D., Rodila, D., Abbaspour, K., & Rouholahnejad, E. (2012). Grid based calibration of SWAT hydrological models. *Natural Hazards and Earth System Sciences, 12*(7), 2411-2423. https://doi.org/10.5194/nhess-12-2411-2012

Hallema, D. W., Robinne, F.-N., & Bladon, K. D. (2018). Reframing the Challenge of Global Wildfire Threats to Water Supplies. *Earth's Future*, *6*(6), 772–776. https://doi.org/10.1029/2018EF000867

Havel, A., Tasdighi, A., & Arabi, M. (2018). Assessing the long-term hydrologic response to wildfires in mountainous regions. *Hydrology and Earth System Sciences*, *22*(25), 2527–2550. https://doi.org/10.5194/hess-2017-604

Health Canada (2017). Guidelines for Canadian Drinking Water Quality—Summary Table. Water and Air Quality Bureau, Healthy Environments and Consumer Safety Branch, Health Canada, Ottawa, Ontario.

Hernandez, A. J., Healey, S. P., Huang, H., & Ramsey, R. D. (2018). Improved prediction of stream flow based on updating land cover maps with remotely sensed forest change detection. Forests, 9(6), 1–19. https://doi.org/10.3390/f9060317

Hohner, A. K., Cawley, K., Oropeza, J., Summers, R. S., & Rosario-Ortiz, F. L. (2016). Drinking water treatment response following a Colorado wildfire. *Water Research*, *105*, 187–198. https://doi.org/10.1016/j.watres.2016.08.034

Hohner, A. K., Terry, L. G., Townsend, E. B., Summers, R. S., & Rosario-Ortiz, F. L. (2017). Water treatment process evaluation of wildfire-affected sediment leachates. *Environmental Science: Water Research and Technology*, *3*(2), 352–365. https://doi.org/10.1039/c6ew00247a

IPCC (2007): Climate Change 2007: Synthesis Report. Contribution of Working Groups I, II and III to the Fourth Assessment Report of the Intergovernmental Panel on Climate Change [Core Writing Team, Pachauri, R.K, & Reisinger, A. (eds.)]. IPCC, Geneva, Switzerland, 104.

IPCC (2013): Climate Change 2013: The Physical Science Basis. Contribution of Working Group I to the Fifth Assessment Report of the Intergovernmental Panel on Climate Change [Stocker, T. F., Qin, D., Plattner, G.-K., Tignor, M., Allen, S. K., Boschung, J., Nauels, A. Xia, Y., Bex, V. & Midgley, P. M. (eds.)]. Cambridge University Press, Cambridge, United Kingdom and New York, NY, USA, 1535.

Kemanian, A. R., Julich, S., Manoranjan, V. S., & Arnold, J. R. (2011). Integrating soil carbon cycling with that of nitrogen and phosphorus in the watershed model SWAT: Theory and model testing. *Ecological Modelling*, *222*(12), 1913–1921. https://doi.org/10.1016/j.ecolmodel.2011.03.017

Krause, P., Boyle, D. P., & Bäse, F. (2005). Advances in Geosciences Comparison of different efficiency criteria for hydrological model assessment. *Advances in Geosciences*, *5*, 89–97. https://doi.org/10.5194/adgeo-5-89-2005

Krishnan, N., Raj, C., Chaubey, I., & Sudheer, K. (2018). Parameter estimation of SWAT and quantification of consequent confidence bands of model simulations. *Environmental Earth Sciences, 77*(470), 1–16. https://doi.org/10.1007/s12665-018-7619-8

Kulig, J. C., Edge, D., Reimer, W. (Bill), Townshend, I., & Lightfoot, N. (2009). Levels of Risk: Perspectives from the Lost Creek Fire. *Australian Journal of Emergency Management*, *24*(2), 33–39.

Larsen, S., Andersen, T., & Hessen, D. O. (2011). Climate change predicted to cause severe increase of organic carbon in lakes. *Global Change Biology*, *17*(2), 1186–1192. https://doi.org/10.1111/j.1365-2486.2010.02257.x

Laudon, H., Buttle, J., Carey, S. K., McDonnell, J., McGuire, K., Seibert, J., Shanley, J., Soulsby, C., & Tetzlaff, D. (2012). Cross-regional prediction of long-term trajectory of stream water DOC response to climate change. *Geophysical Research Letters*, *39*(18), 4–9. https://doi.org/10.1029/2012GL053033

Lessels, J. S., Tetzlaff, D., Carey, S. K., Smith, P., & Soulsby, C. (2015). A coupled hydrology-biogeochemistry model to simulate dissolved organic carbon exports from a permafrost-influenced catchment. *Hydrological Processes, 29*(26), 5383–5396. https://doi.org/10.1002/hyp.10566

Mahat, V., Silins, U., & Anderson, A. (2016). Effects of wildfire on the catchment hydrology in southwest Alberta. *Catena*, *147*, 51–60. https://doi.org/10.1016/j.catena.2016.06.040

Malagó, A., Bouraoui, F., Vigiak, O., Grizzetti, B., & Pastori, M. (2017). Modelling water and nutrient fluxes in the Danube River Basin with SWAT. *Science of the Total Environment*, *603–604*, 196–218. https://doi.org/10.1016/j.scitotenv.2017.05.242

Marlon, J. R., Bartlein, P. J., Gavin, D. G., Long, C. J., Anderson, R. S., Briles, C. E., Brown, K. J., Colombaroli, D., Hallett, D. J., Power, M. J., Scharf, E. A., & Walsh, M. K. (2012). Long-term perspective on wildfires in the western USA. *Proceedings of the National Academy of Sciences*, *109*(9), 3203–3204. https://doi.org/10.1073/pnas.1112839109

Masud, M.B., Ferdous, J., & Faramarzi, M. (2018). Projected changes in hydrological variables in the agricultural region of Alberta, Canada, *Water, 12*(10), DOI: 10.3390/w10121810.

Masud, M. B., Wada, Y., Goss, G., & Faramarzi, M. (2019). Global implications of regional grain production through virtual water trade, Science of the total environment 659, 807–820. DOI: 10.1016/j.scitotenv.2018.12.392.

MNP LLP (2017). A Review of the 2016 Horse River Wildfire. Alberta Agriculture and Forestry Preparedness and Response. <https://wildfire.alberta.ca/resources/reviews/documents/2016HorseRiverWildfireReview-Mar2017.pdf>

Monteith, J.L. (1965). Evaporation and the environment. In The state and movement of water in living organisms. 19th symposia of the Society for Experimental Biology. Cambridge University Press, London, U.K. 205–234.

Moody, J. A., & Martin, D. A. (2001). Post-fire, rainfall intensity-peak discharge relations for three mountainous watersheds in the Western USA. *Hydrological Processes*, *15*(15), 2981–2993. https://doi.org/10.1002/hyp.386

Moody, J. A., & Martin, D. A. (2009). Synthesis of sediment yields after wildland fire in different rainfall regimes in the western United States. *International Journal of Wildland Fire*, *18*, 96–115. https://doi.org/10.1071/WF07162

Moody, J. A., Shakesby, R. A., Robichaud, P. R., Cannon, S. H., & Martin, D. A. (2013). Current research issues related to post-wildfire runoff and erosion processes. *Earth-Science Reviews*, *122*, 10–37. https://doi.org/10.1016/j.earscirev.2013.03.004

Morán-Tejeda, E., Zabalza, J., Rahman, K., Gago-Silva, A., López-Moreno, J. I., Vicente-Serrano, S., Lehmann, A., Tague, C. L., & Beniston, M. (2015). Hydrological impacts of climate and land-use changes in a mountain watershed: Uncertainty estimation based on model comparison. *Ecohydrology*, *8*(8), 1396–1416. https://doi.org/10.1002/eco.1590

Moriasi, D.N., Arnold, J.G., Van Liew, M.W., Bingner, R.L., Harmel, R.D., & Veith, T.L. (2007). Model evaluation guidelines for systematic quantification of accuracy in watershed simulations. *Transactions of the ASABE. 50*(3), 885–900. doi: 10.13031/2013.23153

Moriasi, D.N., Gitau, M.W., Pai, N., & Daggupati, P. (2015). Hydrologic and water quality models: Performance measures and evaluation criteria. *Transactions of the ASABE 58*(6), 1763–1785. DOI 10.13031/trans.58.10715

Nalley, J. O., O'Donnell, D. R., & Litchman, E. (2018). Temperature effects on growth rates and fatty acid content in freshwater algae and cyanobacteria. *Algal Research*, *35*, 500–507. https://doi.org/10.1016/j.algal.2018.09.018

Natural Resources Canada (2017), accessed May 2019, <https://www.nrcan.gc.ca/forests/measuring-reporting/classification/13179>

Natural Resources Canada (2018), accessed July 2019. <https://www.nrcan.gc.ca/our-natural-resources/forests-forestry/sustainable-forest-management/boreal-forest/8-facts-about-canadas-boreal-forest/17394>

Neitsch, S.L., Arnold, J.G., Kiniry, J.R., Williams, J.R. (2011). Soil and water assessment tool theoretical documentation version 2009. Texas Water Resources Institute.

Nguyen, H. H., Recknagel, F., Meyer, W., Frizenschaf, J., & Shrestha, M. K. (2017). Modelling the impacts of altered management practices, land use and climate changes on the water quality of the Millbrook catchment-reservoir system in South Australia. *Journal of Environmental Management, 202*(1), 1–11. https://doi.org/10.1016/j.jenvman.2017.07.014

Ni, X., & Parajuli, P.B. (2018). Evaluation of the impacts of BMPs and tailwater recovery system on surface and groundwater using satellite imagery and SWAT reservoir function. *Agricultural water management 210*, 78–87. https://doi.org/10.1016/j.agwat.2018.07.027

Niraula, R., Kalin, L., Srivastava, P., & Anderson, C. J. (2013). Identifying critical source areas of nonpoint source pollution with SWAT and GWLF. *Ecological Modelling*, *268*, 123–133. https://doi.org/10.1016/j.ecolmodel.2013.08.007

Noske, P. J., Lane, P. N. J., & Sheridan, G. J. (2010). Stream exports of coarse matter and phosphorus following wildfire in NE Victoria, Australia. *Hydrological Processes*, *24*(11), 1514–1529. https://doi.org/10.1002/hyp.7616

Oeurng, C., Sauvage, S., & Sánchez-Pérez, J. M. (2011). Assessment of hydrology, sediment and particulate organic carbon yield in a large agricultural catchment using the SWAT model. *Journal of Hydrology*, *401*(3–4), 145–153. https://doi.org/10.1016/j.jhydrol.2011.02.017

Osborn, G., Stockmal, G., & Haspel, R. (2006). Emergence of the Canadian Rockies and adjacent plains: A comparison of physiography between end-of-Laramide time and the present day. *Geomorphology*, *75*(3–4), 450–477. https://doi.org/10.1016/j.geomorph.2005.07.032

Parton, W.J., Ojima, D.S., Cole, C.V., & Schimel, D.S. (1994). A general model for soil organic matter dynamics: sensitivity to litter chemistry, texture and management. Quantitative modeling of soil forming processes. SSSA spec. 39, Madison, WI, 147–67.

Parton, W.J., Schimel, D.S., Cole, C.V., Ojima, D. (1987). Analysis of factors controlling soil organic matter levels in the Great Plains grasslands. *Soil Science Society of America Journal 51*, 1173–1179. DOI: 10.2136/sssaj1987.03615995005100050015x

Pekel, J.-F., Cottam, A., Gorelick, N., & Belward, A. S. (2016). High-resolution mapping of global surface water and its long-term changes. *Nature*, *540*, 418–422.

https://doi.org/10.1038/nature20584

Plaza-Álvarez, P. A., Lucas-Borja, M. E., Sagra, J., Moya, D., Alfaro-Sánchez, R., González-Romero, J., & De las Heras, J. (2018). Changes in soil water repellency after prescribed burnings in three different Mediterranean forest ecosystems. *Science of the Total Environment*, *644*, 247–255. https://doi.org/10.1016/j.scitotenv.2018.06.364

Pomeroy, J. W., Gray, D. M., Brown, T., Hedstrom, N. R., Quinton, W. L., Granger, R. J., & Carey, S. K. (2007). The cold regions hydrological model: a platform for basing process representation and model structure on physical evidence. *Hydrological Processes*, *21*, 2650–2667. https://doi.org/10.1002/hyp

Porcal, P., Dillon, P.J., & Molot, L.A. (2015). Temperature dependence of photodegradation of dissolved organic matter to dissolved inorganic carbon and particulate organic carbon. *PLoS One 10*(6). DOI: 10.1371/journal.pone.0128884

Qi, J., Li, S., Jamieson, R., Hebb, D., Xing, Z., & Meng, F. R. (2017). Modifying SWAT with an energy balance module to simulate snowmelt for maritime regions. *Environmental Modelling and Software*, *93*, 146–160. https://doi.org/10.1016/j.envsoft.2017.03.007

Qi, J., Li, S., Li, Q., Xing, Z., Bourque, C. P. A., & Meng, F. R. (2016). A new soil-temperature module for SWAT application in regions with seasonal snow cover. *Journal of Hydrology*, *538*, 863–877. https://doi.org/10.1016/j.jhydrol.2016.05.003

Qiu, Z., Wang., L., 2014. Hydrological and Water Quality Assessment in a Suburban Watershed with Mixed Land Uses Using the SWAT Model. *Journal of Hydrologic Engineering 19*(4), 816–827.

Regan, S., Hynds, P., & Flynn, R. (2017). An overview of dissolved organic carbon in groundwater and implications for drinking water safety. *Hydrogeology Journal*, *25*(4), 959–967. https://doi.org/10.1007/s10040-017-1583-3

Rhoades, C. C., Chow, A. T., Covino, T. P., Fegel, T. S., Pierson, D. N., & Rhea, A. E. (2019). The Legacy of a Severe Wildfire on Stream Nitrogen and Carbon in Headwater Catchments. *Ecosystems*, *22*(3), 643–657. https://doi.org/10.1007/s10021-018-0293-6

Robichaud, P. R., Wagenbrenner, J. W., Pierson, F. B., Spaeth, K. E., Ashmun, L. E., & Moffet, C. A. (2016). Infiltration and interrill erosion rates after a wildfire in western Montana, USA. *Catena*, *142*, 77–88. https://doi.org/10.1016/j.catena.2016.01.027

Robinne, F. N., Bladon, K. D., Miller, C., Parisien, M. A., Mathieu, J., & Flannigan, M. D. (2018). A spatial evaluation of global wildfire-water risks to human and natural systems. *Science of the Total Environment, 610–611*, 1193–1206. https://doi.org/10.1016/j.scitotenv.2017.08.112

Robinne, F. N., Bladon, K. D., Silins, U., Emelko, M. B., Flannigan, M. D., Parisien, M. A., Wang, X., Kienzle, S. W., & Dupont, D. P. (2019). A regional-scale index for assessing the exposure of drinking-water sources to wildfires. *Forests, 10*(5), 1–21. https://doi.org/10.3390/f10050384

Robinne, F. N., Miller, C., Parisien, M. A., Emelko, M. B., Bladon, K. D., Silins, U., & Flannigan, M. (2016). A global index for mapping the exposure of water resources to wildfire. *Forests, 7*(1), 1–16. https://doi.org/10.3390/f7010022

Rodrigues, E. L., Jacobi, C. M., & Figueira, J. E. C. (2019). Wildfires and their impact on the water supply of a large neotropical metropolis: A simulation approach. *Science of the Total Environment*, *651*, 1261–1271. https://doi.org/10.1016/j.scitotenv.2018.09.289

Rodríguez-Jeangros, N., Hering, A. S., & McCray, J. E. (2018). Analysis of anthropogenic, climatological, and morphological influences on dissolved organic matter in Rocky Mountain streams. *Water (Switzerland)*, *10*(4), 1–46. https://doi.org/10.3390/w10040534

Rogeau, M.-P., & Armstrong, G. W. (2017). Quantifying the effect of elevation and aspect on fire return intervals in the Canadian Rocky Mountains. *Forest Ecology and Management*, *384*, 248–261. https://doi.org/10.1016/j.foreco.2016.10.035

Rogeau, M.-P., Flannigan, M. D., Hawkes, B. C., Parisien, M.-A., & Arthur, R. (2016). Spatial and temporal variations of fire regimes in the Canadian Rocky Mountains and Foothills of southern Alberta. *International Journal of Wildland Fire*, *25*, 1117–1130. https://doi.org/10.1071/WF15120

Rood, S. B., Samuelson, G. M., Weber, J. K., & Wywrot, K. A. (2005). Twentieth-century decline in streamflows from the hydrographic apex of North America. *Journal of Hydrology*, *306*(1–4), 215–233. https://doi.org/10.1016/j.jhydrol.2004.09.010

Rostami, S., He, J., & Hassan, Q. K. (2018). Riverine water quality response to precipitation and its change. *Environments*, *5*(1), 1–17. https://doi.org/10.3390/environments5010008

Roy, S., Heidel., K., Creager, C., Chung, C., & Grieb., T. (2006). Conceptual model for organic carbon in the Central Valley and Sacramento-San Joaquin Delta. Tetra Tech, Inc: Lafayette, California, USA

Runkel, R.L., Crawford, C.G., & Cohn, T.A. (2004). Load Estimator (LOADEST): A FORTRAN program for estimating constituent loads in streams and rivers. Techniques and Methods 4-A5, https://doi.org/10.3133/tm4A5

Rust, A. J., Hogue, T. S., Saxe, S., & McCray, J. (2018). Post-fire water-quality response in the western United States. *International Journal of Wildland Fire*, *27*(3), 203–216. https://doi.org/10.1071/WF17115

Sempéré, R., Charrière, B., Van Wambeke, F., & Cauwet, G. (2000). Carbon inputs of the Rhône River to the Mediterranean Sea: biogeochemical implications. *Global Biogeochemical Cycles* 14(2), 669–681. https://doi.org/10.1029/1999GB900069

Schindler, D. W., & Donahue, W. F. (2006). An impending water crisis in Canada's western prairie provinces. *Proceedings of the National Academy of Sciences*, *103*(19), 7210–7216. https://doi.org/10.1073/pnas.0601568103

Shakesby, R. A., Bento, C. P. M., Ferreira, C. S. S., Ferreira, A. J. D., Stoof, C. R., Urbanek, E., & Walsh, R. P. D. (2015). Impacts of prescribed fire on soil loss and soil quality: An

assessment based on an experimentally-burned catchment in central Portugal. *Catena*, *128*, 278–293. https://doi.org/10.1016/j.catena.2013.03.012

Shrestha, N. K., Du, X., & Wang, J. (2017). Assessing climate change impacts on fresh water resources of the Athabasca River Basin, Canada. *Science of the Total Environment*, *601–602*, 425–440. https://doi.org/10.1016/j.scitotenv.2017.05.013

Shrestha, N. K., & Wang, J. (2018). Predicting sediment yield and transport dynamics of a cold climate region watershed in changing climate. *Science of the Total Environment*, *625*, 1030–1045. https://doi.org/10.1016/j.scitotenv.2017.12.347

Silins, U., Stone, M., Emelko, M. B., & Bladon, K. D. (2009). Sediment production following severe wildfire and post-fire salvage logging in the Rocky Mountain headwaters of the Oldman River Basin, Alberta. *Catena*, *79*(3), 189–197. https://doi.org/10.1016/j.catena.2009.04.001

Smith, H. G., Sheridan, G. J., Lane, P. N. J., Nyman, P., & Haydon, S. (2011). Wildfire effects on water quality in forest catchments: A review with implications for water supply. *Journal of Hydrology*, *396*(1–2), 170–192. https://doi.org/10.1016/j.jhydrol.2010.10.043

Sosiak, A., & Dixon, J. (2006). Impacts on water quality in the upper Elbow River. *Water Science and Technology*, *53*(10), 309–316. https://doi.org/10.2166/wst.2006.326

Tague, C. L., & Band, L. E. (2004). RHESSys: Regional Hydro-Ecologic Simulation System—An Object-Oriented Approach to Spatially Distributed Modeling of Carbon, Water, and Nutrient Cycling. *Earth Interactions, 8*(19), 1–42. https://doi.org/10.1175/1087-3562(2004)8<1:rrhsso>2.0.co;2

Technical Support Document for Ontario Drinking Water Standards (2006), Objectives and Guidelines, June 2003, Revised June 2006, PIBS 4449e01.

Teshager, A. D., Gassman, P. W., Secchi, S., Schoof, J. T., & Misgna, G. (2016). Modeling Agricultural Watersheds with the Soil and Water Assessment Tool (SWAT): Calibration and Validation with a Novel Procedure for Spatially Explicit HRUs. *Environmental Management*, *57*(4), 894–911. https://doi.org/10.1007/s00267-015-0636-4

Townsend, S. A., & Douglas, M. M. (2000). The effect of a wildfire on stream water quality and catchment water yield in a tropical savanna excluded from fire for 10. *Journal of Hydrology*, *229*, 118–137. Retrieved from http://espace.library.cdu.edu.au/view.php?pid=cdu:1488

Townsend, S. A., & Douglas, M. M. (2004). The effect of a wildfire on stream water quality and catchment water yield in a tropical savanna excluded from fire for 10 years (Kakadu National Park, North Australia). *Water Research*, *38*(13), 3051–3058. https://doi.org/10.1016/j.watres.2004.04.009

Tuppad, P., Douglas-Mankin, K. R., Lee, T., Srinivasan, R., & Arnold, J. G. (2011). Soil and Water Assessment Tool (SWAT) hydrologic/water quality model: Extended capability and wider adoption. *Transactions of the ASABE 54*(5), 1677–1684. DOI: 10.13031/2013.39856

Vaghefi, S.A., Iravani, M., Sauchyn, D., Andreichuk, Y., Goss, G., Faramarzi, M. (2019). Regionalization and parameterization of a hydrologic model significantly affect the cascade of uncertainty in climate-impact projections. *Climate Dynamics, 53*(5–6), 2861–2886. DOI: https://doi.org/10.1007/s00382-019-04664-w

Valeo, C., Xiang, Z., Bouchart, F. J., Yeung, P., & Ryan, M. C. (2007). Climate change impacts in the Elbow River watershed. *Canadian Water Resources Journal*, *32*(4), 285–302. https://doi.org/10.4296/cwrj3204285

Vörösmarty, C. J., McIntyre, P. B., Gessner, M. O., Dudgeon, D., Prusevich, A., Green, P., Gidden, S., Bunn, S. E., Sullivan, C. A., Liermann, R., & Davies, P. M. (2010). Global threats to human water security and river biodiversity. *Nature*, *467*, 555–561. https://doi.org/10.1038/nature09440

Wagner, M. J., Bladon, K. D., Silins, U., Williams, C. H. S., Martens, A. M., Boon, S., MacDonald, R. J., Stone, M., Emelko, M. B., & Anderson, A. (2014). Catchment-scale stream temperature response to land disturbance by wildfire governed by surface – subsurface energy exchange and atmospheric controls. *Journal of Hydrology*, *517*, 328–338. https://doi.org/10.1016/j.jhydrol.2014.05.006

Wang, X., Thompson, D. K., Marshall, G. A., Tymstra, C., Carr, R., & Flannigan, M. D. (2015). Increasing frequency of extreme fire weather in Canada with climate change. *Climatic Change*, *130*(4), 573–586. https://doi.org/10.1007/s10584-015-1375-5

Wei, X., Bailey, R.T., Records, R.M., Wible, T.C., & Arabi, M. (2018). Comprehensive simulation of nitrate transport in coupled surface-subsurface hydrologic systems using the linked SWAT-MODFLOW-RT3D model. *Environmental Modelling & Software* (in press, corrected proof) https://doi.org/10.1016/j.envsoft.2018.06.012

Wijesekara, G. N., Farjad, B., Gupta, A., Qiao, Y., Delaney, P., & Marceau, D. J. (2014). A comprehensive land-use/hydrological modeling system for scenario simulations in the Elbow River watershed, Alberta, Canada. *Environmental Management*, *53*(2), 357–381. https://doi.org/10.1007/s00267-013-0220-8

Wijesekara, G. N., Gupta, A., Valeo, C., Hasbani, J. G., Qiao, Y., Delaney, P., & Marceau, D. J. (2012). Assessing the impact of future land-use changes on hydrological processes in the Elbow River watershed in southern Alberta, Canada. *Journal of Hydrology*, *412–413*, 220–232. https://doi.org/10.1016/j.jhydrol.2011.04.018

Williams, J.R. (1995). Chapter 25: The EPIC model. P. 909–1000. In V.P. Singh (ed) Computer models of watershed hydrology. Water Resources Publications.

Willmore, N. Jensen, H.G. (1960). Alberta's Forests, Government of the Province of Alberta, Department of Lands and Forests, Edmonton.

Worku, T., Khare, D., & Tripathi, S. K. (2017). Modeling runoff–sediment response to land use/land cover changes using integrated GIS and SWAT model in the Beressa watershed. *Environmental Earth Sciences*, *76*(16), 1–14. https://doi.org/10.1007/s12665-017-6883-3

Worrall, F., & Moody, C. (2014). Modeling the rate of turnover of DOC and particulate organic carbon in a UK, peat-hosted stream: Including diurnal cycling in short-residence time systems. *Journal of Geophysical Research: Biogeosciences, 119*(10) 1934-1946. https://doi.org/10.1002/2014JG002671

Wotton, B. M., Nock, C. A., & Flannigan, M. D. (2010). Forest fire occurrence and climate change in Canada. *International Journal of Wildland Fire*, *19*(3), 253–271. https://doi.org/10.1071/WF09002

Writer, J H, McCleskey, R. B., & Murphy, S. F. (2012). Effects of wildfire on source-water quality and aquatic ecosystems, Colorado Front Range. *Wildfire and Water Quality: Processes, Impacts, and Challenges*, (IAHS Publ. 354), 117–123.

Writer, Jeffrey H., Hohner, A., Oropeza, J., Schmidt, A., Cawley, K., & Rosario-Ortiz, F. L. (2014). Water treatment implications after the High Park Wildfire in Colorado. *American Water Works Association*, *106*(4), 189–199. https://doi.org/10.5942/jawwa.2014.106.0055

Yang, Qi, Leon, L. F., Booty, W. G., Wong, I. W., McCrimmon, C., Fong, P., Fong, P., Michiels, P., Vanrobaeys, J., & Benoy, G. (2014). Land Use Change Impacts on Water Quality in Three Lake Winnipeg Watersheds. *Journal of Environment Quality*, *43*(5), 1690–1701. https://doi.org/10.2134/jeq2013.06.0234

Yang, Qichun, & Zhang, X. (2016). Improving SWAT for simulating water and carbon fluxes of forest ecosystems. *Science of the Total Environment*, *569–570*, 1478–1488. https://doi.org/10.1016/j.scitotenv.2016.06.238

Yu, M., Bishop, T. F. A., & Van Ogtrop, F. F. (2019). Assessment of the decadal impact of wildfire on water quality in forested catchments. *Water (Switzerland)*, *11*(3), 1–17. https://doi.org/10.3390/w11030533

Zabaleta, A., Meaurio, M., Ruiz, E., & Antigüedad, I. (2014). Simulation climate change impact on runoff and sediment yield in a small watershed in the Basque Country, northern Spain. *Journal of environmental quality 43*(1), 235–245. doi: 10.2134/jeq2012.0209

Zeiger, S. J., & Hubbart, J. A. (2016). A SWAT model validation of nested-scale contemporaneous streamflow, suspended sediment and nutrients from a multiple-land-use watershed of the central USA. *Science of the Total Environment*, *572*, 232–243. https://doi.org/10.1016/j.scitotenv.2016.07.178

Zhang, X. (2018). Simulating eroded soil organic carbon with the SWAT-C model. *Environmental Modelling and Software*, *102*, 39–48. https://doi.org/10.1016/j.envsoft.2018.01.005

Zhang, X., Izaurralde, R. C., Arnold, J. G., Williams, J. R., & Srinivasan, R. (2013). Modifying the Soil and Water Assessment Tool to simulate cropland carbon flux: Model development and initial evaluation. *Science of the Total Environment, 463–464*, 810–822. https://doi.org/10.1016/j.scitotenv.2013.06.056

APPENDICES

A.1. Data Sources

Table A.1. Data sources used for SWAT model.

Data Set	Source	Notes
Digital elevation model (DEM)	AltaLIS	Year: 2008 Resolution: 30 m
Land use map	GeoBase Land Cover Product	Year: 2000 Resolution: 90 m
Soil map	Agri-Food Canada, Government of Canada	Year: 2011 Resolution: 90 m
Precipitation and temperature data	Alberta Environment and Parks	1980–2017 Daily timestep 5 stations for temperature (some incomplete) 8 stations for precipitation (some incomplete)
Humidity, wind speed and solar radiation	CFSR: National Centers for Environmental Predictions Climate Forecast System Reanalysis	1980–2014 Daily timestep 4 stations (all records complete)
Volumetric discharge	Environment Canada	3 hydrometric flow stations
Water quality data	City of Calgary	1989–2015 Total suspended solid and nutrient concentrations
Historical wildfire data	Alberta Wildfire	1961–2017

A.2. Streamflow Calibration Results.

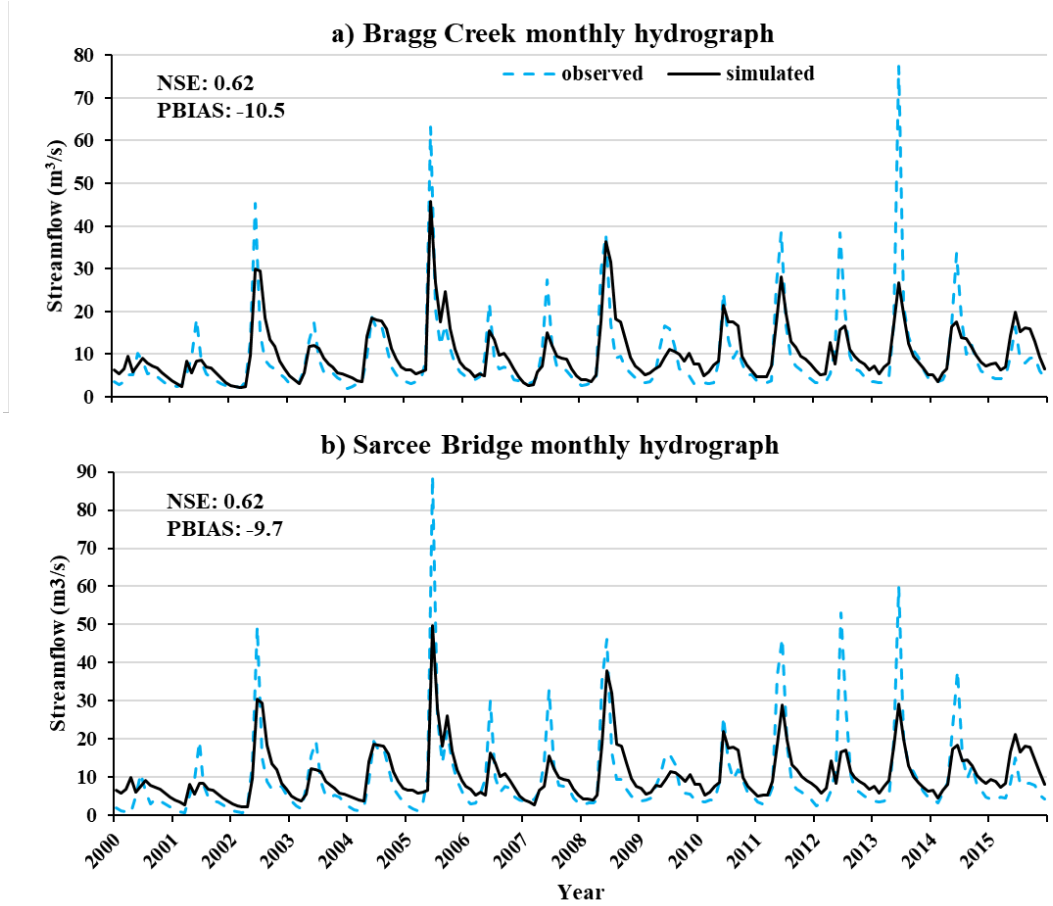

Fig. A.2. Monthly average hydrographs: (a) Bragg Creek; (b) Sarcee Bridge (watershed outlet), (Du et al., 2019a).

Table A.2. Monthly streamflow calibration and validation statistics; Elbow Falls operational from 1986–1995; Bragg Creek and Sarcee Bridge operational from 1986–2015 (Du et al., 2019a).

Stations	Calibration (2000–2015)			Validation (1986–1999)			All (1986–2015)		
	NSE	*R2*	*PBIAS*	*NSE*	*R2*	*PBIAS*	*NSE*	*R2*	*PBIAS*
Elbow Falls	-	-	-	0.62	0.62	-0.3	0.62	0.62	-0.3
Bragg Creek	0.62	0.64	-10.5	0.75	0.73	-9.3	0.66	0.68	-9.9
Sarcee Bridge	0.62	0.67	-9.7	0.70	0.70	-13.3	0.63	0.68	-11.2

A.3. Sediment Calibration Results

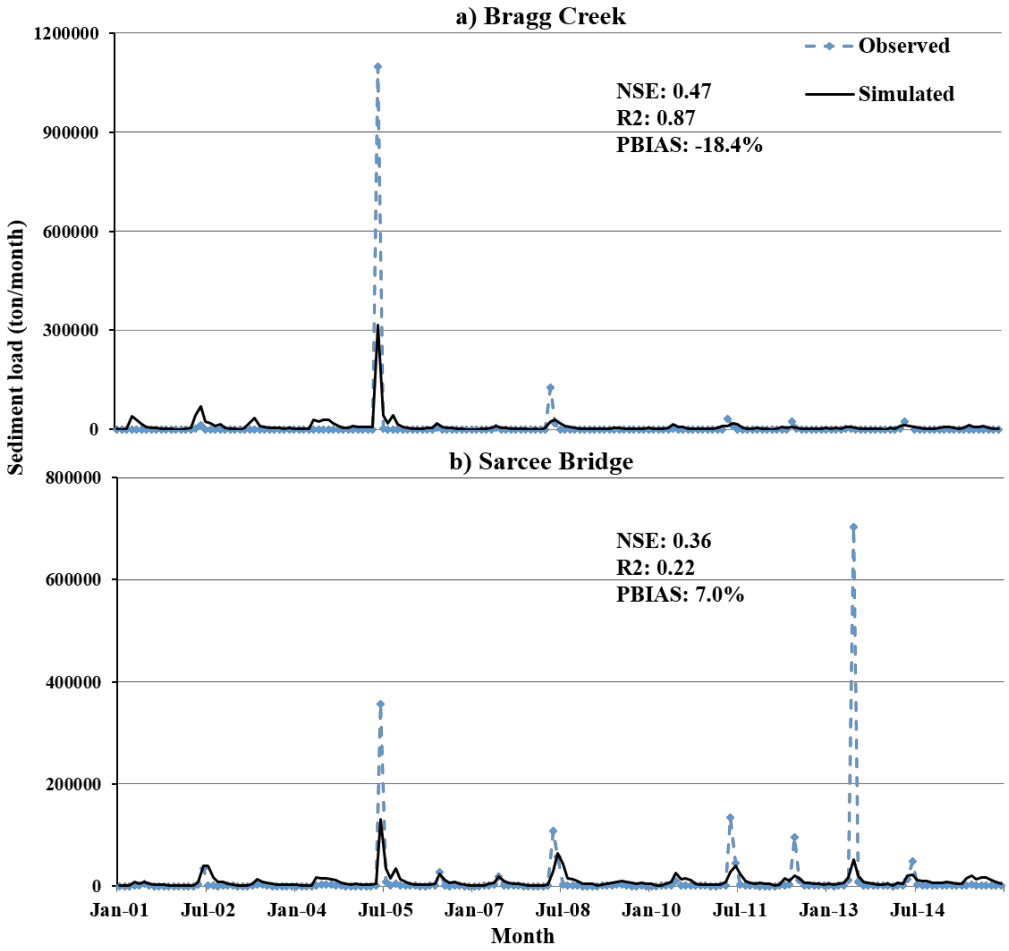

Fig. A.3. Monthly Sediment load simulation results with model performance statistics for the whole simulation period (2001–2015): (a) Bragg Creek; (b) Sarcee Bridge, (Du et al., 2019a).

Table A.3. Monthly sediment load calibration and validation statistics (Du et al., 2019a).

Stations	Calibration (2001–2007)			Validation (2008–2015)		
	NSE	*R2*	*PBIAS*	*NSE*	*R2*	*PBIAS*
Bragg Creek	0.47	0.88	-1.3	0.21	0.27	-95.7
Sarcee Bridge	0.55	0.79	-43.8	0.13	0.29	26.3

A.4. Total Organic Carbon Calibration Results

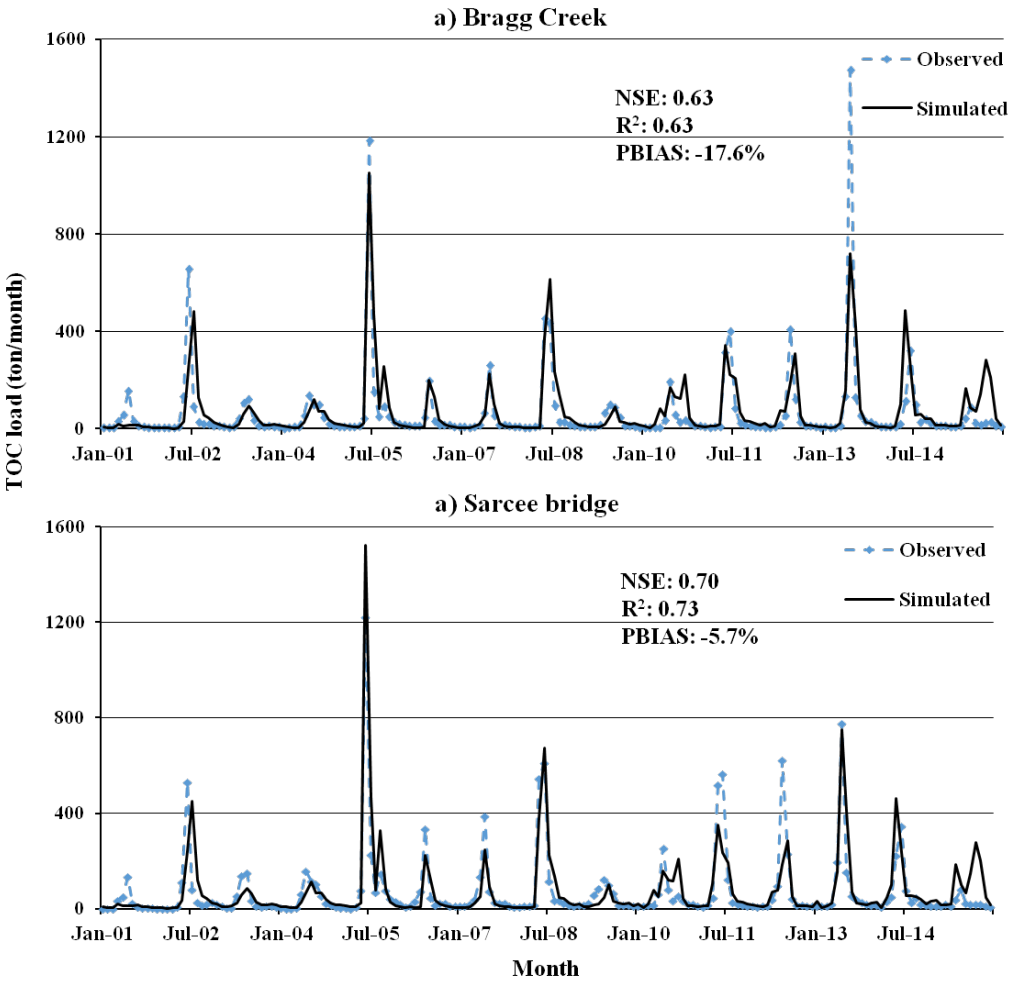

Fig. A.4. Monthly total organic carbon calibration for (a) Bragg Creek and (b) Sarcee Bridge stations; results were improved from Du et al., (2019a).

Table A.4. Monthly TOC load calibration and validation statistics (Du et al., 2019a).

Stations	Calibration (2001–2007)			Validation (2008–2015)		
	NSE	*R2*	*PBIAS*	*NSE*	*R2*	*PBIAS*
Bragg Creek	0.71	0.71	-4.8	0.57	0.58	-27.1
Sarcee Bridge	0.74	0.82	-0.2	0.66	0.66	-9.7